Energy & Environmental Science

Accepted Manuscript

ROYAL SOCIETY OF CHEMISTRY

www.rsc.org/ees

Graphical abstract

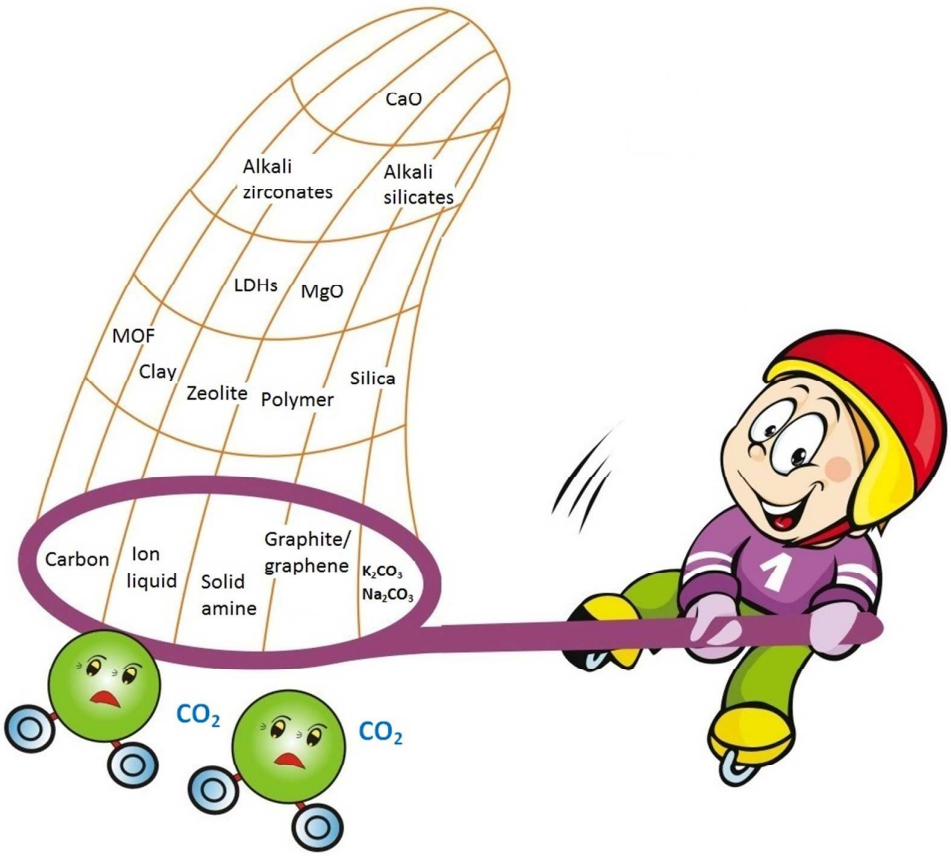

Energy &
Environmental Science

Cite this: DOI: 10.1039/c0xx00000x

www.rsc.org/xxxxxx

Review Articles

Recent Advances in Solid Sorbents for CO_2 Capture and New Development Trends

Junya Wang,[a] Liang Huang,[a] Ruoyan Yang,[a] Zhang Zhang,[a] Jingwen Wu,[a] Yanshan Gao,[a] Qiang Wang,*[a] Dermot O'Hare,[b] Ziyi Zhong*[c]

Received (in XXX, XXX) Xth XXXXXXXXX 20XX, Accepted Xth XXXXXXXXX 20XX

DOI: 10.1039/b000000x

Carbon dioxide (CO_2) capture using solid sorbents has been recognized as a very promising technology that has attracted intense attention from both academic and industrial fields in the last decade. It is astonishing that around 2000 papers have been published from 2011 to 2014 alone, which is less than three years after our first review paper in this journal on solid CO_2 sorbents was published. In this short period, much progress has been made and the major research focuses have more or less changed. Therefore, we feel that it is necessary to give a timely update on solid CO_2 capture materials, although we still have to keep some important literature results published in earlier years so as to keep the good continuity. We believe this work will benefit researchers working in both academic and industrial areas. In this paper, we still organize the CO_2 sorbents according to their working temperatures by classifying them as such: (1) low-temperature (<200 °C), (2) intermediate-temperature (200–400 °C), and (3) high-temperature (> 400 °C). Since the sorption capacity, kinetics, recycling stability and cost are important parameters when evaluating a sorbent, these features will be carefully considered and discussed. In addition, due to the huge amounts of cost-effective CO_2 sorbents demanded and the importance of waste resources, solid CO_2 sorbents prepared from waste resources and their performance are reviewed. Finally, the techno-economic assessments of various CO_2 sorbents and technologies in real applications are briefly discussed.

1. Introduction

CO_2 is one of the major greenhouse gases (GHG)[1] that absorbs heat radiation from Earth's surface which would otherwise have left the atmosphere. Although atmospheric CO_2 is the primary source of carbon in life on Earth and its concentration since the late Precambrian eon has been regulated by photosynthetic organisms, its continuous increase due to the large-scale burning of fossil fuels starting from the industrial revolution has led to the global warming and anthropogenic climate change. It is without a doubt that the many extreme weather events in recent years can be strongly correlated with the increase in atmospheric CO_2 concentration and the GHG effect, which contributes significantly to global warming and its environmental effects, such as the continuous rise of water-level in sea and the increasing number of ocean storms, floods, etc. Although other factors exist, the importance of the aforementioned relationship should not be undermined.[2, 3] Unfortunately, it is predicted that this trend of increasing atmospheric CO_2 concentration will not be altered within next several decades, because fossil fuels will be still the dominant energy source. As measured by Scripps Institute of Oceanography, the CO_2 concentration increased from ca. 315 ppm in March 1958 to 391 ppm in January of 2011, and close to 398 ppm in January 2014.[4]

One of the major anthropogenic sources of CO_2 emission is the power plant. For example, a 500 MW coal-fired power plant will generate ca. 3 million tons of CO_2 per year.[5] Therefore, CO_2 capture and sequestration (CCS) from these large point sources is essential for the reduction of CO_2 emission into atmosphere, which should be applied not only to new power plants but also to the retrofitting of old power plants.[6] Currently there are three approaches or processes to capture CO_2 from these point sources, namely pre-combustion capture, post-combustion capture and oxyfuel combustion.[7] In comparison with the other two processes, the post-combustion capture method is quite competitive in cost but as it involves flue gas, which has a low CO_2 concentration, i.e. typically below 15%, it creates a technical challenge for the development of cost-effective advanced capture processes.[8] Three main technologies including the use of scrubbing solutions, solid

sorbents and membranes are used to separate and capture CO_2 from the flue stream. Among these, solid sorbents have been most commonly investigated for post combustion CO_2 capture in recent years. Unlike liquid sorbents, solid sorbents can be used over a wider temperature range from ambient temperature to 700 ^oC, yielding less waste during cycling, and the spent solid sorbents can be disposed without undue environmental precautions.

In 2011, we published a review paper in Energy and Environmental Sciences on solid CO_2-sorbents for CO_2 capture and their applications.[9] However, within only three years (from 2011 to 2014), we noticed that there have been nearly 2000 new publications in this area, and some types of CO_2-sorbents, such as supported ion liquid, graphite/graphene based materials, boron nitride, clay-based sorbents, zirconium phosphate, metals oxides (TiO_2, NiO, CuO, Fe_3O_4, etc), etc, have been reported. More importantly, some waste-derived CO_2 sorbents, which probably will reduce the cost of the CO_2-sorbents significantly, have appeared.[10] In addition, there are many papers dealing with simulation/modeling studies on the technical and economic evaluations for different types of sorbents. Therefore, we feel that it is necessary to give a timely update on these solid CO_2 sorbents, which may benefit researchers working in both academic and industrial areas.

The solid sorbents may have various chemical or physical interactions with CO_2 molecules. However, following our previous classification, we continue to organize them according to their sorption and desorption temperatures and classify them as (1) low-temperature (< 200 ^oC), (2) intermediate-temperature (200–400 ^oC), and (3) high-temperature (> 400 ^oC) sorbents. Since the sorption capacity, kinetics, recycling stability and cost are important parameters when evaluating a sorbent, these features will be paid with special attention in this review. In addition, due to the potential demand of huge amounts of low cost CO_2 sorbents and the importance of waste resources, many active research activities in this field have appeared. Hence, a detailed review on the preparation of solid CO_2 sorbents from waste resources has been provided as well. Finally, the techno-economic assessments of various CO_2 sorbents and technologies in real applications are briefly discussed.

2. Low-temperature solid CO_2 adsorbents

2.1 Solid amine-based adsorbents

CO_2 removal from flue gas by sorption and stripping with aqueous amines (commonly monoethanolamine (MEA), diethanolamine (DEA) and methyldiethanolamine (MDEA)) has been established since 1930 and is still believed to be a feasible technology.[11, 12] However, this process suffers from a series of inherent problems, including the corrosive nature of the amines, fouling of the process equipment and high regeneration energy, etc.[13] To avoid the above problems, solid adsorbents with loaded organic amines on certain support materials are intensively investigated.[14-18] Compared to the aqueous amine solutions, these solid adsorbents usually require lower capital cost, lower pressure for gas recovery, and less energy for regeneration.[19] Amine-grafted silica was first proposed by Burwell and Leal[20] for SO_2 capture. Since then, amine-impregnated porous supports for CO_2 capture have been widely explored.[21, 22] From 2011 to 2014, many groups have also tried to improve the CO_2 sorption capacity of these amine-based solid adsorbents via the following technical routes: (1) supporting amines on porous materials, (2) selecting proper amines, and (3) enhancing CO_2 diffusion, etc. A vital variable that governs the CO_2 adsorption performance is the support. Up to date, many porous materials including carbon, graphite/grapheme, zeolite, MOF, silica, polymer, clay, and TiO_2 nanotubes, etc., have been investigated. With respect to the support effects, more details will be given in the following sections of 2.2–2.9.

The methods for loading of amine on supports can be classified as (a) impregnation, (b) post-synthesis grafting, and (c) direct condensation.[9] The impregnated samples often have high capture capacities. However, the transport limitations of CO_2 to active sites and the leaching of amines over multiple regeneration cycles limit their performance and long-term viability as CO_2 capture solutions.[23] The leaching problem can be alleviated or solved by covalently attaching amines onto solid surfaces, e.g., hyperbranched amines covalently attached to silica,[9] amine groups functionalized onto silica or alumina supports,[9] or by adding additives to the polyethylenimine (PEI) to increase stability.[23] Another group of amine adsorbents is solid polymeric systems in which the amines are covalently incorporated into the polymer backbone via chemical bonds such as C−C bonds. These C-C bonds usually are more stable than Si−O−C bonds hydrothermally.[23, 24]

The first amine impregnated CO_2 adsorbent (PEI/MCM-41) was developed by Xu et al.[25] in 2002. The adsorbent had a CO_2 capacity of 3.0 mmol g^{-1} at 75 ^oC under a dry 100% CO_2 feed gas. After that, intensive efforts have been made to synthesize amine-based CO_2 adsorbents with better performance, and to know more about the effects of operation temperature, CO_2 partial pressure, textural pore character of the support, and the nature of the amines on the CO_2 capture performance.[26, 27] For the impregnated systems, most studies have shown that supports having a larger pore volume and pore diameter give better adsorption performance. Son et al.[28] impregnated PEI onto five different mesoporous silica materials (i.e.MCM-41, MCM-48, SBA-15, SBA-16, KIT-6) and discovered that the adsorption capacity increased with increase of the pore diameter. Qi et al.[29] synthesized novel nanocomposites based on PEI and tetraethylenepentamine (TEPA) supported on specially designed mesoporous SiO_2 hollow capsules (see Figure 1).[29] They found that TEPA impregnated mesoporous silica capsules achieved adsorption capacities of 6.6 and 5.6 mmol g^{-1} using dry streams containing 100% and 10% CO_2 respectively at 75 ^oC, as well as 7.9 mmol g^{-1} under a humid 10% CO_2 stream, which are the highest reported adsorption capacity so far for the impregnated systems. This high capture capacity can be attributed to the large pore space and open structural character of the supports, which can enable high amine loadings and effective amine distribution, fast CO_2 adsorption kinetics and high CO_2 adsorption capacities.

Amine-silanol interactions are believed to be important for the adsorption of CO_2.[30] The impregnated PEI may not be very stable on the surface of the support. Although the grafted and hyperbranched amines have demonstrated improved CO_2 capture and stability over their impregnated counterparts, there is still reservation that, with increase of the complexity of the sorbents, the number of required steps in sorbent processing, and their associated costs, will also be increased simultaneously. Because of the required scale for CO_2 capture, the production of amine-functionalized and/or amine-impregnated sorbents should be at low cost and environmentally benign.[31] The amines in the polymeric forms may provide solution to the above problems. A class of polymeric amines with potential for CO_2 capture is ion exchanged resins (IER) with amine functionality. These materials showed ability to scrub CO_2 at low concentrations, like that in confined quarters such as marine and space vehicles, or from air.[32, 33] They also have high potential for application in CO_2 capture from fossil energy power plant flue gas. A variety of amine-functionalized IERs have been synthesized and investigated, including primary to quaternary amine functional groups.[23] Alesi. et al.[23] and Hallenbeck et al.[34] reported a primary amine-functionalized polymeric ion-exchange resin with a CO_2 capture capacity of 1.85 and 1.15 mmol g^{-1} at 30 and 70 °C, respectively. The capture capacity of the resin was stable over 18 adsorption/regeneration cycles. Also, the solid CO_2 adsorbents may be further improved by eliminating the use of the inert porous support via tailoring the molecular structures. Wang et al.[35] prepared support-free polyamine porous particles by a precipitation-polymerization method and obtained a CO_2 capture capacity of 2.3 mmol g^{-1}. This solid sorbent is very easy to be regenerated, requiring heating to only 100 °C under a N_2 flow.

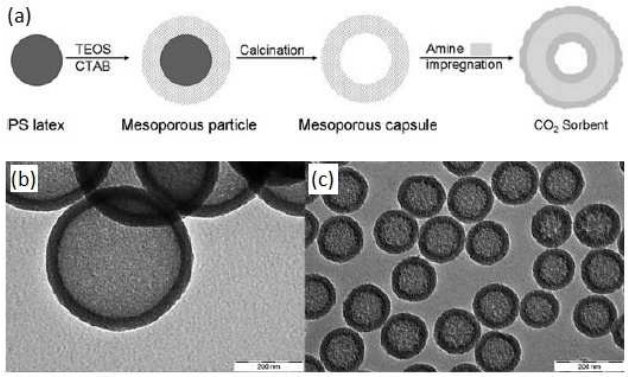

Figure 1. (a) Synthesis of amine impregnated composite sorbents based on mesoporous capsules, and TEM images of two silica supports, (b) MC400/50, and (c) MC160/20 (MC x/y, where x and y represent the approximate diameter and the shell thickness of the mesoporous capsules in nanometres, respectively).[29]

Besides the work on selecting and optimizing the supports, another aspect is to select the proper amines, such as primary amines, secondary amines, tertiary amines, and polyamines etc. Primary amines can form stable complexes with CO_2, capture CO_2 efficiently but are difficult to regenerate.[36] Tertiary amines do not capture CO_2 as efficiently as primary amines, but can be regenerated readily at relatively low temperatures.[36-42] As for the secondary amines, they can offer a compromise between the primary and tertiary amines. Bollini et al.[43] used four different silane coupling agents, three with a single primary, secondary, or tertiary amine at the end of a propyl surface linker, and the fourth with a secondary propylamine separated from a primary amine by an ethyl linker. They found that both amine type and their proximity had a significant effect on oxidative degradation rates. In particular, the supported primary and tertiary amines were stable under the oxidizing conditions used, whereas the secondary amines degraded at elevated treatment temperatures. Among all the studied amines, PEI and TEPA are the mostly used in adsorbent formulations because of their wide availability and efficient characteristics in CO_2 capture.

Previous work mainly emphasized how to advance the support or the amine to improve CO_2 capture performance. There are few strategies to resolve the kinetic barrier for CO_2 inner diffusion. Very recently, Wang et al.[44] proposed a new method to overcome the limitation of the CO_2 kinetic diffusion, which could improve in CO_2 capture performance. They introduced CO_2-neutral surfactant into PEI to create extra CO_2 transfer pathways that could facilitate CO_2 diffusion into the deeper PEI films (Figure 2).[44] Consequently, the sorbents offered more reactive sites and higher utilization efficiency of amine groups, leading to a dramatically enhanced CO_2 dynamic capacity and total capacity. Due to the enhanced CO_2 diffusion, the sorbents could work at room temperature with very good performance. At 30 °C, the surfactant-promoted sorbents achieved a CO_2 capture capacity as high as 3.2 mmol g^{-1} with amine utilization over 50%. Moreover, the surfactant-promoted sorbents also exhibited much better sorption kinetics and regeneration performance. This study provides a cost-efficient and general approach to designing CO_2 solid sorbents with high performance.[44]

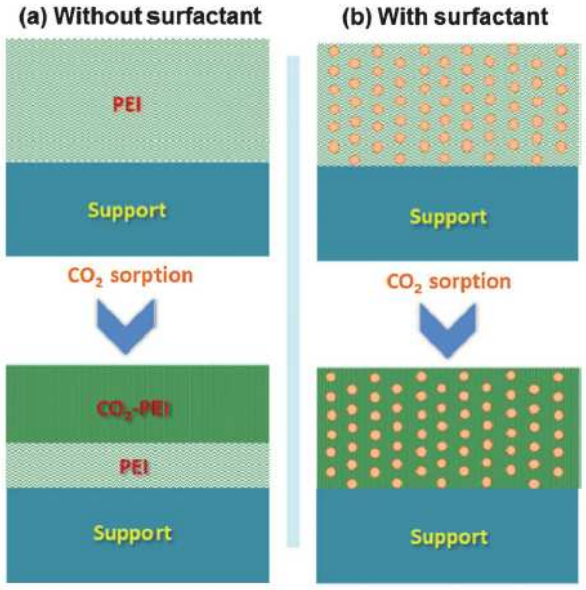

Figure 2. Schematic illustration of the CO_2 sorption process over

the PEI loaded hierarchical porous silica with and without surfactant. [44]

2.2 Carbon-based adsorbents

As mentioned in our previous review paper, carbon-based materials are considered as one of the most promising adsorbents for CO_2 capture,[45] because of their low cost, high surface area, high amenability to pore structure modification and surface functionalization, and relative easiness for regeneration. However, the CO_2 adsorption on carbon materials is "physical" and weak, which makes these adsorbents sensitive to temperature and relatively poor in selectivity. The CO_2 sorption capacity drops dramatically at temperatures associated with power plant flue gas (50–120 ^oC).[46] Prior to 2011, the research activities on carbon-based CO_2 adsorbents were mainly focused on (1) increasing the surface area and tuning the pore structure, and (2) increasing the alkalinity by surface modifications.[9] From 2011 to 2014, continuous efforts have been made to improve the CO_2 adsorption capacity of the carbon-based adsorbents via investigating (1) the quantative influence of the particle shape, size, and pore structure, (2) surface modification via N-doping, amine modification, oxidation, fluorination, and modification with metal oxide, etc., and (3) synthesis of carbon-based hybrid composites.

It is widely agreed that the pore structure and pore size of carbon-based materials can influence their CO_2 capture capacity. Jiménez et al.[47] studied the CO_2 sorption behaviors of several types of carbon nanofibers (platelet, fishbone, and ribbon) and amorphous carbon at 26 ^oC. The results showed that the lower the graphitic component content or the higher the amorphous carbon content in the carbon materials is, the higher the CO_2-sorption capacity will be. Sevilla et al.[48] summarized the CO_2 adsorption capacities of various carbonaceous materials measured at 25 ^oC and 1 bar. As anticipated, the CO_2 adsorption capacity is strongly correlated with the content of narrow carbon nano- and micropores. Lee et al.[49] and Wickramaratne et al.[50] also reported similar results. Therefore, design of carbon adsorbents with high volume of small micropores should be essential for achieving high CO_2 uptake under ambient conditions. Marco-Lozar et al.[51] found that for low CO_2 pressure, the sorbent should have the maximum possible volume of micropores smaller than 0.7 nm. However, the sorbent requires the maximum possible total micropore volume when the capture is performed at high CO_2 pressure. In addition, novel synthesis techniques for preparation of highly efficient carbon-based CO_2 adsorbents are of great interest. For example, Robertson et al.[52] reported a very simple method for the formation of carbon aerogels followed with activation to generate carbon materials with very attractive CO_2 storage capacity (2.7–3.0 mmol g^{-1} at 25 ^oC, 1 bar). Wang et al.[53] reported the synthesis of a series of porous carbons with adjustable high surface areas and narrow micropore size distributions by activation of fungi-based carbon sources with KOH. The resulting porous carbons demonstrated both high CO_2 uptake (5.5 mmol g^{-1}) and high CO_2/N_2 selectivity (27.3) at 0 ^oC and 1 bar.

Many works have proven that the CO_2 capture capacity of activated carbons can be significantly increased by introducing nitrogen functional groups into their structures.[46, 54-60] Nitrogen-containing carbons can be prepared directly from the carbonization of nitrogen-rich chemical precursors, polymers, and ionic liquids, etc. Up to date, various N-doped carbons have been prepared from nitrogen containing small molecules such as dicyandiamide,[61] chitosan, [62] and HNO_3,[63] with a CO_2 uptake of 3.2, 3.9, and 4.3 mmol/g, at 25 ^oC, 1 bar, respectively. In addition, some nitrogen containing polymers such as porous polyimine[64], polypyrrole[65-67], and co-polymerized acrylonitrile and acrylamide,[67] etc have also been used as precursors and the resulting N-doped carbons showed a CO_2 uptake of 5.3 mmol g^{-1} (0 ^oC), 6.2 mmol g^{-1} (0 ^oC), and 3.8 mmol g^{-1} (25 ^oC) at 1 bar, respectively. Sethia et al.[68] synthesized N-doped carbon by carbonization of an ionic liquid and found that it possessed a CO_2 capture capacity of 3.2 mmol g^{-1} at 25 ^oC and 1 bar. Furthermore, such N-doped porous carbons exhibited high CO_2 adsorption rates and good selectivity for CO_2/N_2 separation, and high feasibility for regeneration.[69]

Incorporation of amine groups is also widely used for surface modification. Generally, the modification with amines can be carried out in two ways: (1) impregnation supports using a liquid amine polymer such as PEI, TEPA or DEA,[70-76] and (2) grafting with amino groups.[77-80] In these amine-supported systems, amine-functionalities are dispersed inside the pores of a mesoporous support material, and thereby produce enhanced CO_2 capture performance relative to that of the bulk amines. Among all the studied amines, PEI, which was first used in CO_2 capture by Satyapal et al.[73] to improve CO_2 removal in space aircraft applications, seems to be the most effective one owing to its high adsorption capacity and good cycling stability.[73] For this reason, there are many reports on using PEI to modify carbon materials for enhanced CO_2 capture. [81, 82] For such amine loaded adsorbents, the total pore volume, especially the meso-plus-macro-pore volume, plays a crucial role in determining the CO_2 sorption capacity.[81] In addition to nanoporous carbon, mesoporous carbon materials have also attracted great attention due to their suitability for surface amine doping.[83] Wang et al.[83] reported that, by loading PEI on a well-developed mesoporous carbon, the CO_2 uptake could be increased to 4.82 mmol g^{-1} in 15% CO_2/N_2 at 75 °C.

Amine groups can also be chemically bound to carbon matrix via grafting. Comparing with those introduced by impregnation, the grafted functional groups are more stable or not desorbed during regeneration. For this reason, CO_2 capture on amine-group grafted carbons has been well studied, and most of relating works prior to 2011 were reviewed by Houshmand et al.[84] As reported, amino compounds such as diamines, polyamines, aminosilanes, halogenated amines, and polyaniline (PANI)[85] were grafted onto the surface of carbon materials. It was concluded that a suitable amine compound should be selected based on the type of porosity and type of functional groups most available on the surface. In the past 3 years, the studied amines grafted on carbons include mainly ethylenediamine, diethylenetriamine, tris-(2-aminoethyl)amine, tri-ethylenetetramine,[86] 2-chloroethylamine,[87] (3-aminopropyl)triethoxysilane,[88] etc.

Apart from the above discussed nitrogen doping and amine modification, there are other treatments such as oxidation,[89] fluorination,[90, 91] and modification with metal oxides, etc, for carbon materials. Oxygen functional groups, such as carbonyls, alcohols and ethers, contain an electron-donating oxygen atom that can also participate in electrostatic interactions with CO_2. It is thus expected that the presence of oxygen functional groups on the carbon surface will enhance CO_2 adsorption capacity and selectivity.[89] Plaza et al.[89] found that the oxygen content could be significantly increased from 1.4 wt% up to 15.9 wt% by liquid and gas phase oxidation treatments, and resulted in a greater CO_2 uptake. Oxidation treatment is therefore proposed as a plausible modification technique for developing easy-to-regenerate carbon adsorbents with enhanced CO_2 capture performance. Fluorination method has received a substantial attention because of its potential for uniform modification, short reaction time, low cost, and high efficiency. Fluorination causes defects, changes surface properties, and increases the total number of basic sites with varying degrees of basicity on carbon materials.[91] Bai et al.[90] investigated the influence of oxyfluorination on activated carbon nanofibers for CO_2 storage and found that the CO_2 adsorption efficiency of oxyfluorinated activated carbon nanofibers improved around 16 wt% due to the semi-ionic interaction effect of surface modificated oxygen functional groups with CO_2 molecules. Up to date, many metal oxides including NiO,[92] CuO,[93, 94] and MgO have been doped or loaded on carbon materials to further improve the CO_2 capture capacity. However, one major problem for the metal oxides modified carbon adsorbents is that the enhancement of CO_2 capture capacity is still too moderate, and it seems more works are desired to draw a conclusion whether this type of materials is promising for practical applications or not.

The third major method for improving the CO_2 capture performance of carbon-based materials is making hybrid composites. Up to date, three types of hybrid materials have been reported, which are (1) carbon/MOF,[95] (2) carbon/carbon,[91] and carbon/carbon nitride,[96] etc. For instance, Kong et al.[96] synthesized a composite by growing CNTs on the active ACF via chemical vapor deposition method, and the composite was further modified by branched PEI. The CO_2 adsorption tests proved that the micro-nano composite showed an equilibrium adsorption amount of 1.5 mmol g^{-1}, higher than that of pristine ACF (1.0 mmol g^{-1}). It is believed that the combination of the unique hollow and tubular structure of the CNTs with the micro-nano phase of ACF contributed to the good CO_2 capture property. Carbon-based adsorbents and their CO_2 capture performance are summarized in Table 1.

Table 1. Summary of carbon-based adsorbents and their performance in CO_2 capture.

Carbon type	Surface modification	CO_2 uptake	Reference
Carbon nanofibers	Nil	16.36 mmol g^{-1} at 26 °C, 8 bar	47
Carbonaceous materials	Nil	6.6 mmol g^{-1} at 0 °C, 1 bar	48
Activated carbon fibers	Nil	5.68 mmol g^{-1} at 25 °C, 1 bar	49
Carbon spheres	Nil	8.9 mmol g^{-1} at 0 °C, 1 bar	50
Carbon aerogels	Nil	3.0 mmol g^{-1} at 25 °C, 1 bar	52
Porous carbons	KOH activation	5.5 mmol g^{-1} at 0 °C, 1 bar	53
N-doped mesoporous carbons	N-doped	3.2 mmol g^{-1} at 25 °C, 1 bar	61
N-doped porous carbons	N-doped	3.86 mmol g^{-1} at 25 °C,1 bar	62
N-doped porous carbons	N-doped	4.30 mmol g^{-1} at 25 °C, 1 bar	63
N-doped porous carbon	N-doped	5.60 mmol g^{-1} at 0 °C, 1 bar	97
N-doped porous carbons	N-doped	5.26 mmol g^{-1} at 0 °C, 1 bar	64
N-doped porous carbons	N-doped	6.2 mmol g^{-1} at 0 °C, 1 bar	65
N-doped porous carbons	N-doped	2 mmol g-1 at 25 °C, 1 bar	66
N-doped porous carbons	N-doped	3.8 mmol g-1 at 25 °C, 1 bar	67
Commercial carbon	PEI modified	3.5 mmol g^{-1} at 75 °C and 1 bar	81
Nanoporous carbon	PEI modified	1.09 mmol g^{-1} at 75 °C, 1 bar	82
Mesoporous carbons	PEI modified	4.82 mmol g^{-1} at 75 °C, 1 bar	83
Activated carbons	TREN, TETA modified	1.96 mmol g^{-1} at 25 °C, 1 bar	86
MWCNTs	APTES modified	1.7 mmol g^{-1} at 60 °C, 1 bar	88
MWCNTs	PANI modified	11.7 mmol.g^{-1} at 25 °C, 11 bar	85

Phenolic-resin-derived carbon	oxidation	2.9 mmol.g^{-1}at 25 ^{o}C, 1 bar	[89]
Carbon nanofiber	oxyfluorination	3.68 mmol.g^{-1} at 0 ^{o}C and 1 bar	[90]
Porous carbon	loaded CuO	0.30 mmol g^{-1} at 25 ^{o}C and 1 bar	[93]
Activated carbon	loaded NiO	2.23 mmol g^{-1} at 25 ^{o}C, 1 bar	[92]
MWCNTs/MIL-101	Nil	1.35 mmol g^{-1} at 25 ^{o}C, 10 bar	[95]
CNTs/phenolic resin	Nil	1.2 mmol g^{-1} at 25 ^{o}C, 1.5 bar	[91]
CNTs/ACF	PEI modified	2.75 mmol g^{-1} at 60 ^{o}C, 1 bar	[96]
Mesoporous carbon nitrides	Nil	2.35 mmol g^{-1} at 25 ^{o}C, 1 bar	[97]

2.3 Graphite/graphene-based adsorbents

Graphene is a type of synthetic carbon allotrope which has many superior properties and received tremendous attention in recent years. Although graphite/graphene is generally classified into carbon materials, in order to highlight the rapidly growing research interests in graphite/graphene-based CO_2 adsorbents, we separately summarize the relating work as a new section in this review paper. Prior to 2011, there is no any report on using graphite/graphene for CO_2 capture. However, owing to the high specific surface area and the lowered production cost, many efforts have been made to explore their application in CO_2 capture since 2012. In general, the studies on graphite/grapheme-based materials for CO_2 capture are mainly focused on three aspects, including (1) exfoliation or new structures, (2) surface or edge functionalisation, and (3) synthesized hybrid materials.

To date, several methods have been used to obtain a high specific surface area for graphene, including heat treatment at high temperatures under vacuum condition.[98-103] Modifications of graphene oxide layers with hydroxyl and epoxy surface functional groups employing both organic and inorganic compounds can increase the interlayer spacing of graphene oxide layers.[100] Although the chemical modification and reduction approach can remove most of the oxygen atoms from the surface of graphene oxide, some remaining oxygen atoms and additional functional groups introduced during the chemical modification or reduction may cause the scattering of electrons, which reduces the structural and thermal stability. In addition, these methods are highly costly and energy intensive for large-scale preparation. Meng et al.[104] found that exfoliated graphene nanoplate was highly efficient for CO_2 capture. The exfoliated graphene nanoplates could be expanded from graphite oxide by a low-heat treatment at temperatures ranging from 150 to 400 ^{o}C under vacuum conditions. The effects of the interlayer spacing of the graphene layers and pore structure on the CO_2 capture capacities were studied as a function of the processing conditions. The prepared graphene nanoplates exhibited high CO_2 capture capacities, up to 56.4 mmol g^{-1}, at 25 ^{o}C and 30 bar. The improved CO_2 capture capacity of the graphene nanoplates was attributed to the larger inter-layer spacing and higher interior void volume.[104]

Graphene and graphitic nanoribbons possessing different types of carbon hybridizations exhibit different chemical activity. In particular, the basal plane of the honeycomb lattice of nanoribbons consisting of sp^2-hybridizedcarbon atoms is chemically inert. Interestingly, their bare edges could be more reactive as a result of the presence of extra unpaired electrons, and for multilayer graphene nanoribbons, the presence of terraces and ripples could introduce additional chemical activity.[105] Asai et al.[105] observed a remarkable irreversibility in adsorption of CO_2 (0.26 mmol g^{-1}) on graphitic nanoribbons at ambient temperature, which is distinctly different from the behavior of nanoporous carbon and carbon blacks. The irreversible adsorption of CO_2 is due to the large number of sp^3-hybridized carbon atoms located at the edges.

Graphite has not only properties similar to that of carboneous adsorbents but also the economic advantage of low cost, thus it is considered as a potential CO_2 adsorbent. However, graphite has a weak affinity towards CO_2 and a low surface area, which limit the CO_2 adsorption ability.[101] To overcome these limitations, Hong et al.[106] modified the surface of graphite with amine groups (3-aminopropyl-triethoxysilane, APTS) to increase the basicity, which is favorable for CO_2 adsorption. Graphite showed negligible adsorption ability for CO_2 gas, and graphite oxide had a very low adsorption uptake of 0.074 mmol g^{-1}. However, on the APTS-modified graphite oxide, the CO_2 uptake was significantly increased to 1.16 mmol g^{-1}. The increased basicity appears to be a major factor in enhancing the CO_2 uptake and is related to the amine molecules attached to the surface of the graphite.

Fabrication of graphene-inorganic hybrid materials is another approach to enhancing the CO_2 uptake. Nanoparticles incorporated between graphene sheets effectively prevent the aggregation of the graphene sheets,[107] and the generated high porosity would increase their CO_2 capture performance. By making graphene-Mn_3O_4,[108] graphene/chitosan,[109] graphene/silica,[110] hybrid porous materials, a CO_2 uptake of 2.5, 4.2, and 4.3 mmol g^{-1} at 25 ^{o}C and 1 bar could be achieved, respectively. Mishra et al.[111] prepared Pd decorated graphite nanoplatelets and obtained a CO_2 uptake of 5.1 mmol g^{-1} at 25 ^{o}C and 11 bar. It was concluded that the greater affinity of CO_2 molecules towards Pd nanoparticles is responsible for the increased CO_2 adsorption capacity. Graphite/graphene-based adsorbents and their CO_2 capture performance are summarized in Table 2.

Table 2. Summary of graphite/graphene-based adsorbents and their performance in CO_2 capture.

Schemes	Materials	CO_2 uptake	References
Exfoliation or new structures	graphene nanoplate	56.36 mmol g^{-1} at 25 ^oC, 30 bar	104
Surface or edge functionalisation	graphitic nanoribbons	0.26 mmol g^{-1} at 30 ^oC, 1 bar	105
	graphite	1.16 mmol g^{-1} at 30 ^oC, 1 bar	106
Hybrid materials	graphene-Mn_3O_4	2.50 mmol g^{-1} at 25 ^oC, 0.8 bar	108
	Palladium-graphite nanoplatelets	5.10 mmol g^{-1} at 25 ^oC, 11 bar	111
	graphene-based mesoporous silica	4.32 mmol g^{-1} at 75 ^oC, 1 bar	110
	chitosan-graphene oxide	4.15 mmol g^{-1} at 25 ^oC, 1 bar	109
	polyindole-reduced GO	3 mmol g^{-1} at 25 ^oC,1 bar	112

2.4 Zeolite-based adsorbents

The CO_2 adsorption mechanism on zeolites has been revealed that the physisorption of CO_2 by an ion–dipole interaction or strongly bound carbonate species by bi-coordination.[9] Although zeolites have shown promising results for separating CO_2 from gas mixtures and can potentially be used in the pressure swing adsorption (PSA) process, in general their selectivity for CO_2 over other gases (N_2, CH_4, H_2O, etc.) is still low, and their adsorption capacities rapidly decline with increasing temperature above 30 ^oC and become negligible above 200 ^oC. Previously, we outlined the work on improving the CO_2 capture performance of the zeolite-based CO_2 sorbents in three aspects, including (1) changing the composition and structure of framework, (2) cationic exchange, and (3) zeolite purity. During 2011-2014, more papers have been published in this field, and we noticed that the researches are more focusing on the former two aspects. There is no much work continued in zeolite purity. In addition, researchers started to modify the existing zeolites by either impregnating or grafting various amines to further increase the CO_2 capture capacity. Making zeolite-based hybrid materials is another research direction in this field. A brief summary of research activities of zeolite-based CO_2 sorbents is illustrated in Figure 3.

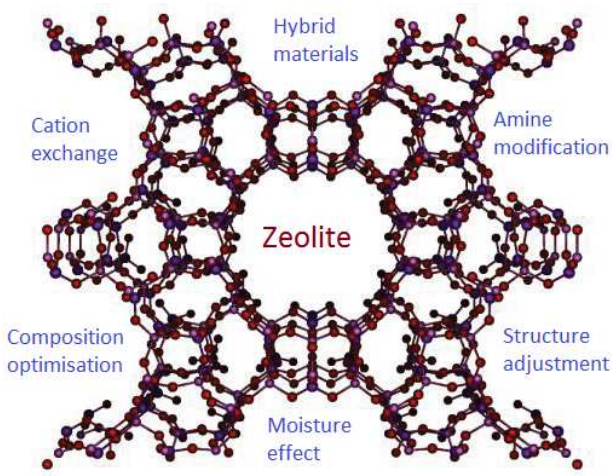

Figure 3. A brief summary of research activities on zeolite-based CO_2 adsorbents.

Prior to 2011, zeolites that were studied included X,[113-115] Y,[116, 117] A,[118] β,[119] ZSM,[120, 121] CHA,[122] FER,[123] and natural zeolites (e.g. ZAPS, ZNT, ZN-19).[124] Among them, zeolite 13X attracted more attention than others.[125-127] In addition, some new zeolites have also been studied, e.g., SAPO-34,[128, 129] SSZ-13,[130] and Rho,[131] etc. For instance, Hudson et al.[130] reported both acidic and copper exchanged forms of SSZ-13, a zeolite containing an 8-ring window, as CO_2 adsorbents. The maximum CO_2 uptake at 1 bar for Cu-SSZ-13 and H-SSZ-13 was 3.75 mmol g^{-1} and 3.98 mmol g^{-1}, respectively. At low CO_2 loadings, the gas molecules preferentially occupy the A-sites located in the center of the 8-ring window (Figure 4). With increasing the CO_2 loading per Cu^{2+}, the CO_2 molecules start to take the end-on CO_2 coordination with Cu^{2+} and occupy at B-sites. Such CO_2 binding mode is believed to be the reason for its high selectivity of CO_2/N_2. Besides the synthesis of novel zeolites for CO_2 capture, methods including controlling the Al distribution[132] and expanding the pore size,[133] etc. are also used to improve the CO_2 capture performance. Nachtigall et al.[132] proved that not only the accessibility of Bronsted sites but also the homogeneity of Al distribution in the FER zeolite could be tuned, which resulted in a new zeolite adsorbent exhibiting a constant heat of CO_2 adsorption. Loganathan et al.[133] reported that the average pore size could be expanded from conventional values of 9–10 nm to as large as ~30 nm, which is favorable for amine tethering.

Another important strategy for improving the CO_2 capture performance of zeolite is cationic exchange. The cations influence the electric field inside the pores as well as the available pore volume, and provide a convenient mean for tuning adsorptive properties of these porous materials. Both Walton et al.[134] and Ridha et al.[135] reported that Li^+ provides the highest CO_2 capture capacity among all the univalent cations. Very recently, Lozinska et al.[136] performed a comprehensive study by preparing a series of univalent cation forms of zeolite Rho ($M_{9.8}Al_{9.8}Si_{38.2}O_{96}$, M = H, Li, Na, K, NH_4, Cs) and ultrastabilized zeolite Rho (US-Rho). The highest uptakes at 0.1 bar, 25 ^oC for both Rho and ZK-5 were obtained on the Li-forms

(Li-Rho, 3.4 mmol g^{-1}; Li-ZK-5, 4.7 mmol g^{-1}). Besides univalent cations, some divalent cations such as Mg^{2+}, Ca^{2+}, Sr^{2+} exchanged zeolites have also been investigated. Bae et al.[137] compared a series of Na^+, Mg^{2+}, and Ca^{2+} exchanged A and X zeolites, and found that Ca-A exhibited the highest CO_2 uptake (3.72 mmol g^{-1}) together with an excellent CO_2 selectivity over N_2. A detailed study of CO_2 adsorption kinetics further showed that the performance of Ca-A was not limited by the slow CO_2 diffusion within the pores. Lee et al.[138] compared the Mg^{2+} and Ca^{2+} exchanged 13X with the Li^+ and K^+ exchanged samples, and found that the CO_2 capture capacity followed the order of $Ca^{2+} > Mg^{2+} > Li^+ > K^+$. Arévalo-Hidalgo et al.[139] reported that by cation exchanging of SAPO-34 with Sr^{2+}, the overall CO_2 adsorption performance could be improved in a remarkable fashion as well. Recently, Hong et al.[140] studied the CO_2 capture performance of cationic exchanged CHA and 13X under high pressure and moderate temperature conditions. The CO_2 adsorption capacity increased in the following order: CaCHA > LiCHA > 13X > NaCHA > MgCHA at 200 °C. The introduction of mesopores in CHA was effective in increasing the CO_2 capture capacity under high pressure conditions. Zeolite 13X was effective as a support material for $Mg(OH)_2$ used in CO_2 capture via carbonation under pre-combustion conditions (20 bar and 200 °C), leading to the full utilization of $Mg(OH)_2$ for CO_2 capture approaching the theoretical maximum (1.42 mmol g^{-1}).

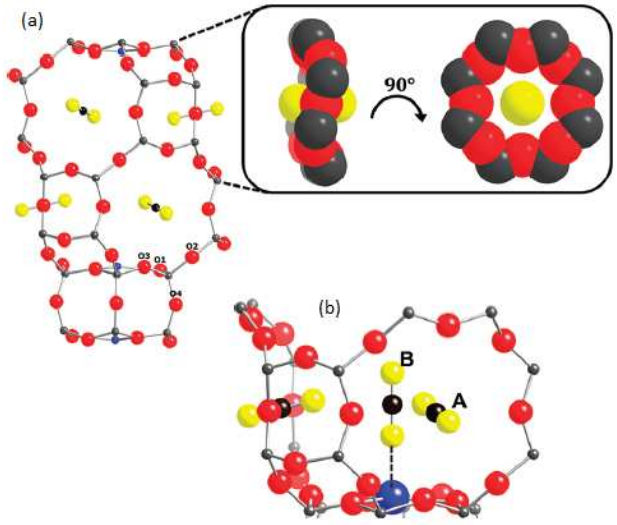

Figure 4. (a) CO_2 adsorption site of Cu-SSZ-13 at 4 K for one complete CHA cage. (b) Cut-away view of the CHA cage showing the primary (A) and secondary (B) CO_2 adsorption sites (black, carbons; yellow, oxygens) for the highest CO_2 dosing.[130]

Recently, one of the active research activities with zeolite is modification with amine groups, either by co-condensation, impregnation or grafting. The amine modified zeolites for CO_2 adsorption had been earlier reported by impregnation method such as zeolite Y,[141] 13X,[142] ZSM-5,[143] A,[144] and SBA-15.[145] Singh et al.[146] observed that the increasing number of nitrogen in the alkyl chain amine group led to the enhanced CO_2 absorption capacity, and the highest absorption capacity was found for TEPA modified zeolite. Su et al.[141] showed that the CO_2 uptake of TEPA treated Zeolite Y was 2.61 mmol g^{-1} at 60 °C. However, due to the small pores of zeolite, it is generally difficult to load large amount of amines using impregnation method. Kim et al.[144] reported a new route to produce TEPA modified zeolite A by embedding method, in which TEPA molecules were directly introduced into the zeolite A precursor gel. The optimum CO_2 adsorption capacity was found in the case of 7.5% TEPA embedded zeolite A, which was 3.75 mmol g^{-1}, much higher than neat zeolite A (2.88 mmol g^{-1}).

To overcome the low thermal stability problem of the adsorbents impregnated with amine, grafting aminosilanes through silylation onto the intrachannel surface of the mesoporous silica has been proposed. In general, the amine-grafted adsorbents exhibited a comparatively higher adsorption rate and higher stability in cyclic runs than the amine-impregnated adsorbents.[147] Chang et al.[148] investigated 3-aminopropyltriethoxysilane (APS) grafted MCM-41, SBA-15, and pore expanded-SBA-15, and found that SBA-15 was the most appropriate support because its pore size could accommodate more amines and avoid blocking CO_2 adsorption. Moreover, its high pore surface area provided a large number of silanol groups, which was more beneficial for aminosilane grafting. Serna-Guerrero et al.[149, 150] synthesized amine-modified MCM-41 and pore-expanded MCM-41 (PE-MCM-41) for CO_2 capture and demonstrated that the larger pore diameter and pore volume of PE-MCM-41 resulted in a higher CO_2 adsorption capacity and greater dynamic adsorption performance than those of MCM-41. The loading and distribution of the introduced amines in zeolites are the two key parameters determining the CO_2 capture performance. Since they are often influenced by the synthesis method, Sanz et al.[151] prepared amino-functionalized SBA-15 materials via co-condensation, grafting and impregnation method respectively, and found that a considerable organic loading was achieved for the grafted sample, in which amino groups were mainly located inside pore channels, thus favouring CO_2 diffusion through the whole structure.[151] Recently, Jing et al.[145] prepared a series of SBA-15 adsorbents grafted with dendritic polyamine including melamine-based ethylene diamine (ED) dendrimers, diethylenetriamine (DETA) dendrimers, triethylenetetramine (TETA) dendrimers, and acrylate-based ED dendrimers. They found that the primary amines were the active groups within all adsorbents and the branched dendrimers could weaken diffusion resistance of CO_2 adsorption. Zeolite-based hybrid material such as SBA-3/cotton fiber composite has also been studied for enhanced CO_2 capture.[152]

As discussed in our previous review paper, in practical applications, moisture is another challenge to zeolite-based adsorbents, since it may compete with CO_2 for the active adsorption sites. Gallei et al.[153] reported that the physical adsorption of CO_2 on CaY- and NiY-zeolite is scanty in the presence of water, because water is preferentially adsorbed onto these surfaces. Later Rege et al.[154] and Brandani et al.[155] observed that H_2O has a strong effect on CO_2 adsorption on type X zeolites. From a thermodynamic viewpoint, the adsorption of CO_2 in the

presence of H_2O is not favored.[156] However, Diaz et al.[116] found that the CO_2 adsorption on Cs- and Na-treated Y zeolites was increased after water treatment, and believed that it was due to the enhanced Brønsted acidity in zeolites after treatment with alkali. In addition, H_2O may have a detrimental effect on the stability of zeolite frameworks. In the presence of CO_2, the acidic conditions may cause dealumination of the zeolite structures, leading to a partial or total destruction of the framework.[157, 158] In general, it is accepted that moisture in the gas flow causes significant decreases in CO_2 adsorption capability as well as in the lifetime of the adsorbents. Zeolite-based adsorbents and their CO_2 capture performance are summarized in Table 3.

Table 3. Summary of zeolite-based CO_2 adsorbents and their performance in CO_2 capture.

Schemes	Materials	CO_2 uptake	References
Structure and composition adjustment	Cu-SSZ-13	3.8 mmol g^{-1} at 25 °C, 1 bar	130
	H-SSZ-13	4.0 mmol g^{-1} at 25 °C, 1 bar	130
		1.2 mmol g^{-1} at 30 °C, 1 bar	133
Cation exchange	Li-Rho	3.4 mmol g^{-1} at 25 °C, 0.1 bar	136
	Li-ZK-5	4.7 mmol g^{-1} at 25 °C, 0.1 bar	136
	Ca-A	3.7 mmol g^{-1} 40 °C 0.15 bar	137
	Zeolite Ca	1.6 mmol g^{-1} at room temperature, 1 bar	138
	Sr^{2+}-SAPO-34	3.0 mmol g^{-1} at 25 °C, 1 bar	139
	CHA and 13X	1.4 mmol g^{-1} at 200 °C, 20 bar	140
Amine modification	TEPA modified zeolite Y	2.6 mmol g^{-1} at 60 °C, 1 bar	141
	TEPA modified zeolite A	3.8 mmol g^{-1} at 25 °C, 1 bar	144
	G-SBA-15-NNN-(10)	2.2 mmol g^{-1} at 40 °C, 4.5 bar	151
Hybrid materials	SBA-3/cotton fiber	2.4 mmol g^{-1} at 75 °C, 1 bar	152

2.5 MOF-based adsorbents

Metal organic frameworks (MOFs), which are constructed from transition metal ions and bridging organic ligands, are a new family of porous materials.[159] Great progress in MOFs-based CO_2 adsorbents has been achieved during the past several years, but new discoveries are still being made constantly as the field is growing quickly.[160-164] Liu et al.[160] wrote a nice review paper on the recent advances in CO_2 adsorption, storage, and separation by MOF. They also discussed some of the important properties of MOF adsorbents that may be crucial for practical applications but are largely overlooked by researchers so far. Zhang et al.[165] briefly reviewed the effect of multifunctional sites on the adsorption capacity and selectivity. Prior to 2011, most efforts were made to increase their CO_2 capture capacity and selectivity by modifying the metal ions and/or organic linkers in MOFs.[9] In the past three years, continuous efforts have been paid to MOFs based-CO_2 adsorbents. However, apart from the modification of metals sites and organic linkers in MOFs, it seems more attention has been paid to (1) novel MOF structures, (2) metal ions doping, (3) functionalization, (4) hybrid materials, and (5) water effect on the structure and stability, etc. More details will be given below.

One important strategy for enhancing the CO_2 capture capacity and selectivity of MOFs is to remove the terminal bound solvent molecules to make the coordinately-unsaturated metal centres exposed. These coordinately unsaturated metal centres act as physisorptive sites for CO_2 molecules enhanced by ion induced dipole interactions,[166] thus efforts have been made to understand the effect of various metals. Caskey et al.[167] studied a family of materials known as MOF-74:M_2(DOBDC) (M = Mg, Co, Ni; DOBDC = 2,5-dioxy-1,4-benzenedicarboxylate). It was found that the coordinately-unsaturated metal centres within the framework of Mg_2(DOBDC) and Ni_2(DOBDC) were the initial sites of interaction with CO_2, and the CO_2 adsorption isotherms measured at different temperatures revealed that the strength of the initial interaction followed the order of Mg > Ni > Co. Wade et al.[168] investigated $M_3(BTC)_2$ isostructural series (M = Cr, Fe, Ni, Zn, Ni, Cu, Mo) and gained insight into the impact of CO_2-metal interactions on CO_2 storage/separation. It was found that in this series the heat of adsorption varied as Ni > Ru > Cu > Mo ≈ Cr. The difference observed among various metals of the series supports the notion that metal identity affects the strength of the initial framework–CO_2 interaction. Notably, $[Ru_3(BTC)_2]$-$[BTC]_{0.5}$, which bears a higher formal charge on the dimetal unit than the other isostructural MOFs, exhibited a slightly higher CO_2 adsorption enthalpy than the Cr, Cu, and Mo analogues. It was attributed to the formation of stronger electrostatic interactions between CO_2 and the Ru_2^{5+} sites. Similarly, Cu-based MOFs (Cu_2(dhtp)), which are structurally homologous to the honeycomb-like M_2(dhtp) series and lanthanide MOFs $(La(BTB)(H_2O)\cdot 3DMF)_n$ have also been prepared for CO_2 capture.[169, 170]

The CO_2 capture performance of MOFs can also be improved by selecting proper organic linker, which can either increase the porosity and specific surface area or provide extra adsorbing sites. For instance, recent studies showed that replacing the phenyl spacers of organic linkers with triple-bond spacers could effectively boost the molecule-accessible surface areas of MOFs and related high-porosity materials.[171, 172] Zheng et al.[173] designed an expanded 4,4-paddlewheel-connected porous MOF-505 analogue from a nanosized rectangular diisophthalate linker containing alkyne groups. The synthesized NJU-Bai12 exhibited excellent CO_2 uptake capacity (23.83 and 19.85 mmol g^{-1} at 20

bar for 0 and 25 °C, respectively) and selective gas adsorption property with a CO_2/CH_4 selectivity of 5.0 and CO_2/N_2 selectivity of 24.6 at room temperature. Park et al.[174] constructed a multi-functional MOF PCN-124 from Cu paddle wheel motifs and a judiciously designed novel ligand bearing carboxylate, pyridine, and amide groups.[174] The open metal sites and amide groups were expected to increase the interaction between the adsorbed CO_2. It has been reported that MOFs constructed from flexible organic components, even if they do not adsorb N_2 and H_2 gases due to the smaller pores of the activated samples than the kinetic diameters of these gases, often selectively adsorb CO_2 since they open the gates for CO_2 that has much higher polarizability (2.51 $Å^3$) and quadrupole moment (1.4×10^{-39} C m^2) than other gases.[175, 176] Hong et al.[177] constructed a MOF (SNU-110) from an organic ligand with flexible joints and found that it exhibited selective CO_2 adsorption over N_2, O_2, H_2, and CH_4 gases. Masoomi et al.[178] synthesized two new three-dimensional porous Zn(II)-based MOFs, containing azine-functionalized pores by using a nonlinear dicarboxylate and linear N-donor ligands. The use of nonfunctionalized and methyl-functionalized N-donor ligands led to the formation of frameworks with different topologies and metal-ligand connectivities and therefore different pore sizes and accessible volumes.

The synthesis of MOFs with different microstructures and morphologies such as 1D tubular,[179] 2D,[180] 3D,[181] and core-shell MOFs,[182] etc. have also attracted great attention for CO_2 capture. Bataille et al.[179] prepared a novel porous tubular 1D-MOF from Cu(II), 1,2-bis(4-pyridyl)ethane and P,P'-diphenyl-diphosphinate by an easy and direct self-assembly process in either needle microcrystal or nanorod form depending on the synthesis conditions. This 1D-MOF compound is comprised of single walled tubules, held together by soft van der Waals interactions (Figure 5). The CO_2 absorption kinetics drastically increased from the micrometric crystals to the nanorods. Yan et al.[180] prepared functionalized 2D MOFs in a tandem manner, which displayed a high thermal stability and moisture resistance. Although their surface areas were moderate, they still had good CO_2 adsorption capacity of 2.9 and 1.9 mmol g^{-1} at 1 bar and 0 and 25 °C, respectively, comparable to that of previously reported MOFs with much higher surface areas. Li et al.[182] designed a core−shell MOF comprising a porous bio-MOF-11/14 mixed core and a less porous bio-MOF-14 shell. The resulting core−shell material exhibited 30% higher CO_2 uptake than bio-MOF-14 and low N_2 uptake in comparison to the core. When the core−shell architecture was destroyed by fracturing the crystallites via grinding, the amount of N_2 adsorbed was doubled but the CO_2 adsorption capacity remained the same. Finally, the more water stable bio-MOF-14 shell serves to prevent the degradation of the water-sensitive core in aqueous environments.

The nonframework ions in an ionic MOF can be exchanged with other metal ions. In order to know how different nonframework ions would affect gas adsorption and separation, a molecular simulation study was performed for CO_2 adsorption in rho-ZMOF exchanged with a series of cations (Na^+, K^+, Rb^+, Cs^+, Mg^{2+}, Ca^{2+}, and Al^{3+}). The isosteric heat and Henry's constant at infinite dilution increases monotonically with increasing charge-to-diameter ratio of cation ($Cs^+ < Rb^+ < K^+ < Na^+ < Ca^{2+} < Mg^{2+} < Al^{3+}$). At low pressures, cations act as preferential adsorption sites for CO_2 and the capacity follows the charge-to-diameter ratio. However, the free volume of framework will become predominant with increasing pressure and Mg-rho-ZMOF appears to possess the highest saturation capacity. Furthermore, the adsorption selectivity of CO_2/H_2 mixture will increases as $Cs^+ < Rb^+ < K^+ < Na^+ < Ca^{2+} < Mg^{2+} \approx Al^{3+}$. This work suggests that the performance of ionic rho-ZMOF can be tailored by cations. Xiang et al.[183] also demonstrated that the CO_2 capture capacity of MOF can be improved by doping certain amount of Li^+. Recently, Li et al.[184] prepared a Zn doped Ni-ZIF-8 nanocomposite with high stability and good CO_2 capture performance (4.25 mmol g^{-1} at 0 °C and 1 bar).

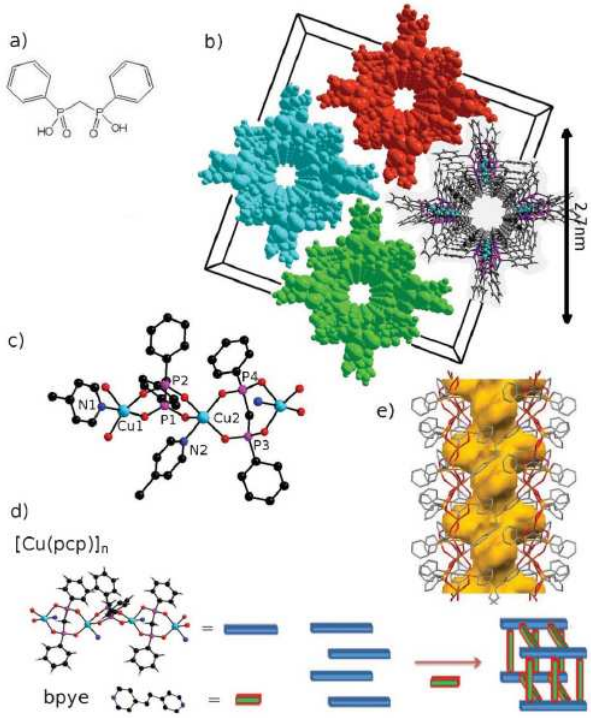

Figure 5. (a) Schematic drawing of the P,P9-diphenyl-diphosphinic acid (H_2 pcp); (b) view of the tubes of 1 packing perpendicular to the c axis (right). Solvent water molecules have been removed for the sake of clarity. The separation of the tubes is enhanced with respect to the real crystal structure in order to highlight the discrete 1D units; (c) a portion of the structure of 1 showing the copper coordination and the pcp bridging mode; (d) schematic representation of the building up of the tube where the blue lines are the pillar $[Cu(pcp)]_n$ polymer connected by bipyridines(green segments). Color code: Cu = light blue, P = purple, O = red, N =blue; (e) a single tube viewed along the c axis. The yellow surface inside is the solvent accessible volume.[179]

For MOFs-based CO_2 adsorbents, one problem is that their CO_2 adsorption capacities are usually not fully utilized at low pressures, particularly below 0.15 bar. One promising solution to this problem is to modify MOFs with amines, carboxyl groups, or some other polar groups. Up to date, various basic amine groups including EDA,[185] 4-picolylamine, 3-picolylamine,[186] dimethylacetamide,[187] acylamide,[188] PEI,[189] etc. have been employed for the purpose. However, although these basic amine groups seem to interact with acidic CO_2 molecules strongly, the amine-functionalized MOFs are not very successful in CO_2 capture. It is believed that the covalent grafting of amine groups onto the aromatic rings in MOFs cannot significantly enhance the affinity of amino groups to CO_2 because of the electron withdrawing effect of benzene ring; while the incorporation of diamine to the open metal sites of MOFs provides a much better CO_2 capture performance at low pressures. [190, 191] The open metal sites can anchor one end of the diamine groups and leave the other end (alkylamines) available to capture CO_2. Believing that impregnation of poly-alkylamines onto MOFs might afford more active amine groups than diamines and maintain the strong interaction between CO_2 and alkylamine groups, Lin et al.[189] studied the PEI incorporated MOF for CO_2 capture. At 100 wt% PEI loading, the CO_2 adsorption capacity at 0.15 bar reached a very competitive value of 4.2 mmol g^{-1} at 25 ^oC, and 3.4 mmol g^{-1} at 50 ^oC, with a high CO_2/N_2 selectivity up to 770 at 25 ^oC, and 1200 at 50 ^oC.[189] Si et al.[192] reported that the structure transition of flexible MOF (MIL-53) could be adjusted by confinement of BNH_x into MIL-53 channels, which yielded a CO_2 adsorption capacity of 4.5 mmol g^{-1} at 0 ^oC and 1 bar. Recently, Hu et al.[193] synthesized a series of alkylamine tethered MIL-101. Grafting alkylamine onto the exposed Cr_{III} centers offered new binding sites and strong interaction with CO_2 molecules and endowed MIL-101 with dramatically enhanced CO_2 uptake capacity and significantly lowered N_2 uptake capacity at low pressures. The trend of enhancement in CO_2 uptake in terms of tethered alkylamine is DETA > ED ≈ 3,3'-diaminodipropylamine > 1-(2-aminoethyl)piperazine whereas the pristine MIL-101 has the lowest CO_2 uptake at 1 bar. MIL-101-DETA has the highest CO_2 adsorption capacity of 3.56 mmol g^{-1} at 23 ^oC and 1 bar. Xiang et al.[194] incorporated carboxyl groups into the MOF framework by the post-synthetic modification approach. All the obtained MOFs exhibited high CO_2 uptake, e.g., 19.8 mmol g^{-1} at 18 bar. The First-principles calculations validated the experimental observation, suggesting that the polar carboxyl group may outperform aromatic amine functionalities for CO_2 sorption at low pressure. The data also indicated that the aromatic imino group loses affinity toward CO_2 significantly, compared with the aromatic amino group. It was believed that, besides the amino groups, incorporating polar acidic[194] or N-containing[184, 195] functionalities into the porous materials might provide an alternative approach for enhancing CO_2 capture. To fully utilize the MOF pore space effectively and improve gas adsorption capacity, incorporation of some other materials such as graphite oxide[196] or carbon[197] has also been explored.[196]

Another practical issue for MOF-based CO_2 adsorbents is the effect of water. It is generally accepted that both the CO_2 adsorption and the selectivity of MOFs decrease in the presence of water, because water molecules compete with CO_2 for the adsorption sites. Barbarao et al.[198] reported that even with 0.1% water in the CO_2/CH_4 mixture the CO_2/CH_4 selectivity in rho-ZMOF decreases by 1 order of magnitude. Yu et al.[199] evaluated the effect of water on Mg-MOF-74 and found that the CO_2 adsorption capacity decreased by the presence of water molecules linked to coordinatively unsaturated metal sites. In order to improve the water-resistant property, Yang et al.[200] synthesized a water-stable Zr-based MOF containing two carboxylic functions grafted on the organic linkers, which showed great promises for CO_2/N_2 gas mixture separation. It not only showed a very good selectivity, relatively high working capacity, but also high water stability. MOF-based adsorbents and their CO_2 capture performance are summarized in Table 4.

Table 4. Summary of MOF-based CO_2 adsorbents and their performance in CO_2 capture.

Schemes	Materials	CO_2 uptakes	References
Modification of metal sites	$Ni_3(BTC)_2$	3.0 mmol g^{-1} at 40 ^oC, 1 bar	168
Selecting proper organic linker	NJU-Bai12	23.8 mmol g^{-1} at 0 ^oC, 20 bar	173
	PCN-124	9.1 mmol g^{-1} at 0 ^oC, 1 bar	174
	SNU-110	6.0 mmol g^{-1} at -78 ^oC, 1 bar	177
Novel structures	1D-MOF	4.0 mmol g^{-1} at -78 ^oC, 1 bar	179
	2D-MOF	2.9 mmol g^{-1} at 0 ^oC, 1 bar	180
	A core–shell MOF	4.1 mmol g^{-1} at 0 ^oC, 1 bar	182
Metal ions doping	Zn(II)-based MOFs	9.2 mmol g^{-1} at -78 ^oC, 1 bar	178
Functionalisation	MOF with PEI	4.2 mmol g^{-1} at 25 ^oC, 0.15 bar	189
	MIL-53 with BNH_x	4.5 mmol g^{-1} at 0 ^oC, 1 bar.	179
	MIL-101-DETA	3.6 mmol g^{-1} at 23 ^oC, 1 bar	193
	UMCM-1-NH_2-MA	19.8 mmol g^{-1} at 25 ^oC, 18 bar	194
Hybrid	MOF-5/graphite oxide	1.1 mmol g^{-1} at 25 ^oC, 4 bar	196

HCM-$Cu_3(BTC)_2$-3	2.8 mmol g^{-1} at 25 °C, 1 bar	197
Zn doped Ni-ZIF-8	4.3 mmol g^{-1} at 0 °C, 1 bar	199

2.6 Silica-based adsorbents

Owing to its high surface area, large pore volume, narrow pore size distribution, and excellent regeneration stability, silica received considerable research interest on CO_2 capture. According to literature, silica is mainly used as support, on which amines are added for capturing CO_2. Therefore, the research activities on silica-based CO_2 adsorbents are mainly focused on making different types of silicas (silica nanoparticles, silica hollow sphere, silica nanotube, silica fume, mesocellular silica foam, macroporous silica, aerogel, etc.) and choosing proper amine groups.

Because substrates often account for above 90% of the absolute sorbent preparation cost[201-203] and are commercially unavailable, the cost-effective, porous and commercially available silica materials thus have been intensively studied for CO_2 capture in these years. Leal et al.[204] functionalized the surface of silica with aminosilane for CO_2 adsorption. After that, adsorption of CO_2 on the surface of amine-functionalized materials using various techniques, amine molecules and silicas, was conducted.[205] Recently, Du et al.[206] reported that rich amine loaded nano-silica adsorbents could be prepared by using polyacrylic acid (PAA) as a multi-functional bridge, which was firstly immobilized onto the surface of silica nanoparticles. Each carboxylic acid group was subsequently reacted with an amine group of alkylamines, hence plenty of remained amines groups could be coated onto silica nanoparticles. The result indicated that SiO_2–PAA–PEI adsorbent possessed a remarkably high CO_2 uptake of approximately 3.8 mmol g^{-1} at 1 bar and 40 °C. Goeppert et al.[207] reported PEI impregnated fumed silica as a promising candidate for capturing CO_2 from dilute sources, including the air, with a CO_2 capture capacity of 2.4 mmol g^{-1}.

Bai et al.[208] and Yu et al.[205] reported the silica hollow spheres are promising support for loading amines for CO_2 capture as well. By loading 50 wt% of TEPA, a high CO_2 adsorption amount of 4.4 mmol g^{-1} was achieved with bimodal meso-/macroporous SiO_2 hollow sphere. Ko et al.[209] prepared various amines (e.g. primary, secondary, tertiary, di-, and tri-amines) immobilized double-walled silica nanotubes (DWSNTs) for CO_2 capture (Figure 6)[209]. The amines on modified DWSNTs showed high CO_2 capture capacity in the order of tri-, di-, primary, secondary, and tertiaryamines, with the maximum capacity of 2.3 mmol g^{-1}. Liu et al.[210] reported the use of amino-modifed silica fume as CO_2 adsorbent. However, its CO_2 capture capacity was not high, only ca. 1.3 mmol g^{-1}. Zhang et al.[211] prepared PEI loaded mesocellular silica foams with a wide range of pore volumes and pore sizes, which achieved a CO_2 capture capacity of 6 mmol g^{-1} at 85 °C and 1 bar.

For amine-functionalized CO_2 adsorbents, the thermal stability is a severe issue that should be considered for practical applications, especially at high temperatures (>135 °C). To have a clear understanding of the thermal stability and cyclic adsorption capacity of PEI and TEPA loaded silica adsorbents, a detailed study was performed by Zhao et al.[196] At the regeneration temperature of 105 °C over 10 cycles, the CO_2 capacities of four types of amine-functionalized sorbents remained stable, and the masses of the sorbents decreased by 5.1%, 0.6%, 0.2%, and 0.1% with increasing molecular weight of amine, indicating that the PEI-based sorbents had excellent thermal stability. The thermal stability was also studied in a fluidized bed at 140 °C for 100 h. The results indicated that the thermal stability was much improved in the fluidized bed because the atmosphere in the fluidized bed contained amine vapor, thus inhibiting amine evaporation. This effective and simple method was first proposed by Zhao et al.[196] to solve amine evaporation issue by entraining some amine vapor into the reactor.

Another method for improving the thermal stability is to introduce the amine groups via chemical grafting. Leal et al.[204] first reported the chemisorption of CO_2 on APS grafted silica gel. However, the sorbent's CO_2 adsorption capacity was low. Yao et al.[212] synthesized APS or 3-(2-aminoethylamino)-propyl-dimethoxymethylsilane (APMS) grafted mesocellular silica foams, which achieved a CO_2 adsorption capacity of 1.54 mmol g^{-1} with 10% (v/v) CO_2 in N_2 at 60 °C. Liu et al.[213] synthesized new covalently tethered CO_2 adsorbents through the in situ polymerization of N-carboxyanhydride of L-alanine from amine-functionalized macroporous silica. This adsorbent showed a high CO_2 adsorption capacity of 3.86 mmol g^{-1} at 50 °C and 1 bar, and good stability over 120 adsorption-desorption cycles. Silica-based adsorbents and their CO_2 capture performance are summarized in Table 5.

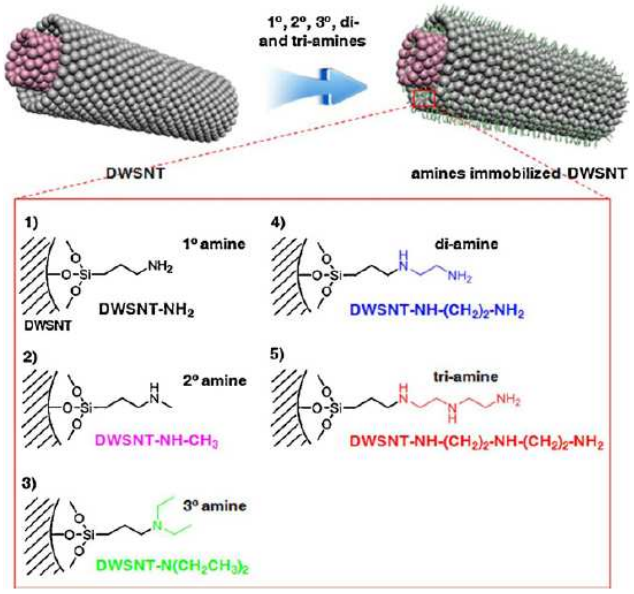

Figure 6. Schematic of primary, secondary, tertiary, di-, and tri-aminosilanes immobilized DWSNTs and their nomenclature.[209]

Table 5. Summary of silica-based CO_2 adsorbents and their performance in CO_2 capture.

Silica types	Surface modifications	CO_2 uptakes	References
Conventional silica	PAA modified	3.8 mmol g^{-1} at 40 °C, 1 bar	206
	PEI modified	2.4 mmol g^{-1} at 25 °C, 1 bar	207
Silica hollow sphere	TEPA modified	4.4 mmol g^{-1} at 110 °C, 1 bar	205
	APTES & BTME modified	1.7 mmol g^{-1} at 0 °C, 1 bar	208
	MCFs PEI modified	6.0 mmol g^{-1} at 85 °C, 1 bar	211
Silica nanotube	Tertiaryamines modified	2.3 mmol g^{-1} at 25 °C, 1 bar	209
Silica fume	Amino-modified	1.3 mmol g^{-1} at 30 °C, 1 bar	210
Chemical grafting	APS grafted	0.7 mmol g^{-1} at 27 °C, 1 bar	204
	APMS grafted	2.0 mmol g^{-1} at 60 °C, 1 bar	212
	APTMS and poly-L-alanine co-grafted	3.9 mmol g^{-1} at 50 °C, 1 bar	213

2.7 Polymer-based adsorbents

Porous polymers, which combine high internal surface area with the synthetic diversity of polymers, have gained an enormous and increasing interest because of their flexibility in structural modification, light weight and high thermal stability. Particularly, porous polymers are promising alternative to the extensively investigated porous inorganic and hybrid materials for CO_2 capture. High CO_2 gas uptakes and good CO_2 selectivities under ambient conditions in a reversible adsorption process are characteristic features for several porous polymers.[214] Up to date, the porous polymers that have been studied for CO_2 capture can be generally categorized into eight groups, which are (1) porous melamine formaldehyde (MF),[215] (2) hypercrosslinked polymers (HCPs),[216-219] (3) conjugated microporous polymers (CMPs),[220-223] (4) polymers with intrinsic microporosity (PIMs),[223-226] (5) polymer with porous aromatic framework (PAF),[227-230] (6) covalent organic polymers (COP),[216, 231, 232] (7) polymer with covalent triazine-based framework (CTF),[214, 233] and (8) molecularly imprinted polymer (MIP),[234] and so on. The synthesis and CO_2 capture behaviors of all the above mentioned porous polymers will be discussed in detail below.

Melamine–formaldehyde (MF) resins, a type of well-known and large scale produced product, has been regarded as cheap and easily available materials for CO_2 adsorption. To fully utilize the surface functional groups of MF, the creation of pores in MF is highly desired. Wilke et al.[215] reported that meso- and microporous melamine resins can be synthesized via hard templating of silica nanoparticles. Porosities of up to 61% and specific mesopore surface areas up to 250 m^2 g^{-1} were achieved, with a CO_2 uptake of 1.6 mmol g^{-1} at 0 °C.

HCPs represent a family of robust microporous organic materials that can exhibit high surface areas up to 2000 m^2 g^{-1}.[235, 236] These materials show excellent chemical robustness and scalability. Moreover, they are quite readily produced on a large scale. Comparing with other materials, the relative low heat of adsorption is another distinct advantage of HCPs. The most extensively studied HCPs are based on a polystyrene network. Hyper-cross-linked polystyrene has shown high CO_2 adsorption capacity (ca. 1.6 mmol g^{-1}) at low pressures which renders it a promising material for selective CO_2/CH_4 separation.[216] Martin et al.[216] prepared a series of HCPs by copolymerisation of p-dichloroxylene and 4,4'-bis(chloromethyl)-1,1'-biphenyl,which constitute a family of low density porous materials with excellent textural development. The maximum CO_2 capture capacity of these materials at 25 °C was 1.7 and 13.4 mmol g^{-1} at 1 and 30 bar, respectively. This type of material was believed to be superior to zeolite-based materials (zeolite 13X, zeolite NaX) and commercial activated carbons.[216] In addition, these polymers have low isosteric heats of CO_2 adsorption and good selectivity towards CO_2. Luo et al.[218] prepared microporous heterocyclic polymers via crosslinking the aromatic heterocyclic molecules. Compared to the other CO_2 capture materials, these microporous materials are more economical at larger scale production and show a remarkable CO_2 adsorption capacities (2.9 mmol g^{-1} at 0 °C and 1 bar.), which are comparable or even higher than those of amine- or carboxylic acid-functionalized materials.

CMPs are a new class of porous materials possessing extended π-conjugation in an amorphous organic framework. Owing to the high flexibility in the selection and design of building blocks and the available control on pore parameters, these polymers can be tailored for use in various applications, such as gas storage, electronics and catalysis.[221] The porous structures of CMPs can be incorporated with a range of chemical functionalities including carboxylic acids, amines, hydroxyl groups, and methyl groups, enabling these materials suitable for CO_2 capture.[221, 223] For instance, Dawson et al.[223] synthesized carboxylic acid- and amine-functionalized CMP networks, CMP-1-COOH and CMP-1-NH_2, and found that CMP-1-COOH showed a higher CO_2 uptake than the non-functionalized sample. The experimental isosteric heats showed the following order in terms of the appended functional groups: –COOH > $(OH)_2$ > NH_2 > H > $(CH_3)_2$. Chen et al.[220] designed a novel kind of functional organic microporous polymers by introducing polar organic groups (P=O and P=S) and electron-rich heterocyclic into the framework to obtain high CO_2 capture capacity. The measured specific surface areas of these polymers were about 600 m^2 g^{-1} and the highest CO_2 uptake was 2.26 mmol g^{-1} (0 °C and 1.0 bar). Interestingly, the polymer containing P=O groups shows greater CO_2 capture capacity than that containing P=S groups at the same temperature. In addition, these polymers show high isosteric heats of CO_2 adsorption (28.6 kJ mol^{-1}), which are competitive to those of some nitrogen-rich networks. Xie et al.[221] synthesized a new porous organic polymer, SNU-C1, by incorporating two different CO_2-attracting groups, namely, carboxy and triazole groups. By

activating SNU-C1 with two different methods, vacuum drying and supercritical-CO_2 treatment, the guest-free phases, SNU-C1-va and SNU-C1-sca, respectively, were obtained. At 25 ^oC and 1 bar, SNU-C1-va and SNU-C1-sca had high CO_2 uptakes of 2.31 mmol g^{-1} and 3.14 mmol g^{-1}, respectively, probably due to the presence of abundant polar groups (carboxy and triazole) exposed on the pore surfaces. Recently, Xie et al.[221] reported a novel class of cobalt/aluminium-coordinated CMPs that exhibited not only outstanding CO_2 capture capacity, but also CO_2 conversion performance at atmospheric pressure and room temperature. The measured CO_2 adsorption capacities of these polymers were ~1.8 mmol g^{-1} at 25 ^oC and 1 bar comparable to those of MOFs. The cobalt-coordinated conjugated microporous polymers can also simultaneously function as heterogeneous catalysts for the reaction of CO_2 and propylene oxide at atmospheric pressure and room temperature, in which the polymers demonstrate better efficiency than a homogeneous salen-cobalt catalyst. By combining the functions of gas storage and catalysts, a direction cost-effective CO_2 reduction processes becomes possible.

Among microporous polymers, PIMs are of great interest because of their relatively slow physical aging, good solubility, high gas permeability and selectivity.[237, 238] Generally, PIMs have a structural combination of rigid ladder-like backbones with sites of contortion, which prevent intra- and/or inter-chain packing and create a large amount of free-volume elements at the same time. Luo et al.[226] synthesized a series of porous polyimides with relatively high BET surface area and a CO_2 uptake of 1.7 mmol g^{-1} at 0 ^oC and 1 bar by polycondensation of melamine and several readily available dianhydride monomers.[226] The relatively low price and nontoxic nature make this material promising for CO_2 capture.

Owing to the ultrahigh surface area and high physicochemical stability, PAFs are amongst the main candidate materials for gas storage and capture. In CO_2 capture, there is inevitably the presence of water or water vapor, thus the hydrothermal stability of a CO_2-sorbent is essential for its large-scale application. Ben et al.[228] reported a series of PAFs, which maintained their original porosity even after boiling in water and 1M HCl for 7 days. PAF-1 showed a high CO_2 uptake of 29.5 mmol g^{-1} at 25 ^oC and 40 bar. Later on, a series of PAFs were prepared by a Yamamoto-type Ullmann reaction containing quadricovalent Si (PAF-3) and Ge (PAF-4).[228] These materials are thermally stable up to 465 ^oC for PAF-3 and 443 ^oC for PAF-4. Gas uptake experiments at low pressure showed that PAF-3 has the highest heat of adsorption of CO_2 (19.2 kJ mol^{-1}).[230] Recently, the same group reported a series of carbonized PAF-1s with enhanced gas storage capacities and isosteric heats of adsorption. Especially, PAF-1-450 showed an adsorption capacity of 4.5 mmol g^{-1} at 0 ^oC and 1 bar. Moreover, it also exhibited excellent CO_2/N_2 and CO_2/CH_4 adsorption selectivity. In addition, these carbonized PAF-1s possess high physicochemical stability. Practical applications in capture of CO_2 lie well within the realm of possibility.[230] By reaction with chlorosulfonic acid, PPN-6 was modified to give PPN-6-SO_3H, which was further neutralized to produce PPN-6-SO_3Li by Lu et al.[228]. At 22 ^oC and 1 bar, the measured CO_2 uptakes of PPN-6-SO_3H (3.6 mmol g^{-1}) and PPN-6-SO_3Li (3.7 mmol g^{-1}) were much higher than that of nongrafted PPN-6 (1.2 mmol g^{-1}). Compared with that of PPN-6-SO_3H, the initial CO_2 uptake for PPN-6-SO_3Li is more pronounced; the Li^+ cation in -SO_3Li has up to three open coordination sites after full activation, which results in stronger interactions with CO_2 molecules.[228] Li et al.[239] explored the performance of designed PAFs using grand canonical Monte Carlo simulations and ab initio calculations, and the results showed that pyridine with one nitrogen atom can provide a strong physisorption site for CO_2, whereas more nitrogen atoms in heterocycles will reduce the interaction, especially at relatively low pressure. It was found that the -COOH group in PAFs plays a key role in holding CO_2 rather than the -NH_2 group.

COPs are another group of porous polymers that show promising potential for CO_2 capture due to high hydrothermal stability and BET specific surface area. Xiang et al.[231] synthesized a series of COPs for the adsorption of H_2, CO_2, CH_4, N_2 and O_2. The CO_2 takeup reached 13.5 mmol g^{-1} at 25 ^oC and 18 bar. COP-1 also exhibited significantly higher selectivity than COP-2, 3 and 4, due to its smaller pore size. Furthermore, these COPs also showed robust capabilities for the removal of CO_2 from natural gas. In order to enhance the gas adsorption properties of the COP-1 material, Xiang et al.[240] proposed a novel lithium-decorating approach in which the alkynyl functionalities in COP-1 were postsynthetically converted to lithium carboxylate groups with the aid of dry ultrapure CO_2. After such modification, the CO_2 uptake in Li@COP-1 was increased from 4.4 to 5 mmol g^{-1} at 25 ^oC and 18 bar.

Additionally, some other types of porous materials such as triazine-based and molecularly imprinted polymers, etc., are also promising for CO_2 capture. Liebl et al.[214] synthesized seven triazine-based porous polyimide (TPI) polymer networks for CO_2 capture. A high CO_2 uptake of 2.45 mmol g^{-1} was obtained at 0 ^oC and 1 bar. It was found that the high degree of functionalization led to comparatively high CO_2 adsorption heats for TPI polymer networks between 29 and 34 kJ mol^{-1}. As a result, the TPI networks showed high CO_2 uptakes relative to their moderate BET equivalent surface areas. Zhao et al.[234] synthesized a series of molecularly imprinted adsorbents for CO_2 capture by molecular self-assembly procedures. Among them, the sample with higher amine content exhibited the highest CO_2 capacity, which maintained steady after 50 adsorption−desorption cycles. The CO_2 adsorption mechanism of molecularly imprinted adsorbents was determined to be physical sorption according to the adsorption enthalpies integrated from the DSC heat flow profiles. The calculated separation factors of CO_2 under 15% CO_2/85% N_2 atmosphere were above 100 for all these adsorbents.

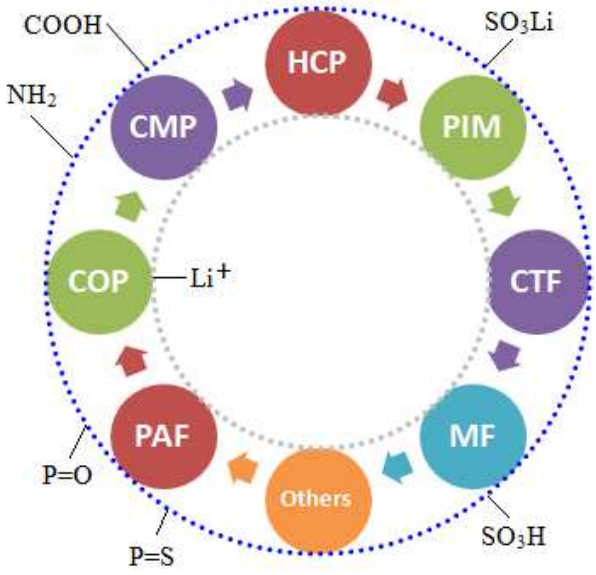

Figure 7. A summary of all the studied porous polymers and the possible modifications for CO_2 capture.

In short, porous polymers have attracted great attention for the low temperature CO_2 capture/separation mainly due to their high surface area and synthetic diversity. All the efforts made to improve the related to porous polymer-based CO_2 adsorbent can be briefly summarized in Figure 7, which can be divided into three main parts: (1) the major one is to change the compositions of polymer framework including HCP, CMP, COP, PAF, PIM, CTF, MF, and so on, (2) the second one is to tune the pore size and specific surface area of the obtained porous polymers, and (3) the third one is to do surface modifications with various groups including COOH, NH_2, P=O, P=S, SO_3Li, SO_3H, Li^+, etc. For the further work, two technical problems should be overcome. One is hydrothermal stability of the adsorbents, and the other one is the adsorption/desorption cyclability. Polymer-based adsorbents and their CO_2 capture performance are summarized in Table 6.

Table 6. Summary of polymer-based CO_2 adsorbents and their performance in CO_2 capture.

Polymer types	Materials	CO_2 uptakes	References
MF	Meso- and microporous MF resins	1.6 mmol g^{-1} at 0 °C, 1bar	215
HCPs	HCPs	13.4 mmol g^{-1} at 25 °C, 1bar	216
	Microporous heterocyclic polymers	2.9 mmol g^{-1} at 0 °C , 1bar	218
CMPs	CMP-1-COOH, CMP-1-NH_2	1.2 mmol g^{-1} at 25 °C, 1 bar	223
	CMP with P=O and P=S groups	2.3 mmol g^{-1} at 0 °C, 1 bar	220
	SNU-C1-va, SNU-C1-sca	3.1 mmol g^{-1} at 25 °C, 1 bar	221
	Co or Al coordinated CMPs	1.8 mmol g^{-1} at 25 °C, 1 bar	241
PIMs	Porous polyimide	1.7 mmol g^{-1} at 0 °C, 1 bar	226
PAFs	PAF-1	29.5 mmol g^{-1} at 25 °C, 40 bar	242
	PAF-1	4.5 mmol g^{-1} at 0 °C, 1 bar	230
	PPN-6-SO_3Li	3.7 mmol g^{-1} at 22 °C, 1 bar	243
	PAF-N4	60.0 mmol g^{-1} at 25 °C, 11 bar	239
COPs	COP-1	13.5 mmol g^{-1} at 25 °C, 18 bar	231
	Li@COP-1	5 mmol g^{-1} at 25 °C, 18 bar	240
CTFs	TPI	2.45 mmol g^{-1} at 0 °C, 1 bar	214
MIPs	MIP1b	0.48 mmol g^{-1} at 60 °C, 1 bar	234

2.8 Clay-based adsorbents

Clay is a general term for a single clay mineral or combination containing one more clay minerals with trace amounts of metal oxides and organic matter.[244] Geologic clay deposits are mostly composed of phyllosilicate minerals containing variable amounts of water trapped in the mineral structure. Acting as a solid sorbent, clay has many advantages: low cost, high surface area,[245] high mechanical and chemical stability, relative easiness in availability, regeneration and production in large enough quantities. The use of clay for CO_2 capture has also attracted some attention recently. Up to date, there are mainly two main kinds of clays, montmorillonite and bentonite, that have been studied for CO_2 capture.

Montmorillonite is a natural inorganic material with a general chemical structure of $(OH)_4Si_8(Al_{4-x}Mg_x)O_{20}$. The crystal structure of montmorillonite consists of two-dimensional layers formed by an octahedral sheet sandwiched between two opposing tetrahedral sheets. As a kind of clay, it has all the merits of clay and is widely studied as an adsorbent or catalyst support.[245] In order to be used for CO_2 capture, the montmorillonites have to be modified with amines, diamines, polyamines or polyoldendrimers, etc. When CO_2-containing gas is passed through a bed of this adsorbent, the immobilized amine reacts with CO_2 forming carbamates, resulting in CO_2 capture.[246] Stevens et al.[247] synthesized diamine modified montmorillonite via water aided exfoliation and grafting route. The material achieved a CO_2 adsorption capacity of 2.4 mmol g^{-1} at 100 °C in pure CO_2 which is predominately associated with chemisorption. The maximum CO_2 adsorption capacity in 15% CO_2 in N_2 was 1.8 mmol g^{-1} at 95 °C. Roth et al.[248] treated montmorillonite nanoclay with

aminopropyltrimethoxysilane (APTMS) and PEI for CO_2 capture. The untreated nanoclay had very low CO_2 capture, but it was considerably increased after doping with amines, particularly with both APTMS and PEI. CO_2 sorption tests showed fast sorption kinetics and capture capacities as high as 1.7 mmol g^{-1} at 1 bar and about 3.9 mmol g^{-1} at ca. 20 bar in the temperature range of 75−85 °C. The regeneration of these nanoclays could be achieved using nitrogen at 100 °C or CO_2 (dry or humid) at 155 °C as the sweep gases. Furthermore, pressure swing operation, employing vacuum at 85 °C, was proven effective in regenerating the adsorbent. This work showed that amine-modified montmorillonite nanoclay has the potential to be a high performing solid adsorbent for CO_2 capture. Azzouz et al.[249] studied the CO_2 capture capacity of montmorillonite intercalated with three soya oil-derived polyglycerol dendrimers with average molecular weights of 500, 1100, and 1700, respectively. It was concluded that intercalation of montmorillonite with polyglycerol dendrimers provided expanded effective adsorbents acting via weak base-like character for the reversible retention of CO_2. This behavior was similar to that observed with polyol-intercalated montmorillonite, confirming once again that the OH groups grafted on the dendritic moiety act as the main adsorption site. In the absence of diffusion hindrance, all organoclays displayed affinity toward CO_2 with adsorption capacity of up to 0.012-0.016 mmol g^{-1}, but with much lower desorption temperatures as compared to amine-based adsorbents. As a common feature of polyalcohol-montmorillonites, these adsorbents exhibited optimum adsorptive properties resulting from a judicious compromise between the highest adsorption capacities and the lowest desorption temperatures. It opens a new prospect in reducing the greenhouse effect by valorizing natural and eco-friendly materials as valuable adsorbents with high levels of regeneration ability and re-usability.

Bentonite is another common raw clay material that has been studied for CO_2 capture. The inner layer is composed of one octahedral alumina sheet placed between two tetrahedral silica sheets. Due to the isomorphous substitutions within the layers of Al^{3+} for Si^{4+}, the surface of bentonite is negatively charged.[250] The sorption features over clay are believed to be related to the nature of the parent clay, and an attempt to rationalize the fact was made by considering the Si/Al ratio, together with textural characteristics.[251] Chen et al.[252] studied the CO_2 capture capacity of PEI modified bentonite. The results showed that bentonite in its natural state showed negligible CO_2 uptake. After amine modification, the CO_2 uptake increased significantly from 0.14 to 1.1 mmol g^{-1}. The PEI-modified bentonites showed high CO_2 capture selectivity over N_2, and exhibited excellent stability in cyclic CO_2 adsorption runs. However, owing to smaller pore volume, the CO_2 uptake of PEI-modified bentonite was lower than those usually achieved by PEI-impregnated mesoporous silicas. In order to deal with this problem, Wang et al.[253] used sulfuric acid treatment, the textural properties, in particular, pore volume and surface area of bentonite, were significantly improved. With the maximum TEPA loading of 50 wt%, the maximum CO_2 breakthrough sorption capacity reached 3 mmol g^{-1} at 75 °C under a dry condition. With the addition of 18% moisture to the simulated flue gas, the CO_2 sorption capacity could be increased to 3 mmol g^{-1} due to the bicarbonate formation under a wet condition. In addition, these adsorbents showed a good regeneration ability and thermal stability below 130 °C.

2.9 Alkali metal carbonate-based adsorbents

With both high sorption capacity and low cost, it is not strange that alkaline metal carbonate solids such as K_2CO_3 and Na_2CO_3 have been paid with attention for CO_2 capture application in the last several years.[254-257] Alkali metal carbonates are suitable for the treatment of flue gases at temperatures below 200 °C.[258, 259] Typically their CO_2 capture takes place within the temperature range of 50–100 °C, while regeneration occurs in the range of 120–200 °C, enabling them potentially applicable to the capture of CO_2 from existing fossil fuel-fired power plants. However, as pointed out in our previous review paper,[9] the main problems for this type sorbents are the slow carbonation reaction rate, poor durability, and temperature limitation, etc.

Prior to 2011, many attempts have been made to resolve the above mentioned problems by dispersing active Na_2CO_3/K_2CO_3 on supports such as Al_2O_3, active carbon, TiO_2, SiO_2, MgO, ZrO_2, etc., so as to enhance the adsorption rate and provide the required attrition resistance in the fluid-bed or transport reactors.[260-266]. In the past three years, similar research efforts have been continued. Wu et al.[267] investigated the CO_2 capture performance of K_2CO_3/Al_2O_3 in a continuous CO_2 sorption−desorption system equipped with three fluidized-bed reactors (two carbonation reactors and one regeneration reactor). The first step of CO_2 removal was higher than 75%, and the total CO_2 removal reached 96% after further sorption in the second step, and it finally reached a fairly constant state. In addition, the CO_2 removal increased with the increase in regeneration temperature, H_2O concentration, and solid circulation, but opposite effect was observed with the increase in carbonation temperature, CO_2 concentration, and fluidization number. After optimizing the operation parameters, the CO_2 removal could reach above 85%. Dong et al.[268] found that both the adsorption capacity and rate can be improved by doping 1–3 wt% of TiO_2 on K_2CO_3/Al_2O_3. Wu et al.[268] found that adding $Ca(OH)_2$ to K_2CO_3/Al_2O_3 can not only increase the CO_2 capture capacity, but also improve its SO_2 resistance. Derevschikov et al.[269] reported that Y_2O_3 could be used as potential support instead of Al_2O_3 for dispersing K_2CO_3.

In order to further improve the durability, Kondakindi et al.[270] proposed a method of coating Na_2CO_3/Al_2O_3 sorbents on metal foils. The results indicated that Na_2CO_3/Al_2O_3 powders showed better performance compared to those of foil samples, but 35 wt% Na_2CO_3/Al_2O_3 sorbent coated on foil showed the highest performance (7.7 mmol g^{-1}). Several foil samples were run through durability tests and showed a loss of about 15% of their capacity through the first 15–20 cycles, and 40–50% loss through 500 cycles. Even after 500 cycles, the coated foil sorbent still showed CO_2 capture performance that could be economically competitive with the current existing methods. For alkali carbonate sorbents, the kinetics of CO_2 sorption and desorption has also been investigated.[271, 272] In addition to alkali carbonates, NaOH was investigated for CO_2 capture as well.[273] The results revealed that for the high CO_2 removal rate, there was an optimal

temperature range of 30–45 °C. Cyclic tests for fine and coarse particles indicated a reduction in reaction rate order after each cycle due to an increase in the reaction product layer thickness, formed on the sorbent.

2.10 Immobilized ionic liquid-based adsorbents

Ionic liquids (ILs) are salts that consist exclusively of ions and short-lived ion pairs, and have a melting points lower than 100 °C.[274] Because ILs have negligible volatility, nonflammable ability, high thermal stability, virtually unlimited chemical tenability and high CO_2 solubility, they have been proposed as attractive alternatives for CO_2 capture.[275-277] Blanchard et al.[278] first observed that significant amounts of CO_2 could be dissolved in imidazolium-based ILs to facilitate the extraction of a dissolved product, without contaminating the product with IL, because IL was insoluble in CO_2. Their study initiated an explosion of interest on CO_2 absorption with ILs, leading to a rapid growth of research activities on this specific topic.[279] The concept of absorption of CO_2 in ILs based on their unique properties providing extra advantages over the traditional processes, including a high level of CO_2 absorption, while the co-absorption of hydrocarbons and corrosion problems are significantly minimized. However, there are two major problems associated with the use of neat ILs for CO_2 capture, which are the cost and the relatively high viscosity. The later will result in low sorption and desorption rates and might limit their eventual use in large-scale CO_2 gas removal [12, 278, 280, 281] In addition, IL is liquid, lack of mechanical strength. To overcome the above mentioned difficulties, several strategies have been explored, including (1) supporting ILs (SILs) on a solid porous support such as membranes, metal organic frameworks (MOFs), and nanoporous polymers, etc, (2) pyridine-containing anion-functionalization, and (3) making ILs in the polymeric form.

One of the innovative developments is new types of membrane systems such as immobilized ionic liquid membranes or supported ionic liquid membranes (SILMs). SILMs consist of an ionic liquid immobilized in a supporting porous membrane by capillary forces.[282] Gas transport in supported liquid membranes occurs through the dissolution-diffusion mechanism. Gas molecules on the inlet absorb into the liquid, diffuse across the membrane, and desorb at the permeate site.[283] Moreover, thermal stability, low volatility and high surface tension make membranes containing ILs more stable than supported liquid membranes. And they also can be regenerated and reused. Hence, the SILMs have been regarding as a promising material for CO_2 capture.[284, 285] Compared to neat ILs, SILMs not only reduce the cost and viscosity of ILs, but also enhance mechanical strength and separation efficiency.[286] For immobilization purposes, not only traditional ionic liquids[287] but also amine-terminated ILs can be applied.[288] Particularly, the amine moiety of these task-specific ILs facilitates selective transport of CO_2.[288] Bara et al.[289] prepared a membrane using gemini ILs and demonstrated several gas separations. The ability to functionalize ILs and modify their properties was further demonstrated by the incorporation of polar substituents that provide enhanced interactions with CO_2.

MOFs seem to be promising supports for ILs because their pore size, volume, and functionality of MOFs are readily tunable in a rational manner,[290] which lead to their wider application and increased efficiency for CO_2 capture. Chen et al.[291] first studied MOF-supported ILs by means of computational methods. It was observed that with increasing the concentration of ILs, the molecules in pores were more uniform and ordered. Therefore, the amount of ionic absorption sites and selectivity could be increased with the increase in IL:MOF ratio. Since a great number of ILs as well as MOFs exist, this research area has a great potential in terms of identifying a proper CO_2 capturing adsorbent.[292, 293] Some nanoporous polymer microspheres have also been used as support for ILs. For example, Wang et al.[294] synthesized three 1-ethyl-3-methylimidazolium amino acide ([EMIM][AA])-type amino acid ILs (AAIL) and immobilized them into nanoporouspoly(methyl methacrylate) (PMMA) microspheres (see Figure 8(a)) for CO_2 removal. The sorbents retained the highly porous structures after AAIL loading and exhibited fast kinetics as well as reasonably high sorption capacity, and could be easily regenerated and reused. As shown in Figure 8(b), the resultant [EMIM][AA]–PMMA sorbents could overcome the high viscosities of the [EMIM][AA]s such that the resultant sorbents exhibited a dramatically enhanced sorption rate (CO_2 adsorption equilibriums could be reached in less than 15 min) due to the high mass transfer area of AAILs after immobilization. When exposed to CO_2 at 40 °C, the adsorption capacity of [EMIM][Arg], [EMIM] [Ala], and [EMIM][Gly] was 1.01, 1.38, and 1.53 mmol g^{-1}, respectively. And they also synthesized 1-ethyl-3-methylimidazoliumlysine ([EMIM][Lys]) and immobilized it in a porous PMMA microsphere support for post-combustion CO_2 capture, exhibited a high CO_2 capacity of 1.67 mmol g^{-1}.[294]

Luo et al.[295] developed a new method for capturing CO_2 using several pyridine-containing anion-functionalized ILs, which include two kinds of interacting sites, by cooperative interactions. A high capacity up to 1.60 mol CO_2 per mol IL and excellent reversibility were achieved by introducing a nitrogen-based interacting site on the phenolate and imidazolate anion. It was found that the multiple site cooperative interaction between two kinds of interacting sites in the anion resulted in superior CO_2 capacities, which originated from the π-electron delocalization that increased Mulliken atomic charge of the nitrogen atom.

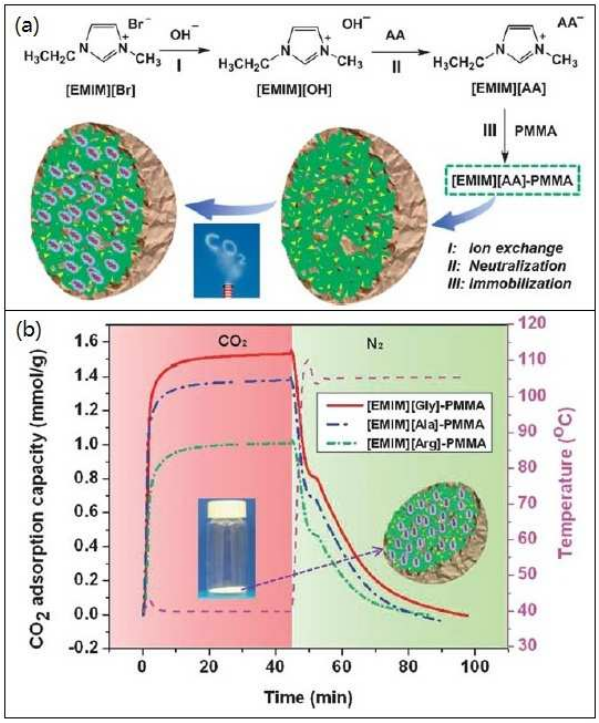

Figure 8. (a) Diagram of synthesis and immobilization of functional[EMIM][AA] for CO_2 capture. (b) CO_2 adsorption/desorption of three different sorbents [EMIM][AA]–PMMA (with an [EMIM][AA] loading of 50 wt% in the sorbents). The inset shows the photo-image of as-prepared [EMIM][AA]–PMMA sorbents.[294]

It is discovered that conversion of ionic monomers into polymeric forms could increase the CO_2 capture efficiency as compared to the room-temperature ILs. Over these poly(ionic liquid)s (PILs), the sorption-desorption rates become faster and the processes are completely reversible.[292, 296-298] Moreover, comparing to the corresponding monomers, both the CO_2 sorption capacity[298, 299] and the selectivity in terms of separation of CO_2 from mixtures of N_2/CO_2, CH_4/CO_2 and O_2/CO_2[298-301] are improved. Further fabrication of the membranes made of PILs can lead to much enhanced mechanical strength as compared to SILMs. For example, the CO_2 sorption capacities of tetraalkylammonium-based ILs polymers are 6.0–7.6 times higher than that of the room-temperature ILs, which are also significantly higher than those of the polymer solids such as poly-methacrylates, polystyrene and polycarbonates.[302-304] In addition, it has be experimentally proved that the desorption of CO_2 from PILs is also fast. Privalova et al.[296] studied the imidazolium-based PILs that consist of poly[2-(1-butylimidazolium-3-yl)ethyl methacrylate] (BIEMA) cation coupled with different counter anions as CO_2 sorbents. An increase in the molecular weight slightly enhanced the CO_2 capture capacity, and the only exception was observed for Br–containing PILs. Moreover, as CO_2 capture and release can be performed at room temperature, no additional heat supply is required for the process. This study uncovers new opportunities for developing alternative CO_2 capture materials with tunable properties and recyclability, which can be considered as additional options for CO_2 mitigation methods.

2.11. Other low-temperature adsorbents

There are some other novel low-temperature adsorbents such as boron nitride (BN), alkali metasilicate, magadiite, which have not been reported prior to 2011.[9] Based on the fact that nitrogen atoms incorporated in a system can act as Lewis base sites for CO_2 chemisorption, the potential application of boron nitride for CO_2 capture and storage thus has gained attention recently.[305-308] In 2011, Jiao et al.[305] and Choi et al.[309] almost simultaneously reported the CO_2 capture by boron nitride materials. Jiao et al.[305] studied the CO_2 capture and activation over graphene-like boron nitride (g-BN) with boron vacancy using density functional theory (DFT), and found that CO_2 can be captured and activated by g-BN with a boron vacancy, followed with dissociation to produce lattice-embedded carbon and surface-adsorbed molecular oxygen. From ab initio calculations, Choi et al.[309] reported strong CO_2 adsorption on boron sites in boron-rich boron nitride nanotube and found it could capture CO_2 effectively at ambient conditions. Sun et al.[306] first demonstrated that by modifying the charge state of the BN nanomaterials, adsorption/desorption of CO_2 on BN nanosheets and nanotubes can be controlled and reversed. Although many works have been performed on boron nitride as CO_2 adsorbents, almost all of the reports, up to now, are still based on theoretical calculations or simulations. To move ahead, a proper design of suitable boron nitrides and the evaluation of their CO_2 capture capacity experimentally are highly demanded.

Although alkali silicates are generally regarded as high-temperature CO_2 sorbents in the temperature range of 500–700 °C, one special kind of alkali silicate, alkali metasilicate (M_2SiO_3 where M is Li, Na, K) has been demonstrated to adsorb CO_2 at low temperatures (30–130 °C).[310-312] Kalinkin et al.[310] studied the CO_2 sorption over M_2SiO_3 (where M is Li, Na, K) in an atmosphere of CO_2. With identical amounts of energy supplied, the CO_2/M_2SiO_3 molar ratio in the samples activated in the medium of CO_2 increased in the order of Li < Na < K. Rodríguez et al.[311] performed a thermo-kinetic analysis of CO_2 sorption over Na_2SiO_3 between room temperature and 130 °C. It was concluded that the quantity of CO_2 absorbed is not high enough to utilize it as CO_2 adsorbent. For alkali metalsilicates, the major problem is that their CO_2 capture capacity is still too low to be practically utilized at present. Vieira et al.[313] prepared a novel adsorbent through the impregnation of PEI into the interlayer space of layered silicate type magadiite and organo-magadiite. Magadiite has an interlayer space that may be modified to diminish diffusional restrictions and the host variable concentration of PEI. These sorbents showed maximum adsorption capacity of 6.11 mmol g^{-1} at 75 °C using 25 wt% impregnated PEI. Clay-based, alkali carbonate-based, and some other types of adsorbents and their CO_2 capture performance are summarized in Table 7.

Table 7. Summary of all clay-based, alkali carbonate-based, immobilized ionic liquid-based, and some other types CO_2 adsorbents and their performance in CO_2 capture.

Adsorbent types	Materials	CO_2 uptakes	References
Clay-based adsorbents	Diamine modified montmorillonite	2.4 mmol g^{-1} at 100 °C, 1 bar	247
	APTMS and PEI modified montmorillonite	3.9 mmol g^{-1} at 85 °C, 20 bar	248
	Polyglycerol dendrimers modifired montmorillonite	0.02 mmol g^{-1} at room temperature, 1 bar	249
	PEI modified bentonite	1.1 mmol g^{-1}. at 75 °C, 1 bar	252
	TEPA modified bentonite	3.0 mmol g^{-1} at 75 °C, 1 bar	253
Alkali carbonate-based adsorbents			267
	TiO_2-Doped K_2CO_3/Al_2O_3	2.5 mmol g^{-1} at 60 °C, 1 bar	268
	$K_2CO_3/Ca(OH)_2/\gamma$-Al_2O_3	2.0 mmol g^{-1} at 60 °C, 1 bar	314
	K_2CO_3/Y_2O_3	0.6 mmol g^{-1} at room temperature, 1 bar	269
	Na_2CO_3/Al_2O_3 coated on foil	7.7 mmol of CO_2 per g of Na_2CO_3 at 150 °C, 1 bar	270
	NaOH	2.5–3 mmol g^{-1} at 25 °C, 1 bar	315
Immobilized ionic liquid-based adsorbents	[EMIM][Gly]-PMMA	1.7 mmol g^{-1} at 25 °C, 1 bar	294
	[EMIM][Lys]-PMMA	1.7 mmol g^{-1} at 40 °C, 1 bar	316
	Pyridine-containing anion-functionalized ILs	1.6 mol CO_2 per mol IL at 20 °C, 1 bar	295
	Imidazolium-based PILs	0.3 mmol g^{-1} at 25 °C, 1 bar	296
Other adsorbents	PEI modified Magadiite	6.1 mmol g^{-1} at 75 °C, 1 bar	313
	Boron nitride	Not mentioned	305
	Boron nitride nanotube	Not mentioned	309
	Boron nitride	Not mentioned	306

3. Intermediate-temperature solid CO_2 sorbents

3.1 LDHs-based sorbents

LDHs derived mixed oxides have been recognized as the important intermediate-temperature CO_2 sorbents.[317-319] In general, LDHs derived mixed oxides possess both high surface area and abundant basic sites, favorable for absorbing acidic CO_2 at 200–400 °C.[320-322] Potentially LDHs-based CO_2 sorbents can be used in the sorption enhanced water gas shift and biomass reforming processes. Previously a lot of efforts were made to improve the CO_2 capture capacity and the long-term stability of LDHs-based sorbents. For Mg-Al-CO_3 LDH, the research focus was on the synthetic conditions,[323] presence of SO_x and H_2O,[324] operation pressures,[319, 325, 326] alkali (K, Cs) doping,[327-330] particle size,[331] and the uploading of LDHs on supports.[332, 333] Later it was shifted to modify the composition of Mg-Al-CO_3 LDH by substituting either the CO_3^{2-} anion, or the divalent and trivalent cations of Mg^{2+} and Al^{3+} with some other anions or cations.[9] In the period of 2011 to 2014, the research activities mainly include the following five aspects: (1) the intercalation of organic anions, (2) the preparation of LDH based hybrid materials, (3) the control of LDH particle size, (4) the method for alkali (Na, K, Cs) doping, and (5) mechanism study.

Recently, Wang et al.[334] demonstrated that the anions affect the thermal stability and morphology, as well as the surface area of LDHs, consequently influencing the CO_2 sorption capacity. Among various LDHs, Mg_3Al_1–CO_3 showed the highest CO_2 sorption capacity of 0.53 mmol g^{-1}, which was much higher than those of other LDHs with HCO_3^-, NO_3^-, SO_4^{2-}, and Cl^- anions (~0.2 mmol g^{-1}). Following this finding, Wang et al.[335] first reported the synthesis of highly efficient intermediate-temperature CO_2 sorbents from organic anion-intercalated LDHs (organo-LDHs). By intercalating long carbon-chain organic anions (e.g. stearate) into LDHs, the CO_2 capture capacity was markedly increased to 1.25 mmol g^{-1}, which is 2.5 times higher than that of traditional LDH-based sorbents (0.5 mmol g^{-1}). The schematic illustration of the structural changes and the CO_2 capture by Mg_3Al_1-CO_3 and Mg_3Al_1-stearate are shown in Figure 9. It is believed that the improved CO_2 capture capacity is due to the following reasons: (1) the decomposition of long carbon-chain anions cracks and splits the LDH plates and creates more surface basicity (O^{2-}) sites; (2) the produced mixed metal oxide mixture has a lower degree of crystallinity; and (3) the formed quasi-amorphous structure is more stable than that from Mg_3Al_1–CO_3. Later Li et al.[306] synthesized the LDH-based precursor by combining both long-carbon-chain stearic anion intercalation and K surface promotion, and obtained a CO_2 capacity up to 1.93 mmol g^{-1} at 300 °C, 1.7 times higher than that of the conventional K_2CO_3-promoted hydrotalcite sorbent (1.11 mmol g^{-1}). The K ion may enter the more spatial interlayer spacing of the stearate-pillared LDH, leading to a better promotion effect of K by forming weak surface chemical bonds.[306] These increased K-species locate on all accessible precursor surfaces forming denser and better dispersed basic sites that can react with CO_2 after calcination.

Garcia-Gallastegui et al.[336] synthesized LDH/GO hybrid for CO_2 capture, and improved both the CO_2 sorption capacity and recyclability. In particular, the absolute CO_2 capture capacity of the LDH was increased by over 60% using only 7 wt % GO as

the support. The synthesis and structure of LDH/graphene oxide (GO) are illustrated in Figure 10. During the precipitation of positively charged Mg-Al LDHs onto negatively charged GO, the mutual electrostatic interactions drive the self-assembly of heterostructured nanohybrids in a "layer-by-layer" fashion.[337] The resultant LDH serves as a spacer to prevent aggregation of individual graphene sheets, particularly after washing out the highly oxidized debris in the GO sample by aqueous base. On the other hand, the GO supports the LDH, improving its dispersion and generating more active sites. Furthermore, based on the compatible degree of surface charge, an in situ LDH precipitation onto base-washed, oxidized, multi-walled carbon nanotubes (MWNTs) was developed to fabricate hybrid materials.[336] MWNTs have an inert nanostructured network, which provides a high surface area that can maximize the gas accessibility, minimize the coarsening effects, and significantly increase the stability of the LDH materials.

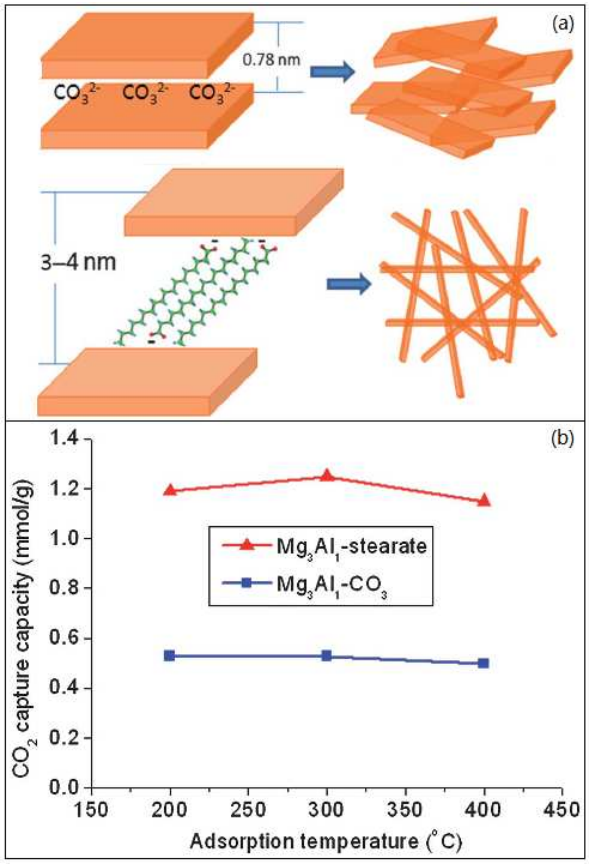

Figure 9. The general schemes of the structural changes of (a) Mg_3Al_1-CO_3 and Mg_3Al_1-stearate into amorphous mixed oxides, (b) Comparison of the CO_2 capture capacity of Mg_3Al_1-CO_3 and Mg_3Al_1-stearate derived CO_2 sorbent.

LDHs have been extensively investigated for decades, and many methods including co-precipitation,[338] urea hydrolysis,[339] structure reconstruction,[340] sol-gel,[341] ion exchange,[342] and reverse microemulsion[343] have been employed. To increase the crystalline degree or to control the morphology of LDHs, the aging process can be further assisted by either hydrothermal treatment,[344] sonication,[345] or microwave irradiation.[346] However, due to the layered structural feature of LDH, it generally prefers to form either "sand rose"[347] or "platelet-like"[348] morphologies. Recently, Wang et al.[349] first synthesized nano-sized spherical Mg_3Al_1-CO_3 LDHs with an average particle size of ca. 20 nm by employing the isoelectric point (IEP) concept. Although the nanospherical LDH only showed a slightly increase in CO_2 capture capacity (0.58 mmol g^{-1}) compared to the "sand rose" LDH (0.53 mmol g^{-1}), the result clearly suggest that the mesoporous structure and big pores of nanospherical LDHs are favorable for the dispersion of doped K_2CO_3 species. After doping K_2CO_3, a much higher CO_2 capture capacity of 1.21 mmol g^{-1} than that of the conventional LDH (0.91 mmol g^{-1}) was obtained.

For the alkali metal carbonate promoted LDHs, most of the previous work used K_2CO_3 as K precursor and H_2O as the solvent. In a recent work, Wang et al.[350] systematically investigated the promoting effect of different alkali metal carbonates such as Li_2CO_3, Na_2CO_3, Rb_2CO_3, and Cs_2CO_3, and of the solvents. The sample doped with Li_2CO_3 showed the highest CO_2 capture capacity (1.05 mmol g^{-1}) at 400 °C and 1 bar, followed by K_2CO_3 (0.96 mmol g^{-1}), Na_2CO_3 (0.83 mmol g^{-1}), Rb_2CO_3 (0.79 mmol g^{-1}), and Cs_2CO_3 (0.75 mmol g^{-1}) doped samples, suggesting that, with the same weight loading, Li_2CO_3 has an even better promotion effect than K_2CO_3. In addition, the solvent has a big impact on CO_2 capture. Besides H_2O, some organic solvents including methanol, ethanol, 1-butanol, and 2-propanol were also used to dissolve K_2CO_3 during the preparation of K_2CO_3/LDH. The results indicated that the capacity was greatly increased when organic solvents were used. The capacity at 400 °C was increased from 0.96 mmol g^{-1} with H_2O to 1.09 mmol g^{-1} with methanol, 1.25 mmol g^{-1} with ethanol, 1.22 mmol g^{-1} with 1-butanol, and 1.33 mmol g^{-1} with 2-propanol. With H_2O as the solvent, the amorphous $MgAlO_x$ mixed oxide was transformed back to LDHs structure again during the preparation. This is reasonable due to the presence of both H_2O and CO_3^{2-} in the mixture. However, with organic solvents, there was no change in the amorphous structure, and this probably results in a better dispersion of K^+ during the impregnation.

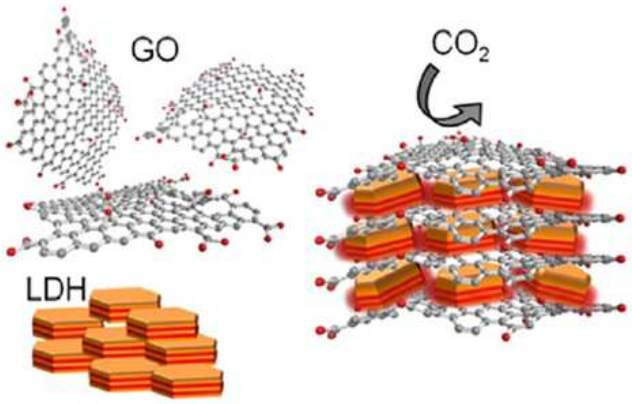

Figure 10. The structure of the LDH−GO hybrid material.[336]

The CO_2 adsorption sites and formation mechanism of LDH-derived metal oxides were investigated by Gao et al.[351], who found that when LDH is optimally calcined there are two mechanisms for the formation of active Mg-O species. One is that the active Mg-O species can be generated by substitution of Mg^{2+} by Al^{3+} in the periclase MgO lattice, as shown in Figure 11(a). To compensate for the positive charge generated by Al^{3+}, the adjacent oxygen anions will become coordinatively unsaturated.[352] With insertion of one Al^{3+} into the periclase MgO lattice, there will be generation of two active Mg-O species. The other one is that a portion of the inserted Al^{3+} might diffuse out of the octahedral sites and become tetrahedrally coordinated in the interlayer. The site formerly occupied by Al^{3+} is left vacant, which consequently produces three active Mg-O species around it, as shown in Figure 11(b). Therefore, the calcination temperature is one of the key parameters that determine the number of active Mg-O species. If it is too low, the Mg-O bonds cannot be broken and the hydroxide phase remains; however, if it is too high, the Mg and Al will start to react and form the $MgAl_2O_4$ spinel oxide. Since each LDH has a different thermal stability, their optimal calcination temperature is different. In addition, this explains why the quasi-amorphous phase obtained by thermal treatment at the lowest possible temperature gives the highest CO_2 capture capacity.

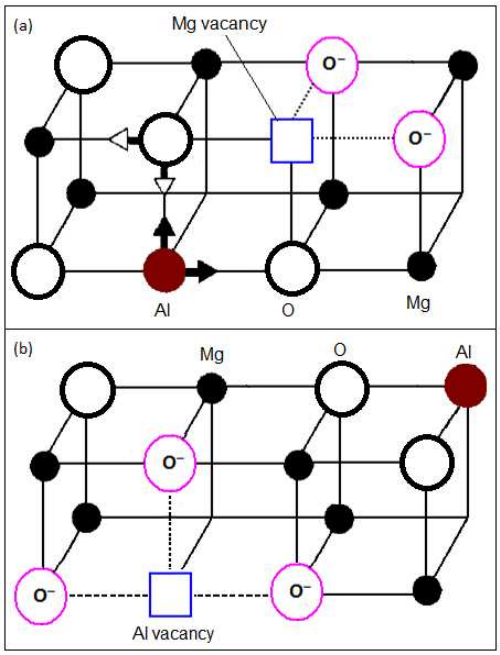

Figure 11. The proposed mechanisms for the formation of active Mg-O species induced by (a) the substitution of Mg by Al and (b) the diffusion of Al atoms out of the octahedral brucite layers.[351]

3.2 MgO-based sorbents

Considering the abundant surface basic sites of the metal oxides and the acidic nature of CO_2, it is expected that some metal oxides can act as CO_2 sorbents. Among various metal oxides, MgO is potential for both carbon capture and long-term CO_2 fixation. Chemically, CO_2 reacts with MgO to form thermodynamically stable $MgCO_3$ ($\triangle H \approx 1100$ kJ mol^{-1}). However, we noticed that there were only few reports using MgO as CO_2 sorbent three years ago. In recent years, much attention has been gained over MgO based sorbents. MgO absorbs CO_2 in the temperature range of 200–400 °C and can be regenerated at relatively low temperatures (~500 °C) compared to CaO-based sorbents,[9, 353] and has a low energy requirement for regeneration.[353-355] However, because of its moderate CO_2 sorption capacity, relative slow sorption kinetics and easiness to lose its surface area during regeneration, the practical application of MgO as a CO_2-sorbent is quite limited.[9] The adsorption sites for CO_2 on MgO are associated with low coordinated Mg^{2+}-O^{2-} sites.[333, 356-358] The acidic CO_2 reacts with basic O^{2-} sites depending on their coordination. Oxygen atoms located at edges and corners of the crystal surfaces have stronger basicity than those in the basal planes.[333] CO_2 adsorbs as monodentate on the edge sites and bidentate on the corner sites.[359] The CO_2 adsorption capacity of commercially available MgO is fairly small (0.5 mmol g^{-1}).[360] In order to enhance the CO_2 capacity of MgO-based sorbents, improvement are mainly focused on (1) decreasing the particle size and synthesis of porous MgO, (2) dispersing MgO nanoparticles on porous supports, (3) modifying MgO with alkali carbonates, and (4) preparation of MgO-based mixed oxides.

An effective method to enhance the efficiency of CO_2 absorption on metal oxide is to decrease the particle size to have more exposed active sites.[361] Bian et al.[361] reported a thermal decomposition method to synthesize mesoporous MgO with high surface area and a narrow pore size distribution, and obtained enhanced CO_2 adsorption capacity as compared with commercially available MgO nanoparticles. Ruminski et al.[362] also proved that the CO_2 sorption capacity of MgO is highly related to surface area. In general, the accessibility of sorption sites and synergistic porous support are crucial for efficient capture sorbate molecules in a gas stream.[363, 364] For this reason, dispersing MgO onto a porous support is intensively investigated.[365-371] Liu et al.[372] prepared MgO nanoparticles (MgO NPs) stabilized by mesoporous carbon (mPC-MgO) through a fast pyrolysis of the $MgCl_2$-loaded waste biomass.[373] The obtained mPC-MgO showed excellent performance in the CO_2 capture process with the maximum capacity of 5.45 mmol g^{-1}, much higher than many other MgO based CO_2 sorbents. The CO_2 capture capacity of the mPC-MgO material kept almost unchanged in 19 runs, and could be regenerated at low temperature. Kim et al.[374] prepared multi-core MgO NPs@C core-shell nanospheres. 3 nm MgO NPs were embedded discretely in the carbon shell, which showed high selectivity for CO_2 over N_2. This composite also showed a high CO_2 uptake capacity (5.3 mmol CO_2 per g MgO) as well as high recyclability.

In addition, much attention has been paid to alkali metal promoted MgO. Potassium carbonate supported on MgO[375] has been reported to be capable of capturing CO_2 at elevated temperatures with good cycling stability. Webley et al.[376]

synthesized K_2CO_3 promoted $MgCO_3$ with a CO_2 uptake of 1.8 mmol g^{-1} at 375 °C and 1 bar. Liu et al.[377] synthesized Cs_2CO_3 doped MgO sorbent, and obtained the maximum CO_2 uptake of 1.9 mmol g^{-1} at 300 °C. The results suggested that the CO_2 chemisorption on Cs_2CO_3-doped MgO formed a mixed Mg−Cs carbonate phase with undetermined stochiometry, and the activation energy of this reaction route was lower than that of the carbonation of MgO at moderate temperatures. The formation of this mixed phase is the reason why Cs_2CO_3-doped MgO shows an improved CO_2 sorption capacity compared to pure MgO sorbent. The activity of MgO can also be improved via mixing with some other metal oxide such as TiO_2,[378, 379] and Al_2O_3,[380] etc. Han et al.[380] prepared nano-structured MgO-Al_2O_3 aerogel adsorbents with different Mg/Al molar ratios. The crystalline structure of MgO-Al_2O_3 aerogel adsorbents was transformed in the sequence of Al_2O_3 → $MgAl_2O_4$ → MgO-$MgAl_2O_4$ with increasing Mg/Al molar ratio from 0 to 3. The sorbents with Mg/Al = 0.5 with the highest medium basicity showed the best CO_2 capture capacity of 0.5 mmol g^{-1}. Although intensive efforts have been made to improve the capacity of MgO, the reported absorption capacities of MgO-based systems are still not high enough, which is likely to limit its wide use for CO_2 capture.[381] LDH-based and MgO-based adsorbents and their CO_2 capture performance are summarized in Table 8.

Table 8. Summary of LDH-based and MgO-based CO_2 adsorbents and their performance in CO_2 capture.

Adsorbent types	Schemes	Materials	CO_2 uptakes	References
LDH-based adsorbents	Intercalation of organic anions	Mg_3Al_1-stearate LDHs	1.3 mmol g^{-1} at 200 °C, 1 bar	335
	Hybrid materials	MgAl-CO_3 LDH/GO	0.5 mmol g^{-1} at 300 °C, 1 bar	336
	Control of particle size	nano-sized spherical Mg_3Al_1-CO_3 LDHs	0.6 mmol g^{-1} at 200 °C, 1 bar	349
	Alkali doping	Mg_3Al_1-stearate LDHs + K_2CO_3	1.9 mmol g^{-1} at 300 °C, 1 bar	382
		nano-sized spherical Mg_3Al_1-CO_3 LDHs + K_2CO_3	1.2 mmol g^{-1} at 200 °C, 1 bar	349
MgO-based adsorbents	Dispersing on supports	mPC-MgO	5.5 mmol g^{-1} at 80 °C, 1 bar	372
		MgO NPs@C	7.7 mmol g^{-1} at 27 °C, 1 bar	374
	Alkali doping	$MgCO_3$ + K_2CO_3	1.8 mmol g^{-1} at 375 °C, 1 bar	376
		MgO + Cs_2CO_3	1.9 mmol g^{-1} at 300 °C, 1 bar	377
	Preparation of mixed oxides	MgO/TiO_2 (4:6)	0.5 mmol g^{-1} at 25 °C, 1 bar	378, 379
		MgO-Al_2O_3 aerogel	0.5 mmol g^{-1} at 200 °C, 1 bar	380

4. High-temperature solid CO_2 sorbents

4.1 CaO-based sorbents

Calcium oxide (CaO) based materials are a type of high-temperature CO_2 sorbents with high theoretical sorption capacity and low cost. It has attracted tremendous attention owning to a number of its advantages.[383] A very nice review paper on the calcium looping cycle for large-scale CO_2 capture has been published by Blamey et al.[384] CaO-based sorbents can be used in both pre-combustion and post-combustion processes, which follow similar principles.[385-388] The whole CO_2 sorption process can be divided into two distinct steps. In the first step, CO_2 is chemically adsorbed on the surface of the sorbent; and in the second step, CO_2 diffuses into the bulk of the sorbent.[389] Thus, the exothermic carbonation reaction is characterized by two stages: (1) an initial fast surface reaction controlled by the reaction kinetics, and a (2) slower reaction restricted by the diffusion of CO_2 in the $CaCO_3$ product. In our previous review paper, we have pointed out that the main problem for calcium-based materials is the low reversibility of the carbonation reaction due to the sintering of sorbent particles. We noticed that, in the past three years, great efforts have been devoted to the improvement of sintering-resistant properties of CaO-based sorbents, which include (1) improving the synthesis method, (2) changing morphology and microstructure, (3) surface modification, (4) synthesis of CaO-based mixed oxides, (5) increasing attribution resistance, (6) reactivating the degraded sorbents, and (7) influence of SO_2, etc.

Various methods have been employed to decrease the particle size and increase the surface area of CaO, including precipitation reaction, bubble templating, interfacial reaction, ion liquid-assisted hydrothermal and solvothermal processes, etc.[390] For instance, with coprecipitation method, different calcium precursors could lead to CaO samples with different properties. Karami et al.[391] prepared CaO sorbents from $CaCl_2$ and $Ca(NO_3)_2$ respectively, and concluded $CaCl_2$ is a better precursor. The sol-gel method is well explored to produce reactive CaO sorbents. [392-394] Xu et al.[393] synthesized CaO-based sorbents composed of active CaO and inert $Ca_9Al_6O_{18}$ (acted as the support matrix) by a sol-gel method. In comparison with pure CaO, the sol-gel-derived sorbents had smaller grain sizes, larger surface areas, and highly interconnected pore networks as well as uniform distribution of CaO and $Ca_9Al_6O_{18}$. The synthetic sorbents exhibited high reactivity and stability in 35 carbonation-calcination cycles. With the CaO content of 70, 80, and 90 wt %, the CO_2 capture capacity at the 35th cycle was 11.4, 11.8, and 13.4 mmol g^{-1}, respectively. Similar results were also observed by Santos et al.[392] and Luo et al.[394]. Moreover, López-Periago et al.[395] reported that the

performance of CaO-based sorbents could be improved via preparation under supercritical condition.

Moreover, it is possible to obtain $CaCO_3$ with different degrees of purity and textural properties by utilizing various solvents, surfactants or organic additives.[390] Recently, Liu et al.[396] reported that the performance of CaO was enhanced by forming novel mesoscopic hollow spheres of $CaO/Ca_{12}Al_{14}O_{33}$ with tunable cavity size (Figure 12). It was believed that the void space in the hollow structures can buffer against the local large volume change during carbonation/calcination cycles, and is able to alleviate the pulverization and aggregation problem of the sorbent material, hence improving the cycling performance. Contrary to the microporous sorbents (< 2 nm), the mesoscopic sorbents (2–50 nm) are less susceptible to pore blockage and plugging through the increase of volume, while still retain a large surface area to ensure rapid kinetics. Furthermore, the inert $Ca_{12}Al_{14}O_{33}$ binders can effectively separate the CaO particles and thus act as a physical barrier to prevent sintering and aggregation of the CaO nanoparticles. The CO_2 capture capacity of the hollow sorbents was only slightly decreased after 30 cyclic runs, with remaining of about 91–98% adsorption capacities, which was much higher than that (23%) of the CaO sorbent calcined from a commercial $CaCO_3$ precursor.[396]

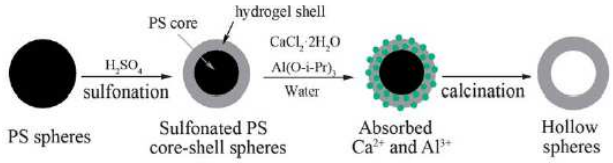

Figure 12. Diagram of the formation mechanism of the $CaO/Ca_{12}Al_{14}O_{33}$ hollowspheres.

To minimize the loss of activity and improve the life cycle performance of limestone, one method is to treat limestone with organic acids (acetic acid, formic acid, oxalic acid, etc)[397] or mineral acids (HCl, HBr, HI, and HNO_3)[398] to increase the sorbent porosity thus enhance the CO_2 capture capacity.[379, 399] Ridha et al.[397, 400] carried out a comprehensive assessment of the treatment on limestone with various organic acids to explore feasibility of this approach for modifying sorbents. The results showed that after 20 cycles, the carbonation conversion of limestone treated with acetic acid, vinegar, formic acid, and oxalic acid was 33.1%, 21.1%, 31%, and 35.2%, respectively, in contrast to 18.9% of the untreated limestone, clearly proving that the treatment with organic acids improved the sintering-resistance properties of the modified sorbent. However, the activities of these sorbents were declined in a similar fashion to that of untreated limestone. Moreover, the treated sorbents which performed well for CO_2 capture also performed well for SO_2 capture, leading their CO_2 capture capacity to decline at least as rapidly as the untreated natural sorbent or even more. Al-Jeboori et al.[398] studied the effects of mineral-acid (HCl, HBr, HI, and HNO_3) doping on the long-term reactivity of limestone-based sorbents, and found that limestones doped with low concentrations of a dopant led to a significant improvement in long-term carrying capacity, whereas doping to a greater extent yielded a marked reduction in capacity. It was proposed that the doping could shift the pore sizes in the calcined limestone to those of approximately the optimal diameter for repeated reaction.

For pure CaO sorbent, although its CO_2 capture capacity can be somehow improved by utilizing different synthesis methods, alerting the morphologies, crystal structures and porosities, or pretreatment with organic acids etc, the enhancement is still too marginal in most cases. Recently, it has been well established that the performance of CaO based sorbent can be significantly improved by the physically or chemically modification of pure CaO. As pointed out in our previous review paper,[9] a feasible way to enhance the stability of the CaO-based sorbents is to incorporate CaO particles into inert materials, which acts as structural supports or matrices. These inert materials include Al_2O_3,[401-405] MgO,[406, 407] TiO_2,[408] $KMnO_4$,[409] SiO_2,[410] $Ce_xZr_yO_z$,[411] La_2O_3,[412] $LaAl_xMg_yO_3$,[411] $CaZrO_3$,[413] etc. Among all the studied CaO-based mixed oxides sorbents, the most investigated is aluminum-containing material.[401, 402, 414] Martavaltzi et al.[415] prepared $CaO–Ca_{12}Al_{14}O_{33}$ sorbents by using different calcium precursors, $Ca(OH)_2$ and $Ca(CH_3COO)_2$, and found that the sorbent derived from $Ca(CH_3COO)_2$ exhibited higher CO_2 uptake ability, because the low tortuosity in its pores allowed easy access of CO_2 to the active sites of the sorbent. Liu et al.[406] developed a simple wet-mixing method to prepare sintering-resistant CaO-based sorbents using calcium L-lactate and aluminum lactate, and found that the support was not $Ca_{12}Al_{14}O_{33}$ but $Ca_9Al_6O_{18}$. Zhou et al.[416] synthesized a series of CaO-based CO_2 sorbents from various calcium and aluminum precursors by a wet-mixing method. The as-prepared sorbents consisted of active CaO and inert support materials that could be Al_2O_3, $Ca_{12}Al_{14}O_{33}$ or $Ca_9Al_6O_{18}$, depending on calcium and aluminum precursors used in the preparation process. Compared to pure CaO, most of the synthetic CaO-based sorbents showed much higher CO_2 capture capability and stability over multiple carbonation/calcinations cycles, which was ascribed to the relatively high specific surface area of the sorbents, the bimodal pore-size distribution with a fair number of small pores, and the inert support material that can effectively prevent or delay sintering of CaO particles. Among these synthetic sorbents the $CaO–Ca_9Al_6O_{18}$ sorbent with a CaO content of 80 wt% derived from calcium citrate and aluminum nitrate exhibited the best performance for CO_2 capture. Its CO_2 capture capacity decreased from 0.59 at the first cycle to 0.51 at the 28th cycle and correspondingly, the carbonation conversion reduced from 0.94 to 0.81, demonstrating high reactivity and stability of this sorbent over long-term cyclic operation.[416] Recently, Amos et al.[417] reported that the stability of CaO supported on mesoporous $Ca_xAl_yO_z$ is superior to that supported on macro/mesoporous hierarchical $Ca_xAl_yO_z$, and it was believed that the formed CaO layer might be too on the surface of macro/mesoporous structure.

MgO is another well studied supporting material for enhancing the sintering-resistant properties of CaO.[406, 418] Mabry et al.[419] revealed that the best MgO:CaO ratio was 0.6, which maintained its capacity at 86% of its original uptake even after 50 cycles. Wu

et al.[412] reported that TiO_2 can also be used for the improvement of sorption properties of CaO-based sorbent. Li et al.[409] demonstrated that the addition of $KMnO_4$ improved the long-term performance of $CaCO_3$, resulting in directly measured conversion as high as 0.35 after 100 cycles, while the untreated $CaCO_3$ retained conversion less than 0.16 under the same reaction conditions. Huang et al.[410] reported that the sorption capacity and long-term durability can be enhanced by using highly ordered mesoporous SBA-15 molecular sieves as carriers. Durability tests showed that the CO_2 adsorption ratio remained at 80% after 40 cyclic runs. Similar results have also been reported by Sanchez-Jimenez et al.[420] The silica supported CaO exhibited a stable CaO conversion under Ca-looping conditions. A 10 wt% CaO impregnated sorbent reached a stable conversion above 0.6, which was much larger than the residual conversion of CaO derived from natural limestone (between 0.07 and 0.08). Zhao et al.[413] synthesized CaO sorbent modified with $CaZrO_3$ which was in the form of ≤ 0.5 μm cuboid and 20−80 nm particles dispersed within the porous matrix of $CaO/CaCO_3$. The sample of 10 wt% $CaZrO_3$/90 wt% CaO showed an initial rise in CO_2 uptake capacity in the first 10 carbonation-decarbonation cycles, increasing from 7.0 mmol g^{-1} in cycle 1 to 8.4 mmol g^{-1} in cycle 10 and stabilizing at this value for the remainder of the 30 cycles tested, with carbonation at 650 °C in 15% CO_2 and calcination at 800 °C in air.

In addition to dispersing the CaO on inert supports, another scheme is to make CaO@porous metal oxides core@shell composite adsorbents. Li et al.[421] prepared $CaCO_3$@mesoporous silica in a core-shell structure (denoted as $CaCO_3$@$mSiO_2$) as a high-performance CO_2 sorbent. The improved carbonation conversion retention of the ($CaCO_3$@5.6 wt% $mSiO_2$)-based pellet sorbent was around 25% after 50 cycles of decarbonation/carbonation, which was higher than that of the $CaCO_3$-based sorbent (13%). It was believed that the mesoporous silica can serve as a stable framework structure and diffusion barrier for the improvement of the stable reversibility of the cyclic reaction.

It is well known that limestones are quite fragile, but the main factors and the mechanism on their attrition have not been well clarified, especially during calcination/carbonation for CO_2 capture.[422] Recently attempts have been made to improve the attrition resistance and CO_2 uptake of the Ca-based sorbent by making pellets with aluminate cement. Chen et al.[423] investigated the effects of various factors on attrition, and found they follow the order of temperature > superficial gas velocity > exposure time > pressure. CO_2 release during calcination of sorbents is the main reason for sorbent attrition and comminution. A slow decay in CO_2 capture capacity was observed for the pellets during cycling, because of the exposure of inner core of CaO sorbents by attrition and enhanced sintering resistance by adding the aluminate cement in the sorbent during pelletization. Chen et al.[424] further demonstrated that a much slower decay during multiple cycles could be obtained by adding 5–10 wt% pores forming agent. This was attributed to the large number of mesopores generated by the use of chemical agents and the exposure of inner core of CaO sorbents due to the attrition, which are in favor of CO_2 capture.

One important issue for CaO based sorbents for practical applications is how to reactivate the degraded sorbents.[425, 426] The reactivation of CaO using steam hydration has been widely reported in the literature, and there is an agreement on the fact that the positive effect of hydration is due to the improved morphology of the sorbent.[427, 428] It is suggested that the hydration causes the formation of cracks in the CaO particles, creating channels extending to the interior of the particles and, thus, improving CO_2 capture.[429] The formation of larger pores because of hydration also improves the performance of the sorbents because they become less susceptible to pore blockage.[430] Yin et al.[431] found that the water hydration of calcined limestone was independent of the factors, such as particle size, hydration duration, hydration temperature, and pre-calcination temperature. Also the conversion of hydrated limestone could not be further enhanced by ultrasonic hydration. In contrast, the synthetic CaO/cement sorbent showed strong dependence on those factors. In addition, the CaO conversion of the synthetic CaO/cement sorbent could be recovered to more than 80% by ultrasonic hydration. Li et al.[432] and Chen et al.[423, 433] modified the CaO derived from limestone in water with addition of ethanol and calcium lignosulfonate respectively and improved the conversion of CaO to nearly 60% after 15 cycles. Martínez et al.[434] found that if the reactivation of the sorbent by hydration was carried out at every cycle, the residual carrying capacity of the sorbent can be increased by a factor of 6.6. However, the steam consumption in these conditions may be unacceptably high (estimated over 1.2 mol of H_2O/mol of CO_2 captured). They also suggested that the reactivation by hydration may not be attractive in systems operating with particles that have moderate life spans.

Considering the fact that SO_2 is also produced from fossil fuel combustion, and can be captured by the Ca-based sorbents, it is necessary to investigate the effect of SO_2 on CO_2 capture behavior.[435, 436] Unfortunately, it is found that SO_2 in calcium looping systems decreases sorbent activity, as SO_2 irreversibly forms $CaSO_4$.[437-440] Sun et al.[441] reported that SO_2 impeded cyclic CO_2 capture because of pore blockage by sulfate products, resulting primarily from direct sulfation during the later stage of each cycle. This adverse effect of SO_2 was confirmed by Ryu et al.[442] and Lu and Smirniotis.[443] Therefore, despite the fact that sorbent performance can be influenced to some extent by altering carbonation and calcination conditions, the presence of SO_2 must be avoided if the objective is CO_2 capture from flue gas. Symonds et al.[444] suggested that the best way to avoid the effect of SO_2 is to desulfurize the flue gases in a separate reactor.[444, 445]

Up to date, all the research efforts regarding to CaO-based CO_2 sorbents can be briefly summarized in Figure 13. By utilizing different synthesis methods or pretreating limestone with acids, pure CaO particles with higher specific surface areas and smaller particle size, or special microstructures (e.g. hollow CaO, mesoporous CaO, etc) can be obtained. In order to further improve its performance, a more feasible approach is to make CaO-based mixed oxides type CO_2 sorbents. By incorporating

CaO particles into inert materials that act as structural supports or matrices, the durability can be significantly improved. Since CaO based CO_2 sorbents is very promising for practical applications, some other important issues have also been investigated, for instance the attribution, degraded sorbent reactivation, and the effect of SO_2, etc.[385] CaO-based adsorbents and their CO_2 capture performance are summarized in Table 9.

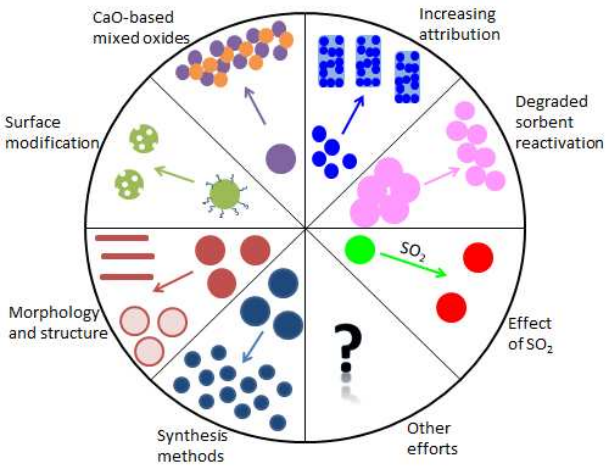

Figure 13. A brief summary of all efforts for improving the CO_2 capture capacity and sintering-resistant properties of CaO based sorbents.

Table 9. Summary of CaO-based sorbents and their performance in CO_2 capture.

Schemes	Materials	CO_2 uptakes at 1 bar	References
Improving synthesis method	CaO by coprecipitation	15.9 mmol g^{-1} after 17 cycles, sorption: 700 °C, desorption: 850 °C, 35% CO_2 in N_2	391
	CaO by sol-gel	5.5 mmol g^{-1} after 70 cycles, sorption: 700 °C, desorption: 800 °C, 15% CO_2 in N_2	392
	CaO by sol-gel	13.4 mmol g^{-1} after 35 cycles, sorption: 650 °C, desorption: 800 °C, 15% CO_2 in N_2	393
	CaO by sol-gel	11.6 mmol g^{-1} after 20 cycles, sorption: 650 °C, desorption: 800 °C, 15% CO_2 in N_2	394
	Synthetic CaO	14.8 mmol g^{-1} after 25 cycles, sorption: 750 °C, desorption: 900 °C, 20% CO_2 in N_2	395
Changing morphology and microstructure	CaO-$Ga_{12}Al_{14}O_{33}$ hollow sphere	14.1 mmol g^{-1} after 30 cycles, sorption: 650 °C, desorption: 900 °C, 100% CO_2	396
Surface modification	Organic acids modified CaO powder	5.7 mmol g^{-1} after 20 cycles, sorption: 650 °C, desorption: 850 °C, 15% CO_2 in N_2	397
	Organic acid modified CaO pellets	2.3 mmol g^{-1} after 20 cycles, sorption: 650 °C, desorption: 850 °C, 15% CO_2 in N_2	446
	Mineral acids modified CaO powders	6.8 mmol g^{-1} after13 cycles, sorption: 700 °C, desorption: 900 °C, 15% CO_2 in N_2	398
	Formic acid modified	7.0 mmol g^{-1} after 20 cycles, sorption: 650 °C, desorption: 850 °C, 15% CO_2 in N_2	400
Synthesis of mixed oxides	CaO-$Ga_9Al_6O_{18}$	13.4 mmol g^{-1} at 650 °C, 1 bar	416
	CaO/$Ca_xAl_yO_z$	9.8 mmol g^{-1} after 30 cycles, sorption: 700 °C, desorption: 850 °C, 15% CO_2 in N_2	417
	CaO/meso-SiC	3.0 mmol g^{-1} after 30 cycles, sorption: 690 °C, desorption: 850 °C, 15% CO_2 in N_2	417
	CaO/$Ca_{12}Al_{14}O_{33}$	7.3 mmol g^{-1} after 30 cycles, sorption: 690 °C, desorption: 850 °C, 15% CO_2 in N_2	415
	CaO/$Ca_{12}Al_{14}O_{33}$ nanospheres	13.9 mmol g^{-1} after 30 cycles, sorption: 650 °C, desorption: 900 °C, 15% CO_2 in N_2	447
	CaO-MgO	15.9 mmol g^{-1} after 50 cycles, sorption: 750 °C, desorption: 750 °C, 100% CO_2	419
	CaO-SiO_2	2 mmol g^{-1} after 50 cycles, sorption: 650 °C, desorption: 850 °C, 15% CO_2 in N_2	420
	CaO-$CaZrO_3$	8.4 mmol g^{-1} after 30 cycles, sorption: 650 °C, desorption: 800 °C, 15% CO_2 in N_2	413
	$CaCO_3$@meso porous silica	8.6 mmol g^{-1} after 50 cycles, sorption: 650 °C, desorption: 850 °C, 15% CO_2 in N_2	421

4.2 Alkali zirconates-based sorbents

Alkali zirconates such as Li_2ZrO_3 is another group of well-studied high-temperature CO_2 sorbents. The main obstacle for the practical application of Li_2ZrO_3 is its kinetic limitation. Previous efforts were made to improve its CO_2 capture performance via (1) changing the crystal structures, and (2) substituting partially substituting Li^+ with Na^+ or K^+. However, during the past three years, it seems the research activities with this type of materials were somehow declined, with only few papers published.

Previously, Li_2ZrO_3 was often prepared using solid-state

reaction method by mechanically mixing the starting materials of ZrO_2 and Li_2CO_3 and heating the mixture at high temperatures for a long time. Consequently, sintering at high temperatures normally results in large particle sizes of Li_2ZrO_3. To synthesize Li_2ZrO_3 sorbents with fine particle size, a liquid phase method has been applied.[448, 449] But the prepared Li_2ZrO_3 sorbents didn't possess the desired CO_2 capture properties due to a heterogeneous distribution of Li and Zr species in it. Alternatively, a citrate method was developed to synthesize Li_2ZrO_3 sorbents with improved CO_2 capture properties, which exhibited a faster CO_2 uptake rate and a higher, nearly stoichiometric absorption capacity at 550 ^oC and a CO_2 partial pressure of 0.5 bar. However, at lower CO_2 partial pressures, the sorbents still showed relatively lower uptakes.[450] Xiao et al.[450] synthesized K-doped Li_2ZrO_3 sorbents with excellent CO_2 capture properties via a citrate route, better than the Li_2ZrO_3-based ones, especially at low CO_2 partial pressures. At 550 ^oC and a CO_2 partial pressure of 0.25 bar, the CO_2 uptake in the K-doped Li_2ZrO_3 with an optimized molar ratio of K : Li : Zr at 0.2:1.6:1 reached 5.2 mmol g^{-1} within 15 min.

In addition to the synthesis work, some kinetic studies and modeling have also been performed to obtain a clearer understanding to the CO_2 sorption and desorption processes. Jiménez et al.[451] investigated the CO_2 sorption kinetics parameters including the reaction order, rate constant, apparent, intrinsic and diffusional activation energies on Na_2ZrO_3. A global reaction rate of first order in CO_2 and a strong dependence on temperature was found. The approximate solution to the shrinking core model was used to fit the data. Modeling results indicated the surface reaction as the main resistance to the reaction rate, controlling reaction kinetics with only a minor contribution of the product layer diffusion resistance toward the end of the reaction. Duan et al.[452] investigated the structural, electronic, and phonon properties of Li_8ZrO_6 using density functional theory and lattice phonon dynamics. The results indicated that the lithium zirconate with a lower Li_2O/ZrO_2 ratio has a lower turnover temperature. Hence, by mixing or doping two or more materials to form a new composite, it is possible to find or synthesize CO_2 sorbents that can fit the industrial needs for optimal performance. In short, the main problem for alkali zirconates-based CO_2 sorbents is still the slow kinetics and severely sintering during sorption/desorption cycles, and more works are highly desired for their practical applications.

4.3 Alkali silicates-based sorbents

In our previous review paper, alkali silicates were only briefly mentioned without a deep discussion.[9] However, tremendous efforts have been paid to this type of materials in the last few years. Up to date, a series of alkali silicates including Li_4SiO_4,[453] $Li_{4-x}Na_xSiO_4$,[454] $Li_{4+x}(Si_{1-x}Al_x)O_4$,[454] $Li_{4-x}(Si_{1-x}Al_x)O_4$,[454] Li_8SiO_6,[455, 456] $Li_6Si_2O_7$,[456] $Li_2Si_2O_5$,[456] $Li_2Si_3O_7$,[456] $CaSiO_3$,[457] $(OH)_3Al_2O_3SiOH$[458] have been studied for CO_2 absorption at high temperatures. The first alkali silicate that was reported for high-temperature CO_2 capture is Li_4SiO_4.[459-461] Since Li_4SiO_4 is synthesized from SiO_2, instead of ZrO_2 as for Li_2ZrO_4, it has been expected to be a promising CO_2 absorbent in the range of 500–850 ^oC. The main advantages of these materials are their high CO_2 capture capacity and relative lower regeneration temperatures (<750 ^oC) as compared to other high-temperature CO_2 sorbents such as CaO, and their excellent stability that allow operations over a significant number of cycles without losing their sorption capacity. Furthermore, Li_4SiO_4 shows lower costs of the raw materials involved comparing the expensive ZrO_2 with the cheaper SiO_2.[462] The absorption is ascribed to the mechanism whereby lithium oxide (Li_2O) in the Li_4SiO_4 crystal structure reacts reversibly with CO_2 as shown in Figure 14[463] and equation (1). Since Li_4SiO_4 has a considerably lower temperature for CO_2 emission in comparison with the CaO absorbent, the reaction between Li_4SiO_4 and CO_2 is easily reversible.

$$Li_4SiO_4 + CO_2 \rightarrow Li_2SiO_3 + Li_2CO_3 \quad (1)$$

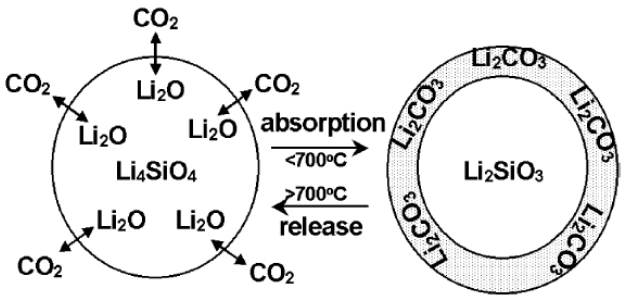

Figure 14. Reaction model of CO_2 absorption and emission by lithium silicate.[463]

The theoretical maximum CO_2 absorption is 1 mole for every mole of Li_4SiO_4. As a result, a capacity of more than 8.2 mmol g^{-1} should be possible. In practice, absorption up to around 8.0 mmol g^{-1} could be obtained at a temperature of 700 ^oC followed by complete release at 850 ^oC. In a typical measurement, Li_4SiO_4 absorbed CO_2 at a rate > 50 mg g^{-1} min^{-1} at 500 ^oC (which was roughly 30 times faster than Li_2ZrO_3 as reported by Kato et al.[464]) with a feed gas containing 20% CO_2. When the CO_2 concentration was lowered to 2% in the feed gas, the rate of CO_2 absorption by Li_2ZrO_3 became extremely low (< 0.23 mmol g^{-1} absorption after 50 min), while that of Li_4SiO_4 was 7.5 mg g^{-1} min and more than 5.7 mmol g^{-1} absorption could be achieved within 50 min. Therefore, the replacement of ZrO_2 with SiO_2 not only reduces the absorbent weight by 23%, but also significantly improves the CO_2 absorption rate and amount. Essaki et al.[465] found that the CO_2 absorption property of Li_4SiO_4 pellets was strongly affected by the absorption temperature. With 10% CO_2, the fastest CO_2 absorption was observed at the temperature between 550 and 600 ^oC. Only a very small amount of CO_2 absorption was observed at temperatures higher than 600 ^oC.

In most reports the studies were carried out in CO_2 atmospheres without the use of steam. The typical steam content during sorption enhanced hydrogen production processes is higher than 30%. Therefore, it is necessary to know the effect of

steam addition on the capture and regeneration properties and stability of these materials is important. Ochoa-Fernández et al.[466] observed that the presence of water in the form of steam could enhance the capture and regeneration rates. However, a large decay in the capacity was observed when compared to the performance of the sorbents in dry conditions. Another influencing parameter is the concentration of SO_2. Pacciani et al.[467] studied the influence of SO_2 on CO_2 absorption over Li_4SiO_4 and demonstrated that the presence of SO_2, even at concentrations as low as 0.002% resulted in an irreversible reaction with the absorbent and a decrease in CO_2 capacity. Analysis of SO_2-exposed samples revealed that the absorbent reacted chemically and irreversibly with SO_2 at 550 ^oC forming Li_2SO_4. It was thus suggested that industrial applications of Li_4SiO_4 should require desulfurization of flue gas prior to contacting the absorbent.

In order to further improve the CO_2 capture performance of Li_4SiO_4 sorbents, improvements have been made in several aspects, including (1) microstructural modification, (2) alkali promotion, (3) transition metal doping, (4) Li substitution by Na, etc. Romero-Ibarra et al.[468] proved ball milling could significantly increase the surface area (by 10 times) and enhance CO_2 uptake and durability. Seggiani et al.[462, 469] modified Li_4SiO_4 with different alkali carbonates (K_2CO_3, Na_2CO_3), binary (K_2CO_3/Li_2CO_3, Na_2CO_3/Li_2CO_3) and ternary ($K_2CO_3/Na_2CO_3/Li_2CO_3$) eutectic mixtures, and found that all the promoters noticeably improved the CO_2 uptake rate and sorption capacity. At the optimum absorption temperature of 580 ^oC, Li_4SiO_4 added with 30 wt% of K_2CO_3 or Na_2CO_3 showed the best CO_2 absorption proprieties with a sorption capacity of 5.2 mmol $g^{-1}_{sorbent}$ corresponding to a Li_4SiO_4 conversion of about 80%. However, the addition of Na_2CO_3 caused sintering during multiple sorption/desorption cycles reducing significantly the sorption capacity within the defined sorption time. Whereas, the sample added with 30 wt% K_2CO_3 maintained its original capacity during 25 CO_2 sorption/desorption cycles, showing an much higher cyclic stability.

Since the reaction of Li_4SiO_4 with CO_2 is assumed to occur at the outer surface of the crystal grain, ion diffusion of Li^+ and O^{2-} is required to facilitate the reaction with CO_2 to form lithium carbonate (Li_2CO_3).[470] Hence, generating defects in crystalline Li_4SiO_4 by appropriate doping of foreign elements is likely to improve the reactivity. This can be concluded from studies where interstitial Li^+ are created due to substitution of Si^{4+} by Al^{3+} or where vacancies originate from replacement of Li^+ by Al^{3+}. In both cases, Li^+-mobility and conductivity are increased as compared to that in non-modified Li_4SiO_4.[471, 472] However, since Li^+ is much smaller compared to O^{2-}, diffusion of the latter should be the limiting part of ion availability at the reaction surface. Hence doping vacancies into the Li_4SiO_4 lattice, which is assumed to facilitate O^{2-} hopping, is intended to improve reactivity substantially.[473] Gauer et al.[473] investigated doping of Li_4SiO_4 with hetero elements such as aluminum (Al) or iron (Fe) to improve its CO_2 capture capacity. An obviously higher reactivity of $Li_{3.7}Al_{0.1}SiO_4$ compared to $Li_{4.1}Al_{0.1}Si_{0.9}O_4$ proved the vacancy doping to be superior to interstitial doping regarding absorption of CO_2. The use of Fe instead of Al in $Li_{3.7}Fe_{0.1}SiO_4$ seems to be further advantageous since CO_2 is desorbed easier. In comparison, K-doped Li_4SiO_4 reveals problems with CO_2 emission even if absorption can be performed at slightly lower temperatures. Anyway, Fe doped Li_4SiO_4 should be recognized as a very promising modification for improved CO_2 absorption from about 500 ^oC. Ortiz-Landeros et al.[474] investigated the structural and thermochemical chemisorption of CO_2 on $Li_{4+x}(Si_{1-x}Al_x)O_4$ and $Li_{4-x}(Si_{1-x}V_x)O_4$ solid solutions, and found that the addition of Al and V had significant but differently influence on the CO_2 chemisorption process. On $Li_{4-x}(Si_{1-x}V_x)O_4$ samples, the CO_2 chemisorption is considerably diminished, while on $Li_{4+x}(Si_{1-x}Al_x)O_4$ samples, the CO_2 capture is markedly improved. In these two solid solutions, the product external shell is composed of Li_2CO_3 and Li_2SiO_3 in both cases, and the unique difference is the presence of Li_3VO_4 or $LiAlO_2$. Since Li_3VO_4 has a smaller lithium diffusion coefficient than Li_2CO_3, Li_2SiO_3 and $LiAlO_4$, the presence of Li_3VO_4 on the external shell must reduce the CO_2 chemisorption by decreasing the lithium diffusion.

It has been well demonstrated that some alkaline solid solutions, such as lithium-sodium zirconates ($Li_{2-x}Na_xZrO_3$) and lithium-potassium zirconates ($Li_{2-x}K_xZrO_3$), present better CO_2 capture properties than the pure lithium or sodium zirconates.[475-477] Moreover, it has been reported that even small quantities of a doping component, such as potassium, enhances the CO_2 capture capacity of lithium ceramics.[478] For this reason, Mejia-Trejo et al.[454] studied the synthesis of $Li_{4-x}Na_xSiO_4$ solid solutions and its performance for CO_2 capture. The $Li_{3.85}Na_{0.15}SiO_4$ sample showed a significant improvement on the CO_2 absorption, getting a total CO_2 absorption equal to 4.4 mmol g^{-1}. Also, the absorption seemed to be faster in this sample.

Apart from Li_4SiO_4 based sorbents, other lithium silicates have also been investigated as high-temperature CO_2 sorbents. Durán-Muñoz et al.[455] explored the CO_2 capture properties of a high lithium-content silicate (Li_8SiO_6) and found that it absorbed CO_2 over a wide range of temperatures. A CO_2 uptake of 11.8 mmol g^{-1} was achieved. The CO_2 chemisorption in the Li_8SiO_6 sample occurs via a two-step mechanism depending on the temperature range. Initially, the Li_8SiO_6 chemisorbs 2 moles of CO_2 to produce Li_4SiO_4, which subsequently traps a third mole of CO_2 to produce Li_2SiO_3 and an additional Li_2CO_3. However, the second reaction process only occurs at $T \leq 550$ ^oC. Later on, Duan et al.[456] investigated CO_2 capture properties of lithium silicates with different ratios of Li_2O/SiO_2 via an ab initio thermodynamic and experimental approach. By increasing the Li_2O/SiO_2 ratio (from $Li_2Si_3O_7$ up to Li_8SiO_6), the corresponding lithium silicates were found to have higher CO_2 capture capacities, higher turnover temperatures, and higher heats of reaction. Obviously, the lithium silicate with higher Li_2O/SiO_2 ratio will require more energy input to be regenerated at higher temperature. For the Li_2O-richlithium silicates (Li_8SiO_6, Li_4SiO_4, $Li_6Si_2O_7$), when the capture temperature is lower than the turnover temperature of Li_2SiO_3, they can absorb CO_2 to form Li_2CO_3 and SiO_2 with high CO_2 capture capacity. However, if the capture temperature is above the turnover temperature of Li_2SiO_3, the products will be Li_2CO_3 and Li_2SiO_3 with low CO_2 capture capacity. The SiO_2-

rich lithium silicates ($Li_2Si_2O_5$, $Li_2Si_3O_7$) can thermodynamically absorb CO_2 at relatively low temperature with low capture capacity. However, if the temperature is too low, the kinetics of CO_2 capture reaction is too slow. Wang et al.[457] reported the absorption of CO_2 on $CaSiO_3$ at high temperatures and realized that $CaSiO_3$ commenced to absorb CO_2 at 400 °C and ended at 800 °C with about 28.72% CO_2 absorption efficiency while using 15% CO_2. CO_2 sorption-desorption cycles were also stable. Alkali silicates-based adsorbents and their CO_2 capture performance are summarized in Table 10.

Table 10. Summary of alkali silicates-based sorbents and their performance in CO_2 capture.

Schemes	Materials	CO_2 uptakes	References
Microstructure modification	Li_4SiO_4	6.3 mmol g^{-1} at 500 °C, 20% CO_2	464
	Li_4SiO_4 pellet	6.3 mmol g^{-1} at 600 °C, 15% CO_2	465
	Li_4SiO_4	6.6 mmol g^{-1} at 525 °C, 10% CO_2	466
	Li_4SiO_4 pellet	6.8 mmol g^{-1} at 550 °C, 14.7% CO_2	479
	Li_4SiO_4	6.3 mmol g^{-1} after 16 cycles, sorption: 700 °C, desorption: 700 °C, 50% CO_2	480
	Li_4SiO_4	3.5 mmol g^{-1} after 10 cycles, sorption: 550 °C, desorption: 550 °C, 100% CO_2	468
Alkali promotions	Li_4SiO_4+ K_2CO_3/Na_2CO_3	5 mmol g^{-1} after 20 cycles, sorption: 580 °C, desorption: 700 °C, 4% CO_2	462
	Li_4SiO_4+ K_2CO_3 + Li_2TiO_3	5.7 mmol g^{-1} at 650 °C, 15% CO_2	467
Transition metal doping	Al and Fe doped Li_4SiO_4	5 mmol g^{-1} at 650 °C, 100% CO_2	473
	$Li_{4+x}(Si_{1-x}Al_x)O_4$	3.9 mmol g^{-1} at 700 °C, 100% CO_2	474
Li substitution by Na	$Li_{4-x}Na_xSiO_4$	4.4 mmol g^{-1} at 680 °C, 100% CO_2	454
	Li_8SiO_6	11.6 mmol g^{-1} at 650 °C, 100% CO_2	455
	Li_8SiO_6	7.0 mmol g^{-1} at 600 °C, 100% CO_2	456
	$CaSiO_3$	3.5 mmol g^{-1} after 10 cycles, sorption: 700 °C, desorption: 800 °C, 15%	457

5. Solid CO_2 sorbents from waste resource

Current waste management practices involving landfill contribute toward climate change, and may lead to water and soil contamination, and local air pollution. To minimize or address the growing environmental concerns associated with increasing amounts of waste being landfilled, many research activities are focusing on the development of new waste management strategies such as the preparation of useful materials from wastes. With the demand of huge amount of solid CO_2 sorbents, the development of low-cost materials that can sorb CO_2 efficiently will undoubtedly enhance the competitiveness of adsorptive separation for CO_2 capture in flue gas applications.[481] In 2012, Olivares-Marin et al.[481] published the first review paper on the preparation and application of CO_2 sorbents from waste precursors, including coal by-products, biomass products, water treatment by-products, household residues, and some other wastes, etc. Since then, there has been evidenced with active research activities in this area. To emphasize the importance, here we separately set a section to update the CO_2-sorbents from waste resource, although some of the CO_2-sorbents are discussed in the previous sections but obtained with different resources.

5.1 Carbon based CO_2 adsorbents from waste resource

According to United Nation Environment Programme (UNEP), globally 140 billion metric tons of biomass is produced per year from agriculture.[482] To fully resource these biomass wastes, one promising approach is to convert them into functional materials, such as carbon based CO_2 adsorbents. Up to date, various biomass wastes have been studied for the preparation of carbon-based CO_2 adsorbents, which can be categorized into four groups: (1) nut shells including almond shell,[483, 484] coconut shell,[485] palm shell,[486] (2) wood processing residues including sawdust,[48] chips and barks,[487] and poplar anthers,[488] etc, (3) food residues including coffee grounds,[489] bagasse,[490] celtuce leaves,[491] (4) marine macroalgae,[492] and (5) pitch, etc.

Nut shells are available in large quantities and contain high content of carbon element, which should be an ideal precursor for preparation of carbon-based CO_2 adsorbents. Plaza et al.[493, 494] prepared a series of carbon adsorbents from olive stones and almond, with a CO_2 capture capacities of 2.7 mmol g^{-1} at 25 °C, which are even higher than that of commercial activated carbons. The basic surface oxides formed during the carbonisation and activation processes have a beneficial effect on the CO_2 adsorption, and the pore size distribution also plays an important role in it, especially at low partial pressures.[483, 484] Vargas et al.[486] prepared activated carbon honeycomb-monoliths with different textural properties from African palm shells, which achieved a CO_2 sorption capacity of 5.8 mmol g^{-1} at 0 °C and 1 bar. Ello et al.[485] prepared microporous carbon from coconut shell and its maximum CO_2 uptake at 1 bar reached 3.9 and 5.6 mmol g^{-1} at 25 and 0 °C, respectively.

Another type of common biomass precursor for the preparation of carbon-based CO_2 adsorbents is wood processing wastes, such

as substandard kraft cellulose, hydrolysis lignin, chips, bark, and sawdust, etc. Dobele et al.[487] and Sevilla et al.[48] reported that the porous carbons obtained from solid waste of birch wood and sawdust could achieve a high CO_2 uptake of 3.6 and 4.8 mmol g^{-1} at 25 ^oC and 1 bar. Every spring innumerable brown granular poplar anthers fall on the land, and most of them are directly burnt as waste, which causes environmental pollution as well. Song et al.[488] synthesized nitrogen-containing granular porous carbons with developed porosities and controlled surface chemical properties from poplar anthers, and a CO_2 capture capacity as high as 51.3 mmol g^{-1} was achieved at 25 ^oC and 50 bar.

The third kind of biomass precursor for making carbon based CO_2 adsorbent is food residues such as coffee grounds,[489] bagasse,[490] and celtuce leaves,[491] etc. Coffee grounds can be considered as pollutant due to its high carbon content, which will consume large amount of oxygen for their degradation.[495] Plaza et al.[489] produced the microporous carbons from coffee grounds, which presented CO_2 adsorption capacities up to 4.8 mmol g^{-1} at 0 ^oC, and 3.0 mmol g^{-1} at 25 ^oC. Wang et al.[491] reported that porous carbons could be prepared from waste celtuce leaves, as shown in Figure 15(a).[487] The as-prepared porous carbon had a very high specific surface area of 3404 m^2 g^{-1} and a large pore volume of 1.88 cm^3 g^{-1}. The porous carbon exhibited an excellent CO_2 adsorption capacity at ambient pressures of up to 6.04 and 4.36 mmol g^{-1} at 0 and 25 °C, respectively.

The fourth approach for the preparation of carbon based CO_2 adsorbents is from ocean pollutant. Enteromorpha prolifera is a marine macroalgae that is becoming more common due to eutrophication and sequentially forms green tides, which impact ocean transportation, tourism and water quality. It is believed that the potentiality and feasibility for preparation of carbon-based CO_2 adsorbent from ocean pollutant is high if this kind of biomass can be utilized effectively.[492] Zhang et al.[492] synthesized nitrogen-containing porous carbon from enteromorpha prolifera with as much as 2.6% nitrogen in the as-prepared state, and it had a hierarchical structure with interconnected microporosity, mesoporosity and macroporosity. The inorganic minerals in the carbon matrix contributed to the development of mesoporosity and macroporosity by functioning as an in situ hard template. These carbons featured with high CO_2 capacity (2.4 mmol g^{-1} at 0 ^oC) and facile regeneration at room temperature (recovered 89% at 25 ^oC after eight cycles).

The fifth approach is for the preparation of carbon based CO_2 adsorbents is from pitch, which has been proposed by Wahby et al.[496] Recently, both Casco et al.[497] and Lee et al.[498] reported the synthesis of porous carbon by chemical activation of pitch using KOH. They found that such obtained carbon materials are good candidates for CO_2 capture, with a capacity of ca. 3.8–4.6 mmol g^{-1}.

5.2 Silica-based CO_2 adsorbents from waste resource

Besides carbon, solid waste is often used to make silica. Lin et al.[499] prepared silica spherical particles (MSPs) using sodium silicate extracted from TFT-LCD industrial waste powder inorganic acids including hydrochloric acids and nitric acids were employed to acidify the silicate supernatant to form activated silica precursors. The MSPs (HNO_3), which was synthesized in the presence of nitric acids exhibited high surface area (776 m^2 g^{-1}), mesopore size (5.3 nm) as well as large pore volume (1.15 cm^3 g^{-1}), and it was further applied as a support of adsorbent for CO_2 capture. It was demonstrated that TEPA-impregnated MSPs (HNO_3) adsorbent presented high adsorption performance (2.77 mol g^{-1}), superior to those of TEPA-SBA-15 and TEPA-MCM-41 manufactured from pure silica chemicals under the same test conditions. The results suggested that low-cost MSPs (HNO_3) prepared using silicate solution from TFT-LCD waste powder via spray approach is a promising CO_2 adsorbents.

5.3 CaO-based CO_2 sorbents from waste resource

For the preparation of CaO-based CO_2 sorbents, generally two types of wastes have been used, which are (1) eggshells and mussel shell,[500] shell fish, and cuttle fishbones,[501-503] and (2) paper industrial solid waste.[504] It is estimated that more than 45 million kg of eggshell waste are produced annually in the United States.[505] Eggshell waste is a serious concern for food industry due to the cost and environmental problems associated with their landfill, as each shell has adhered protein-rich membrane which attracts rats and other vermin.[506] However, eggshell waste, which contains 95% calcium carbonate ($CaCO_3$), presents itself as inexpensive calcium-based CO_2 sorbent. Ives et al.[500] found that the performance of eggshells and mussel shells derived CaO-based sorbents over the course of up to ~50 cycles of calcination and carbonation was significantly superior to limestone derived CaO sorbent. Sacia et al.[501] tested the eggshell waste for CO_2 capture via cyclic carbonation-calcination reactions. The regeneration of spent sorbents with acetic acid provided a 38% improvement in CaO conversion over untreated shells after ten cycles. The eggshell membrane contains highly valuable Type X collagen, which can be recovered through the course of shell pretreatment to increase process feasibility (Figure 15(b)). This scheme allows for sustainable generation of CaO sorbents while also transforming a current waste material into a value-added product. CaO sorbent has also been prepared from high calcium content alimentary wastes including egg shells, shellfish shells and cuttlefish bones by Castilho et al.[502] These results indicate that alimentary wastes with high calcium content can be used to produce CO_2 sorbents thus contributing to mitigate the anthropogenic carbon and the environment contamination with alimentary wastes.[502]

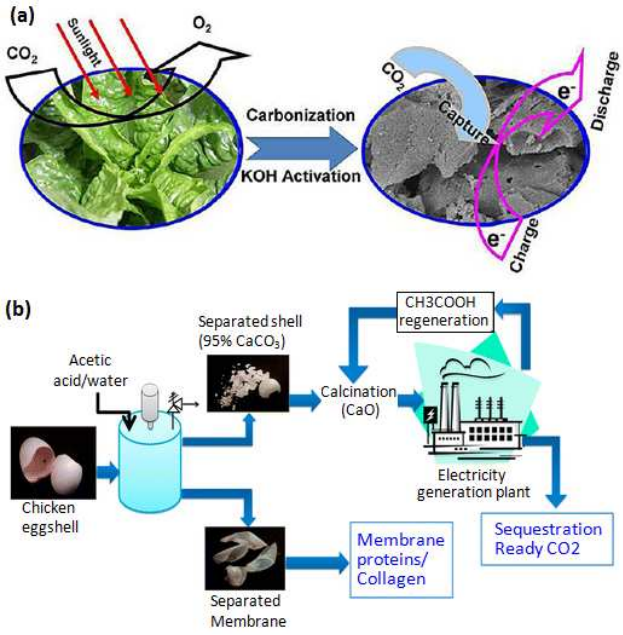

Figure 15. (a) The synthesis scheme of porous carbon from waste celtuce leaves.[487] (b) The synthesis scheme of CaO based CO_2 sorbents from eggshells.[501]

Every year, very large amounts of calcium-based solid wastes such as carbide slag (from the chlor-alkali industry), red mud (from the aluminum industry), and lime mud (from the paper industry) containing $Ca(OH)_2$ or $CaCO_3$ are produced. Lime mud is a solid waste produced as part of the process that turns wood chips into pulp for paper. Li et al.[504] investigated the sequential SO_2 and CO_2 capture behaviour of lime mud in the calcium looping process. In order to minimize the unfavorable effects of impurities such as Na and Cl on CO_2 and SO_2 capture by lime mud, the lime mud was prewashed with distilled water. The carbonation conversions of the raw lime mud and treated lime mud were stable with the number of cycles, and were about 0.21 and 0.36 after 100 cycles, respectively. Compared with the natural limestone, the treated lime mud exhibited a lower carbonation conversion during the first five cycles; however, it showed a higher carbonation conversion after five cycles. The ultimate carbonation conversions of the treated lime mud and the raw one were 4.8 and 2.8 times greater than that of the limestone, respectively.

5.4 Alkali silicate-based CO_2 sorbents from waste resource

For the synthesis of alkali silicate based CO_2 sorbents, three types of wastes have been utilized, which include (1) fly ash (FA),[507] (2) rice husk ash,[488, 508] and (3) diatomite,[480, 509] etc. FA is the finely divided mineral residue resulting from the combustion of ground or powdered coal in power plants. The disposal of FA causes significant economic and environmental problems all over the world. Olivares-Marin et al.[507] synthesized several Li_4SiO_4-based sorbents from FAs for CO_2 capture at high temperatures. Under the optimal experimental conditions (600 °C and 40 mol% K_2CO_3), the maximum CO_2 sorption capacity for the sorbent derived from FA was 2.4 mmol g^{-1}. The Li_4SiO_4-based sorbents could maintain its original capacity during 10 cycle processes and reach the plateau of maximum capture capacity in less than 15 min, while pure Li_4SiO_4 presented a continual upward tendency in the 15 min of the capture stage but didn't achieve the equilibrium capacity.

Table 11. Summary of solid sorbents synthesized from waste resource and their performance in CO_2 capture.

Sorbents	Waste type	CO_2 uptake	Reference
Carbon	Olive stones	2.43 mmol g^{-1} at 25 °C, 1 bar	506
	Almond shell	2.66 mmol g^{-1} at 25 °C, 1 bar	507
	African palm shells	5.8 mmol g^{-1} at 0 °C, 1 bar	486
	Coconut shell	5.6 mmol g^{-1}at 0 °C, 1 bar	485
	Birch wood	15.91mmol g^{-1} at 25 °C, 20 bar	487
	Starch and cellulose, sawdust	4.8 mmol g^{-1} at 25 °C, 1 bar	48
	Coffee grounds	4.8 mmol g^{-1} at 0 °C, 1 bar	489
	Bagasse	0.2 mmol g^{-1} 75 °C, 1 bar	490
	Celtuce leaves	6.04 mmol g^{-1} at 0 °C, 1 bar	491
	Enteromorpha prolifera	2.40 mmol g^{-1} at 0 °C, 1 bar	492
Silica	Industrial waste powder Inorganic acids	2.77 mol g^{-1} at 25 °C, 1 bar	499
CaO	Eggshell waste	14.29 mmol g^{-1} at 700 °C, 1 bar	501
	Egg shells	6.82 mmol g^{-1} at 700 °C, 1 bar	502
	Scallops	6.36 mmol g^{-1} at 700 °C, 1 bar	502
	Cuttlefish bones	4.09 mmol g^{-1} at 700 °C, 1 bar	502
	Lime mud	7.14 mmol g^{-1} at 700 °C, 1 bar	504
Alkali	Fly ash	2.40 mmol g^{-1} at 600 °C, 1	507

silicate		bar	
	Rice husk ash	7.36 mmol g^{-1} at 710 ^{o}C, 1 bar	510
	Diatomite	6.50 mmol g^{-1} at 620 ^{o}C, 1 bar	480

Compared with FA, rice husk ash has higher amorphous SiO_2 content. Moreover, it also contains some metals, which may generate high-performance Li_4SiO_4-based sorbents for CO_2 capture. Wang et al.[508] synthesized highly efficient Li_4SiO_4-based sorbents for CO_2 capture from rice husk ash. At 650 ^{o}C, the sorption of CO_2 increased to 4.1 mmol g^{-1} within 2.5 h. More importantly, the CO_2 uptake remained almost unchanged even after 15 cycles. It seems that the presence of metals in the Li_4SiO_4-based sorbent promoted the reaction kinetic of the CO_2 sorption when compared with pure Li_4SiO_4. Isothermal analysis further indicated the activation energies of the Li_4SiO_4-based sorbents prepared from rice husk ash are smaller than that of pure Li_4SiO_4. Later on, its CO_2 capture capacity was further increased to 6.92 mmol g^{-1} via citric acid pretreatment of rice husk ash by the same group.[488]

Taking into account the significant content of SiO_2 in diatomite, the synthesis of Li_4SiO_4-based CO_2 sorbent from diatomite has also been proposed, with the aim to further decrease the cost of Li_4SiO_4. Shan et al.[480] demonstrated that the SiO_2 source has an important influence on CO_2 sorption properties. The sample with diatomite had higher sorption capacity and sorption rate than that with pure SiO_2 at the same retaining time. The maximum sorption capacity of the sample with diatomite reached 6.5 mmol g^{-1}, being 78% of the theoretical sorption capacity. In addition, lower activation energies of the sample with diatomite for the chemisorption process and diffusion process were also observed, which was attributed to the structural differences caused by the aluminum and other elements present on the diatomite. Solid CO_2 sorbents synthesized from waste resource and their performance for CO_2 capture are summarized in Table 11.

6. Techno-economic assessment of CO_2 sorbents in real applications

For the research of CO_2 capture, besides the development of efficient CO_2 sorbents, another important and urgent issue is the techno-economic assessment of these sorbents/technologies in real applications. However, we will not give too much detail due to the limited length allowed for this review.[511, 512] Recently, Zhao et al.[511] performed a critical review of the techno-economic models for the retrofitting of conventional pulverised-coal power plants for post-combustion CO_2 capture. They compared four promising technologies for the post-combustion CO_2 capture that can be retrofitted to a conventional pulverised-coal power plant. By comparing the efficiency penalty and cost indicators of CO_2 capture using (i) chilled ammonia, (ii) alkali-metal carbonates, (iii) membranes or (iv) calcium looping to the benchmark MEA scrubbing process, it was found that calcium looping technology resulted in the lowest efficiency penalty (4.6%-points) and cost of post-combustion CO_2 capture (36.3% increase in levelised cost of electricity). In addition, the cost of CO_2 avoided by employing calcium looping for post-combustion CO_2 capture can be as low as 29 USD_{2010} per tCO_2. On these three criteria, calcium looping performs more than twice as well as the benchmark MEA post-combustion CO_2 capture process.[511]

Hurst et al.[512] examined the lifecycle greenhouse gas emissions of a 500 MW_e pulverised coal-fired power plant with post-combustion calcium looping and off-shore geological storage. calcium looping uses solid CO_2-sorbent derived from abundant and non-toxic limestone and is currently being piloted at the 1–2 MW_{th} scale in Europe (Spain and Germany). This technology promises to be very competitive with the more mature chemical absorption processes, with the potential to reduce the efficiency and cost penalties of CO_2 capture. It has been demonstrated that the emission intensity of a coal-fired power plant with calcium looping is at least comparable with one using MEA-solvent technology (i.e., ~229 gCO_2e/kWh vs. 225 gCO_2e/kWh). However, there is significant potential for additional emissions reduction when considering the recarbonation of exhausted sorbent in landfill.[512] Dean et al.[513] have demonstrated that it is possible to use the spent sorbent from a promising CO_2 capture process, the calcium looping cycle, for cement production, which might be able to further reduce the cost of CO_2 capture.

To have a thorough understanding to the impact of site-specific factors on the feasibility of CO_2 capture at industrial plant level, Berghout et al.[514] did a techno-economic analysis and made an inventory of potential implementation or operational challenges related to the precombustion, postcombustion, and oxyfuel CO_2 capture technologies applied to five industrial plants from various industrial sectors. The results showed that CO_2 capture at the boilers, furnaces, catalytic crackers and gasifier of the refineries resulted in CO_2 reductions of 64–75% for oxyfuel and pre-combustion technology. For the post-combustion configurations, CO_2 was also captured from the hydrogen plants, combined heat and power plants and gas turbine, resulting in CO_2 reductions of 81–87%. By combining oxyfuel and pre-combustion with post-combustion technology for the hydrogen plants and utilities, significantly higher CO_2 reductions (80–96%) were calculated for the refineries. While combining oxyfuel and postcombustion technology resulted in higher CO_2 avoidance costs, the combination of pre- and post-combustion technology showed slower CO_2 avoidance costs (6–17%), due to economies of scale of shared absorbers and strippers. The study also suggests that CO_2 avoidance costs also depend significantly on industrial plants, not only because of the difference in economies of scale, but also in CO_2 concentrations in flue gases. Implementation issues associated with short term configurations revolve mainly around retrofitting process units. Although retrofitting is technically feasible for all three capture technologies, it still should be proved on a commercial scale. The long term results are more indicative than the short term results, due to cost data uncertainty and the long time frame in which possible plant layout changes may take place. Expectations for the long term are that the focus will shift from retrofit issues to the replacement of old process units with new-built capture-ready process units. Furthermore,

long term configurations will probably have minimal spatial constraints in (new-built) plant lay outs, capture technologies that are highly integrated with core processes, and optimized utility plants. These factors are expected to have a damping effect on the projected long term CO_2 avoidance costs.[514]

The cement industry is a significant industrial greenhouse gas (GHG) emitter, and the emission reduction is expected to be achieved via application of CCS technologies. However, the successful implementation of CO_2 capture technologies in the cement industry will depend not only on the technical performance, but also on the assessment of energy recovery potential. Hence, Vatopoulos et al.[515] assessed the viability of three CO_2 capture technologies for the cement manufacturing process. Post-combustion absorptive capture (MEA) and oxy-combustion options are concepts already used by other industries and currently explored by the power sector; calcium looping post-combustion capture technology (CL) is an emerging technology that has not been assessed before in a comparative manner. The comparison was carried out in terms of specific energy consumption, CO_2 footprint, CO_2 capture energy penalty, raw material consumption and energy recovery potential, by modeling of the integration of these process concepts with a reference cement plant. The results showed that for the same capture efficiency (85%), calcium looping has an advantage as the specific energy consumption increases by 18%. In the case of MEA the increase is 45%. CL also has considerably higher energy recovery potential, which can also further reduce its CO_2 footprint. However, chemical looping demonstrates a higher complexity of integration with an existing cement plant. Oxy-combustion, though showing lower capture efficiency (60%), results in lower specific energy consumption than the base case cement plant, which causes a negative CO_2 capture penalty. These results contribute to the identification of the most suitable CO_2 reducing strategy for the cement industry.[515]

The technical and economic assessment of sorption enhanced water gas shift (SEWGS) as an innovative technology for CO_2 capture has been well investigated. In this process, CO_2 capture or removal of CO_2 from the products of WGS reaction is expected to shift the reaction to the desired direction for H_2 production and CO reduction. Gazzani et al.[516] evaluated the thermodynamic performances of CO_2 capture in natural gas combined cycle with SEWGS. The SEWGS working conditions were optimized in terms of carbon capture ratio and purity of the CO_2 separated as well as number of vessels adopted. Moreover, two different types of sorbent, Sorbent Alfa and Sorbent Beta, were considered in order to evaluate the impact of sorbent cyclic capacity on system performances. Results showed that SEWGS with Sorbent Alfa could avoid 91% of CO_2 emissions and reduce the efficiency penalty of amine scrubbing technologies from 8.4% to 7.2%. However, no significant impact of CO_2 purity on system performances was determined. While for the adoption of Sorbent Beta, which has an improved capacity of 60% than Sorbent Alfa, further reduction in specific primary energy consumption for CO_2 avoidance together with vessel number were observed. The best overall performance in terms of specific primary energy consumption for CO_2 avoided had a net electrical efficiency of 51.93 % and CO_2 avoidance of 86%. Manzolini et al.[516] did the economic assessment for CO_2 capture in natural gas combined cycle with SEWGS. Results showed that with reference sorbent performances the calculated cost of CO_2 avoided is about 58 € t^{-1} CO_2, which is lower than reference MDEA (64 € t^{-1} CO_2) but higher than MEA (48.5 € t^{-1} CO_2). The adoption of a sorbent with improved performances brings down the cost of CO_2 avoided down to 49 € t^{-1} CO_2, which is comparable to post combustion technology. This is a consequence of reforming sections costs which penalizes pre-combustion technologies: specific investment costs for SEWGS cases are 15% higher than MEA. Finally, as far as SEWGS working conditions are concerned, the optimal CO_2 capture rate depends on the sorbent cyclic capacity ranging from 90% to 95%, while the selected CO_2 purity is 99%. Knoope et al.[517] investigated the technological and economic prospects of integrated gasification facilities for power (IGCC) and Fischer–Tropsch (FT) liquid production with and without CCS over time. For this purpose, a component based experience curve was constructed and applied to identify the potential performance improvement of integrated gasification facilities. The results also indicated that substantial cost reductions and performance improvements are possible, especially for IGCC with CCS. Afterwards, Chen et al.[518] investigated the IGCC process incorporated with CaO sorbent by modeling and simulating using Aspen Plus software. The results showed IGCC with CaO sorption-enhanced process has a satisfactory system performance. Even though the net electricity efficiency was not as high as expected, just around 30–33%, the system had a high CO_2 capture efficiency of ca. 97% and low pollutant emissions. Moreover, compared with conventional IGCC–CCS, the schematic diagram of the IGCC–CCS process is simplified.

Conclusions

In this paper, the most recent research progress in solid CO_2 capture materials has been thoroughly reviewed. All the materials are divided into three main groups according to their working temperature ranges, which are (1) low temperature CO_2 adsorbent (< 200 ^oC), (2) intermediate temperature CO_2 sorbents (200–400 ^oC), and high temperature CO_2 sorbents (> 400 ^oC). The low temperature CO_2 sorbents can be further classified into two groups. The first group includes carbon-based (including graphite/graphene-based), zeolite-based, MOF-based, silica-based, polymer-based, and clay-based, etc, which adsorb CO_2 mainly by physical interaction. The second group includes solid amine-based, alkali metal carbonate-based, immobilized ion liquid-based, and alkali metasilicates, etc, which capture CO_2 mainly by chemical binding. For the first group, the CO_2 capture can be mainly attributed to their high specific surface areas and nano-sized pores, etc, due to which their selectivity towards CO_2 is relatively low. In order to improve their CO_2 capture capacity and selectivity, several schemes have been developed, such as microstructure and morphology control, composition optimisation, cation exchange, surface modification, hybrid materials, etc. In particular, impregnating or grafting certain types of solid amines and ILs on the above porous materials has been well recognized as promising approaches. For these low temperature CO_2 adsorbents, much effort has been directed towards enhancing

their thermal stability, resistance to moisture, selectivity, durability, and kinetics, etc. Of course, another big concern is the cost of the materials, which is crucial for large scale industrial applications. For intermediate temperature CO_2 sorbents, LDHs derived mixed oxides and MgO represent the majority. Much progress has been made during the last 3 years, including the use of organic anions to enlarge the interlayer distance, the preparation of LDH hybrid materials, the control of LDH particle size, and the method for alkali carbonates doping. Some more in-depth mechanism investigations have also been performed. Up to date, the CO_2 sorption capacity of LDH derived sorbents already seems very promising and the major remaining issue is to figure out how to maintain its mechanical strength in the presence of steam and at high temperatures. Although intensive efforts have been made to improve the capacity of MgO, the reported sorption capacities of MgO-based systems are still not high enough, hence potentially limiting its wide use for CO_2 capture. For high temperature CO_2 sorbents, CaO has a high CO_2 uptake capacity, but suffers severely from sintering during regeneration. One of the most feasible approaches is to incorporate CaO particles into inert materials that act as structural supports or matrices, by which the durability can be significantly improved. For the practical applications of CaO-based materials, some other important issues should be considered as well, for instance, the attribution, degraded sorbent reactivation, and the effect of SO_2, etc. The research activities on alkali zirconates have somehow declined and more attention has been directed towards alkali silicates. For instance, Li_4SiO_4 has shown high CO_2 capture capacity and relatively lower regeneration temperatures (<750 ^oC) when compared to CaO, and it is also cheaper in raw materials when compared to alkali zirconates.

Another important part of this review paper is the preparation of CO_2 sorbents from waste resources, such as carbon-based adsorbent from various nut shells, wood and food residues, silica-based adsorbent from industrial waste, CaO-based sorbents from egg shells, fishbones, paper industrial solid wastes, and alkali silicates from fly ash, rice husk ash, and diatomite. Finally, the techno-economic assessments of several CO_2 sorbents /technologies in real applications have been briefly reviewed. All results have shown that it is very promising and necessary to integrate the CO_2 sorbents into the current operating systems, either for decreasing the energy penalty or capturing CO_2.

Acknowledgements

This work is supported by the Fundamental Research Funds for the Central Universities (TD-JC-2013-3), the Beijing Nova Programme (Z131109000413013), the Program for New Century Excellent Talents in University (NCET-12-0787), the National Natural Science Foundation of China (51308045), the Key Laboratory of Functional Inorganic Material Chemistry (Heilongjiang University), and the Foundation of State Key Laboratory of Coal Conversion (Grant No. J14-15-309), Institute of Coal Chemistry, Chinese Academy of Sciences. Z. Z thanks the kind support of ICES under A*Star to this research and collaboration.

Notes and references

[a] *College of Environmental Science and Engineering, Beijing Forestry University, 35 Qinghua East Road, Haidian District, Beijing 100083, P. R. China. Tel: +86-13699130626; E-mail: qiang.wang.ox@gmail.com, qiangwang@bjfu.edu.cn*

[b] *Chemistry Research Laboratory, Department of Chemistry, University of Oxford, Mansfield Road, Oxford, OX1 3TA, UK*

[c] *Institute of Chemical and Engineering Sciences, Agency for Science, Technology and Research in Singapore (A*STAR), 1 Pesek Road, Jurong Island, 627833 Singapore. Tel: +65-67963809; E-mail: zhong_ziyi@ices.a-star.edu.sg*

‡ Footnotes should appear here. These might include comments relevant to but not central to the matter under discussion, limited experimental and spectral data, and crystallographic data.

References

1. M. Mikkelsen, M. Jørgensn and F. C. Krebs, *Energy Environ. Sci.*, 2010, **3**, 43.
2. P. N. Pearson and M. R. Palmer, *Nature*, 2000, **406**, 695.
3. J. Lu, M. Cheng, Y. Ji and Z. Hui, *J. Fuel Chem. Technol.*, 2009, **37**, 740.
4. *http:// srippscO2.ucsd.edu/data/atmospheric_CO2.html*.
5. W. Liu, D. King, J. Liu, B. Johnson, Y. Wang and Z. Yang, *JOM*, 2009, **61**, 36.
6. E. A. Roth, S. Agarwal and R. K. Gupta, *Energy Fuels*, 2013, **27**, 4129.
7. M. K. Mondal, H. K. Balsora and P. Varshney, *Energy*, 2012, **46**, 431.
8. J. D. Figueroa, T. Fout, S. Plasynski, H. McIlvried and R. D. Srivastava, *Int. J. Greenhouse Gas Control*, 2008, **2**, 9.
9. Q. Wang, J. Luo, Z. Zhong and A. Borgna, *Energy Environ. Sci.*, 2011, **4**, 42.
10. M. Olivares-Marin and M. Maroto-Valer, *Greenhouse Gases Sci. Technol.*, 2012, **2**, 20.
11. *US Pat.,* 1783901, 1930.
12. G. T. Rochelle, *Science*, 2009, **325**, 1652.
13. B. P. Mandal and S. S. Bandyopadhyay, *Chem. Eng. Sci.*, 2006, **61**, 5440.
14. M. L. Gray, Y. Soong, K. J. Champagne, J. Baltrus, R. W. Stevens Jr., P. Toochinda and S. S. C. Chuang, *Sep. Purif. Technol.*, 2004, **35**, 31.
15. R. V. Siriwardane, M. S. Shen, E. P. Fisher and J. A. Poston, *Energy Fuels*, 2001, **15**, 279.

16. T. Tsuda, T. Fujiwara, Y. Takteani and T. Saeguas, *Chem. Lett.*, 1992, **21**, 2161.

17. S. Lee, T. P. Filburn, M. Gray, J. W. Park and H. J. Song, *Ind. Eng. Chem. Res*, 2008, **47**, 7419.

18. M. Schladt, T. P. Fiburn and J. J. Helble, *Ind. Eng. Chem. Res.*, 2007, **46**, 1590.

19. R. A. Khatri, S. S. C. Chuang, Y. Soong and M. Gray, *Energy Fuels*, 2006, **20**, 1514.

20. R. L. Burwell and O. Leal, *J. Chem. Soc., Chem. Commun.*, 1974, 342.

21. *US Pat.,* 6364938B1, 2000.

22. *US Pat.,* 2002083833A1, 2002.

23. W. R. Alesi and J. R. Kitchin, *Ind. Eng. Chem. Res*, 2012, **51**, 6907.

24. B. Ochiai, K. Yokota, A. Fujii, D. Nagai and T. Endo, *Macromolecules*, 2008, **41**, 1229.

25. X. Xu, C. Song, J.M. Andresen, B.G. Miller and A.W. Scaroni, *Energy Fuels*, 2002, **16**, 1463.

26. N. Linneen, R. Pfeffer and Y. S. Lin, *Microporous Mesoporous Mater.*, 2013, **176**, 123.

27. J.M. Chem, P. Bollini, S.A. Didas and C.W. Jones, *J. Mater. Chem.*, 2011, **21**, 15100.

28. W.J. Son, J.S. Choi and W.S. Ahn, *Microporous Mesoporous Mater.*, 2008, **113**, 31.

29. G. Qi, Y. Wang, L. Estevez, X. Duan, N. Anako, A. H. A. Park, W. Li, C. W. Jones and E. P. Giannelis, *Energy Environ. Sci.*, 2011, **4**, 444.

30. A. Danon, P. C. Stair and E. Weitz, *J. Phys. Chem. C*, 2011, **115**, 11540.

31. D. J. Fauth, M. L. Gray, H. W. Pennline, H. M. Krutka, S. Sjostrom and A. M. Ault, *Energy Fuels*, 2012, **26**, 2483.

32. K. S. Lackner, *Eur. Phys. J. Special Topics*, 2009, **176**, 93.

33. T. Wang, K. S. Lackner and A. Wright, *Environ. Sci. Technol.*, 2011, **45**, 6670.

34. A. P. Hallenbeck and J. R. Kitchin, *Ind. Eng. Chem. Res*, 2013, **52**, 10788.

35. H. B. Wang, P. G. Jessop and G. Liu, *ACS Macro Letters*, 2012, **1**, 944.

36. A. L. Chaffee, G. P. Knowles, Z. Liang, J. Zhang, P. Xiao and P. A. Webley, *Int. J. Greenhouse Gas Control*, 2007, **1**, 11.

37. M. B. Yue, L. B. Sun, Y. Cao, Y. Wang, Z. J. Wang and J. H. Zhu, *Chem. Eur. J.*, 2008, **14**, 3442.

38. Y. Belmabkhout, R. Serna-Guerrero and A. Sayari, *Ind. Eng. Chem. Res.*, 2010, **49**, 359.

39. R. Sanz, G. Calleja, S. Arencibia and E. S. Sanz-Perez, *Appl. Surf. Sci.*, 2010, **256**, 5323.

40. A. Diaf, J. L. Garcia and E. J. Bechman, *J. Appl. Polym. Sci.*, 1994, **53**, 857.

41. A. Diaf and E. J. Bechman, *React. Funct. Polym.*, 1995, **27**, 45.

42. Y. Liu, Q. Ye, M. Shen, J. Shi, J. Chen, H. Pan and Y. Shi, *Environ. Sci. Technol.*, 2011, **45**, 5710.

43. P. Bollini, S. Choi, J. H. Drese and C. W. Jones, *Energy Fuels*, 2011, **25**, 2416.

44. J. Wang, D. Long, H. Zhou, Q. Chen, X. Liu and L. Ling, *Energy Environ. Sci.*, 2012, **5**, 5742.

45. T. C. Drage, O. Kozynchenko, C. Pevida, M. G. Plaza, F. Rubiera, J. J. Pis, C. E. Snape and S. Tennison, *Energy Proc.*, 2009, **1**, 599.

46. A. Arenillas, K. M. Smith, T. C. Drage and C. E. Snape, *Fuel*, 2005, **84**, 2204.

47. V. Jiménez, A. Ramírez-Lucas, J. A. Díaz, P. Sánchez and A. Romero, *Environ. Sci. Technol.*, 2012, **46**, 7407.

48. M. Sevilla and A. B. Fuertes, *Energy Environ. Sci.*, 2011, **4**, 1765.

49. S. Y. Lee and S. J. Park, *J. Colloid Interface Sci.*, 2013, **389**, 230.

50. N. P. Wickramaratne and M. Jaroniec, *J. Mater. Chem. A*, 2013, **1**, 112.

51. J. P. Marco-Lozar, M. Kunowsky, F. Suarez-Garcia and A. Linares-Solano, *Carbon*, 2014, **72**, 125.

52. C. Robertson and R. Mokaya, *Microporous Mesoporous Mater.*, 2013, **179**, 151.

53. J. Wang, A. Heerwig, M. R. Lohe, M. Oschatz, L. Borchardt and S. Kaskel, *J. Mater. Chem.*, 2012, **22**, 13911.

54. T. C. Drage, A. Arenillas, K. M. Smith, C. Pevida, S. Piippo and C. E. Snape, *Fuel*, 2007, **86**, 22.

55. M. L. Gray, Y. Soong, K. J. Champagne, J. Baltrus, R. W. Stevens, P. Toochinda and S. S. C. Chuang, *Sep. Purif. Technol.*, 2004, **35**, 31.

56. H. Y. Huang and R. T. Yang, *Ind. Eng. Chem. Res.*, 2003, **42**, 2427.

57. M. M. Maroto-Valer, Z. Tang and Y. Zhang, *Fuel Process. Technol.*, 2005, **86**, 1487.

58. J. Przepiórski, M. Skrodzewicz and A. W. Morawski, *Appl. Surf. Sci.*, 2004, **225**, 235.

59. M. G. Plaza, C. Pevida, A. Arenillas, F. Rubiera and J. J. Pis, *Fuel*, 2007, **86**, 2204.

60. M. G. Plaza, C. Pevida, B. Arias, J. Fermoso, A. Arenillas, F. Rubiera and J. J. Pis, *J. Them. Anal. Cal.*, 2008, **92**, 601.

61. J. Wei, D. Zhou, Z. Sun, Y. Deng, Y. Xia and D. Zhao, *Adv. Funct. Mater.*, 2013, **23**, 2322.

62. X. Fan, L. Zhang, G. Zhang, Z. Shu and J. Shi, *Carbon*, 2013, **61**, 423.

63. X. Ma, M. Cao and C. Hu, *J. Mater. Chem. A*, 2013, **1**, 913.

64. J. Wang, I. Senkovska, M. Oschatz, M. R. Lohe, L. Borchardt, A. Heerwig, Q. Liu and S. Kaskel, *J. Mater. Chem. A*, 2013, **1**, 10951.

65. M. Sevilla, P. Valle-Vigón and A. B. Fuertes, *Adv. Funct. Mater.*, 2011, **21**, 2781.

66. L.-Y. Meng, W. Meng, T. Chen and L. Y. Jin, *J. Appl. Polym. Sci.*, 2014, in press.

67. J. Yu, M. Guo, F. Muhammad, A. Wang, F. Zhang, Q. Li and G. Zhu, *Carbon*, 2014, **69**, 502.

68. G. Sethia and A. Sayari, *Energy Fuels*, 2014, **28**, 2727.

69. S. Feng, W. Li, Q. Shi, Y. Li, J. Chen, Y. Ling, A. M. Asiri and D. Zhao, *Chem. Commun.*, 2014, **50**, 329.

70. R. S. Franchi, P. J. E. Harlick and A. Sayari, *Ind. Eng. Chem. Res.*, 2005, **44**, 8007.

71. S. H. Liu, C. H. Wu, H. K. Lee and S. B. Liu, *Top. Catal.*, 2010, **53**, 210.

72. X. Ma, X. Wang and C. Song, *J. Am. Chem. Soc.*, 2009, **131**, 5777.

73. S. Satyapal, T. Filburn, John Trela and J. Strange, *Energy Fuels*, 2001, **15**, 250.

74. W. J. Son, J. S. Choi and W. S. Ahn, *Microporous Mesoporous Mater.*, 2008, **113**, 31.

75. X. Wang, H. Li, H. Liu and X. Hou, *Microporous Mesoporous Mater.*, 2011, **142**, 564.

76. M. B. Yue, Y. Chun, Y. Cao, X. Dong and J. H. Zhu, *Adv. Funct. Mater.*, 2006, **16**, 1717.

77. P. J. E. Harlick and A. Sayari, *Ind. Eng. Chem. Res.*, 2007, **46**, 446.

78. N. Hiyoshi, K. Yogo and T. Yashima, *Microporous Mesoporous Mater.*, 2005, **84**, 357.

79. G. P. Knowles, S. W. Delaney and A. L. Chaffee, *Ind. Eng. Chem. Res*, 2006, **45**, 2626.

80. R. Serna-Guerrero, Y. Belmabkhout and A. Sayari, *Chem. Eng. J.*, 2010, **158**, 513.

81. D. Wang, X. Ma, C. Sentorun-Shalaby and C. Song, *Ind. Eng. Chem. Res.*, 2012, **51**, 3048.

82. Z. Tang, Z. Han, G. Yang and J. Yang, *Appl. Surf. Sci.*, 2013, **277**, 47.

83. J. Wang, H. Chen, H. Zhou, X. Liu, W. Qiao, D. Long and L. Ling, *J. Environ. Sci.*, 2013, **25**, 124.

84. A. Houshmand, W. M. A. Wan Daud and M. S. Shafeeyan, *Sep. Sci. Technol.*, 2011, **46**, 1098.

85. A. Kumar Mishra and S. Ramaprabhu, *RSC Adv.*, 2012, **2**, 1746.

86. D. I. Jang and S. J. Park, *Bull. Korean Chem. Soc.*, 2011, **32**, 3377.

87. A. Houshmand, M. S. Shafeeyan, A. Arami-Niya and W. M. A. W. Daud, *J. Taiwan Inst. Chem. E.*, 2013, **44**, 774.

88. M. M. Gui, Y. X. Yap, S. P. Chai and A. R. Mohamed, *Int. J. Greenhouse Gas Control*, 2013, **14**, 65.

89. M. G. Plaza, K. J. Thurecht, C. Pevida, F. Rubiera, J. J. Pis, C. E. Snape and T. C. Drage, *Fuel Process. Technol.*, 2013, **110**, 53.

90. B. C. Bai, J. G. Kim, J. S. Im, S. C. Jung and Y. S. Lee, *Carbon lett.*, 2011, **12**, 236.

91. J.-Y. Jung, H.-R. Yu, S. J. In, Y. C. Choi and Y.-S. Lee, *J. Nanomater.*, 2013, **2013**, 1.

92. D.-I. Jang and S.-J. Park, *Fuel*, 2012, **102**, 439.

93. B.-J. Kim, K.-S. Cho and S.-J. Park, *J. Colloid Interface Sci.*, 2010, **342**, 575.

94. B. J. Park and S. J. Park, *J. Mater. Sci. Lett.*, 1999, **18**, 1607.

95. M. Anbia and V. Hoseini, *Chem. Eng. J.*, 2012, **191**, 326.

96. Y. Kong, L. Jin and J. Qiu, *Sci. Total. Environ.*, 2013, **463-464**, 192.

97. L. Liu, Q. F. Deng, X. X. Hou and Z. Y. Yuan, *J. Mater. Chem.*, 2012, **22**, 15540.

98. B. Z. Jang and A. Zhamu, *J. Mater. Sci.*, 2008, **43**, 5092.

99. W. Lv, D. M. Tang, Y. B. He, C. H. You, Z. Q. Shi, X. C. Chen, C. M. Chen, P. X. Hou, C. Liu and Q. H. Yang, *ACS Nano*, 2009, **24**, 3730.

100. A. K. Mishra and S. Ramaprabhu, *J. Mater. Chem.*, 2012, **22**, 3708.

101. H. B. Zhang, J. W. Wang, Q. Yan, W. G. Zheng, C. Chen and Z. Z. Yu, *J. Mater. Chem.*, 2011, **21**, 5392.

102. L. L. Zhang, X. Zhao, M. D. Stoller, Y. Zhu, H. Ji, S. Murali, Y. Wu, S. Perales, B. Clevenger and R. S. Ruoff, *Nano Lett.*, 2012, **12**, 1806.

103. Y. Zhu, S. Murali, M. D. Stoller, K. J. Ganesh, W. Cai, P. J. Ferreira, A. Pirkle, R. M. Wallace, K. A. Cychosz, M. Thommes, D. Su, E. A. Stach and R. S. Ruoff, *Science*, 2011, **332**, 1537.

104. L. Y. Meng and S. J. Park, *J. Colloid Interface Sci.*, 2012, **386**, 285.

105. M. Asai, T. Ohba, T. Iwanaga, H. Kanoh, M. Endo, J. Campos-Delgado, M. Terrones, K. Nakai and K. Kaneko, *J. Am. Chem. Soc.*, 2011, **133**, 14880.

106. S.-M. Hong, S. H. Kim and K. B. Lee, *Energy Fuels*, 2013, **27**, 3358.

107. Y. Zhu, S. Murali, W. Cai, X. Li, J. W. Suk, J. R. Potts and R. S. Ruoff, *Adv. Mater.*, 2010, **22**, 3906.

108. D. Zhou, Q. Liu, Q. Cheng, Y. Zhao, Y. Cui, T. Wang and B. Han, *Chin. Sci. Bull.*, 2012, **57**, 3059.

109. A. A. Alhwaige, T. Agag, H. Ishida and S. Qutubuddin, *RSC Adv.*, 2013, **3**, 16011.

110. S. Yang, L. Zhan, X. Xu, Y. Wang, L. Ling and X. Feng, *Adv. Mater.*, 2013, **25**, 2130.

111. A. K. Mishra and S. Ramaprabhu, *Chem. Eng. J.*, 2012, **187**, 10.

112. M. Saleh, V. Chandra, K. C. Kemp and K. S. Kim, *Nanotechnology*, 2013, **24**, 255702.

113. R. S. D. Ko and L. T. Biegler, *Ind. Eng. Chem. Res.*, 2003, **42**, 339.

114. P. Xiao, J. Zhang, P. Webley, G. Li, R. Singh and R. Todd, *Adsorption*, 2008, **14**, 575.

115. Z. Liang, M. Marshall and A. L. Chaffee, *Energy Proc.*, 2009, **1**, 1265.

116. E. Díaz, E. Muñoz, A. Vega and S. Ordocnez, *Ind. Eng. Chem. Res.*, 2008, **47**, 412.

117. J. Pires and M. Brotas de Carvalho, *J. Mol. Catal.*, 1993, **85**, 295.

118. J. Merel, M. Clausse and F. Meunier, *Ind. Eng. Chem. Res.*, 2008, **47**, 209.

119. P. Li and F. H. Tezel, *Microporous Mesoporous Mater.*, 2007, **98**, 94.

120. S. K. Wirawan and D. Creaser, *Microporous Mesoporous Mater.*, 2006, **91**, 196.

121. B. Bonelli, B. Onida, B. Fubini, C. Otero Arean and E. Garrone, *Langmuir*, 2000, **16**, 4976.

122. J. Zhang, R. Singh and P. A. Webley, *Microporous Mesoporous Mater.*, 2008, **111**, 478.

123. A. Zukal, A. Pulido, B. Gil, P. Nachtigall, O. Bludsky, M. Rubesand and J. Cejka, *Phys. Chem. Chem. Phys.*, 2010, **12**, 6413.

124. R. Hernández-Huesca, L. Díaz and G. Aguilar-Armenta, *Sep. Purif. Technol.*, 1999, **15**, 163.

125. F. Su and C. Lu, *Energy Environ. Sci.*, 2012, **5**, 9021.

126. Z. Liu, C. Shen, F. V. S. Lopes, P. Li, J. Yu, C. A. Grande and A. E. Rodrigues, *Sep. Sci. Technol.*, 2013, **48**, 388.

127. D. P. Bezerra, R. S. Oliveira, R. S. Vieira, C. L. Cavalcante and D. C. S. Azevedo, *Adsorption*, 2011, **17**, 235.

128. M. Salmasi, S. Fatemi, M. Doroudian Rad and F. Jadidi, *Int. J. Environ. Sci. Technol.*, 2013, **10**, 1067.

129. S. Mahzoon and S. Fatemi, *Sep. Sci. Technol.*, 2014, **49**, 55.

130. M. R. Hudson, W. L. Queen, J. A. Mason, D. W. Fickel, R. F. Lobo and C. M. Brown, *J. Am. Chem. Soc.*, 2012, **134**, 1970.

131. S. Araki, Y. Kiyohara, S. Tanaka and Y. Miyake, *J. Colloid. Interface. Sci.*, 2012, **388**, 185.

132. P. Nachtigall, L. Grajciar, J. Perez-Pariente, A. B. Pinar, A. Zukal and J. Cejka, *Phys. Chem. Chem. Phys.*, 2012, **14**, 1117.

133. S. Loganathan, M. Tikmani and A. K. Ghoshal, *Langmuir*, 2013, **29**, 3491.

134. K. S. Walton, M. B. Abney and M. D. LeVan, *Microporous Mesoporous Mater.*, 2006, **91**, 78.

135. F. N. Ridha, Y. X. Yang and P. A. Webley, *Microporous Mesoporous Mater.*, 2009, **117**, 497.

136. M. M. Lozinska, E. Mangano, J. P. Mowat, A. M. Shepherd, R. F. Howe, S. P. Thompson, J. E. Parker, S. Brandani and P. A. Wright, *J. Am. Chem. Soc.*, 2012, **134**, 17628.

137. T. H. Bae, M. R. Hudson, J. A. Mason, W. L. Queen, J. J. Dutton, K. Sumida, K. J. Micklash, S. S. Kaye, C. M. Brown and J. R. Long, *Energy Environ. Sci.*, 2013, **6**, 128.

138. K. M. Lee, Y. H. Lim, C. J. Park and Y. M. Jo, *Ind. Eng. Chem. Res*, 2012, **51**, 1355.

139. A. G. Arévalo-Hidalgo, N. E. Almodóvar-Arbelo and A. J. Hernández-Maldonado, *Ind. Eng. Chem. Res.*, 2011, **50**, 10259.

140. S.-H. Hong, M.-S. Jang, S. J. Cho and W.-S. Ahn, *Chem. Commun.*, 2014, **50**, 4927.

141. F. Su, C. Lu, S. C. Kuo and W. Zeng, *Energy Fuels*, 2010, **24**, 1441.

142. P. D. Jadhav, R. V. Chatti, R. B. Biniwale, N. K. Labhsetwar, S. Devotta and S. S. Rayalu, *Energy Fuels*, 2007, **21**, 3555.

143. L.-Y. Lin, J.-T. Kuo and H. Bai, *J. Hazard. Mater.*, 2011, **192**, 255.

144.Y.-K. Kim, Y.-H. Mo, J. Lee, H.-S. You, C.-K. Yi, Y. C. Park and S.-E. Park, *J. Nanosci. Nanotechnol.*, 2013, **13**, 2703.

145.Y. Jing, L. Wei, Y. Wang and Y. Yu, *Microporous Mesoporous Mater.*, 2014, **183**, 124.

146.P. Singh, J. P. M. Niederer and G. F. Versteeg, *Chem. Eng. Res. Des.*, 2009, **87**, 135.

147.C. H. Yu, C. H. Huang and C. S. Tan, *Aerosol Air Quality Res.*, 2012, **12**, 745.

148.F.Y. Chang, K.J. Chao, H.H. Cheng and C.S. Tan, *Sep. Purif. Technol.*, 2009, **70**, 87.

149.R. Serna-Guerrero, Y. Belmabkhout and A. Sayari, *Chem. Eng. J.*, 2010, **158**, 513.

150.R. Serna-Guerrero, Y. Belmabkhout and A. Sayari, *Chem. Eng. J.*, 2010, **161**, 173.

151.R. Sanz, G. Calleja, A. Arencibia and E. S. Sanz-Pérez, *Microporous Mesoporous Mater.*, 2012, **158**, 309.

152.K. K. Han, L. Ma, H. M. Zhao, X. Li, Y. Chun and J. H. Zhu, *Microporous Mesoporous Mater.*, 2012, **151**, 157.

153.E. Gallei and G. Stumpf, *J. Colloid Interface Sci.*, 1976, **55**, 415.

154.S. U. Rege and R. T. Yang, *Chem. Eng. Sci.*, 2001, **56**, 3781.

155.F. Brandani and D. M. Ruthven, *Ind. Eng. Chem. Res.*, 2004, **43**, 8339.

156.J. Janchena, D. T. F. Mohlmannb and H. Stach, *Stud. Surf. Sci. Catal.*, 2007, **170**, 2116.

157.A. Ertan and F. Çakicioglu-Özkan, *Adsorption*, 2005, **11**, 151.

158.K.-M. Lee, Y.-H. Lim and Y.-M. Jo, *Environ. Technol.*, 2012, **33**, 77.

159.Y. S. Bae, K. L. Mulfort, H. Frost, P. Ryan, S. Punnathanam, L. J. Broadbelt, J. T. Hupp and R. Q. Snurr, *Langmuir*, 2008, **24**, 8592.

160.Y. Liu, Z. U. Wang and H.-C. Zhou, *Greenhouse Gases Sci. Technol.*, 2012, **2**, 239.

161.X. Peng, X. Cheng and D. Cao, *J. Mater. Chem.*, 2011, **21**, 11259.

162.Z. Xiang, D. Cao, J. Lan, W. Wang and D. P. Broom, *Energy Environ. Sci.*, 2010, **3**, 1469.

163.Z. Xiang, X. Peng, X. Cheng, X. Li and D. Cao, *J. Phys. Chem. C*, 2011, **115**, 19864.

164.A. G. Kontos, V. Likodimos, C. M. Veziri, E. Kouvelos, N. Moustakas, G. N. Karanikolos, G. E. Romanos and P. Falaras, *ChemSusChem*, 2014, **7**, 1696.

165.Z. Zhang, Y. Zhao, Q. Gong, Z. Li and J. Li, *Chem. Commun.*, 2013, **49**, 653.

166.H. Wu, J. M. Simmons, G. Srinivas, W. Zhou and T. Yildirim, *J. Phys. Chem. Lett.*, 2010, **1**, 1946.

167.S. R. Caskey, A. G. Wong-Foy and A. J. Matzger, *J. Am. Chem. Soc.*, 2008, **130**, 10870.

168.C. R. Wade and M. Dinca, *Dalton Trans.*, 2012, **41**, 7931.

169.B. Mu, F. Li, Y. Huang and K. S. Walton, *J. Mater. Chem.*, 2012, **22**, 10172.

170.R. Sanz, F. Martinez, G. Orcajo, L. Wojtas and D. Briones, *Dalton Trans.*, 2013, **42**, 2392.

171.O. K. Farha, A. O. Yazaydin, I. Eryazici, C. D. Malliakas, B. G. Hauser, M. G. Kanatzidis, S. T. Nguyen, R. Q. Snurr and J. T. Hupp, *Nat. Chem.*, 2010, **2**, 944.

172.O. K. Farha, C. E. Wilmer, I. Eryazici, B. G. Hauser, P. A. Parilla, K. O'Neill, A. A. Sarjeant, S. T. Nguyen, R. Q. Snurr and J. T. Hupp, *J. Am. Chem. Soc.*, 2012, **134**, 9860.

173.B. Zheng, R. Yun, J. Bai, Z. Lu, L. Du and Y. Li, *Inorg. Chem.*, 2013, **52**, 2823.

174.J. Park, J. R. Li, Y. P. Chen, J. Yu, A. A. Yakovenko, Z. U. Wang, L. B. Sun, P. B. Balbuena and H. C. Zhou, *Chem. Commun.*, 2012, **48**, 9995.

175.H. S. Choi and M. P. Suh, *Angew. Chem., Int. Ed.*, 2009, **48**, 6865.

176.S. Henke, A. Schneemann, A. Wutscher and R. A. Fischer, *J. Am. Chem. Soc.*, 2012, **134**, 9464.

177.D. H. Hong and M. P. Suh, *Chem. Commun.*, 2012, **48**, 9168.

178.M. Y. Masoomi, K. C. Stylianou, A. Morsali, P. Retailleau and D. Maspoch, *Cryst. Growth Des.*, 2014, **14**, 2092.

179.T. Bataille, S. Bracco, A. Comotti, F. Costantino, A. Guerri, A. Ienco and F. Marmottini, *CrystEngComm*, 2012, **14**, 7170.

180.Q. Yan, Y. Lin, P. Wu, L. Zhao, L. Cao, L. Peng, C. Kong and L. Chen, *ChemPlusChem*, 2013, **78**, 86.

181.P. Sarawade, H. Tan and V. Polshettiwar, *ACS Sustainable Chem. Eng.*, 2012, **1**, 66.

182.T. Li, J. E. Sullivan and N. L. Rosi, *J. Am. Chem. Soc.*, 2013, **135**, 9984.

183.Z. Xiang, Z. Hu, D. Cao, W. Yang, J. Lu, B. Han and W. Wang, *Angew. Chem. Int. Ed.*, 2011, **50**, 491.

184.R. Li, X. Ren, X. Feng, X. Li, C. Hu and B. Wang, *Chem. Commun.*, 2014, **50**, 6894.

185.Q. Wang, W. Xia, W. Guo, L. An, D. Xia and R. Zou, *Chem. Asian. J.*, 2013, **8**, 1879.

186.C. Montoro, E. García, S. Calero, M. A. Pérez-Fernández, A. L. López, E. Barea and J. A. R. Navarro, *J. Mater. Chem.*, 2012, **22**, 10155.

187.J. Duan, Z. Yang, J. Bai, B. Zheng, Y. Li and S. Li, *Chem. Commun.*, 2012, **48**, 3058.

188.B. Zheng, H. Liu, Z. Wang, X. Yu, P. Yi and J. Bai, *CrystEngComm*, 2013, **15**, 3517.

189.Y. Lin, Q. Yan, C. Kong and L. Chen, *Sci. Rep.*, 2013, **3**, 1859.

190.S. N. Brune and D. R. Bobbitt, *Anal. Chem.*, 1992, **64**, 166.

191.R. Haldar, S. K. Reddy, V. M. Suresh, S. Mohapatra, S. Balasubramanian and T. K. Maji, *Chem. Eur. J.*, 2014, **20**, 4347.

192.X. Si, J. Zhang, F. Li, C. Jiao, S. Wang, S. Liu, Z. Li, H. Zhou, L. Sun and F. Xu, *Dalton Trans.*, 2012, **41**, 3119-3122.

193.Y. Hu, W. M. Verdegaal, S.-H. Yu and H.-L. Jiang, *ChemSusChem*, 2014, **7**, 734.

194.Z. Xiang, S. Leng and D. Cao, *J. Phys. Chem. C*, 2012, **116**, 10573.

195.K. Liu, B. Li, Y. Li, X. Li, F. Yang, G. Zeng, Y. Peng, Z. Zhang, G. Li, Z. Shi, S. Feng and D. Song, *Chem. Commun.*, 2014, **50**, 5031.

196.Y. Zhao, H. Ding and Q. Zhong, *Appl. Surf. Sci.*, 2013, **284**, 138.

197.D. Qian, C. Lei, G. P. Hao, W. C. Li and A. H. Lu, *ACS Appl. Mater. Interf.*, 2012, **4**, 6125.

198.R. Babarao and J. W. Jiang, *Energy Environ. Sci.*, 2009, **2**, 1088.

199.J. Yu and P. B. Balbuena, *J. Phys. Chem. C*, 2013, **117**, 3383.

200.Q. Yang, S. B. Vaesen, F. Ragon, A. D. Wiersum, D. Wu, A. Lago, T. Devic, C. Martineau, F. Taulelle, P. L. Llewellyn, H. Jobic, C. Zhong, C. Serre, G. D. Weireld and G. Maurin, *Angew. Chem. Int. Ed.*, 2013, **52**, 10316.

201.D. Wang, C. Sentorun-Shalaby, X. Ma and C. Song, *Energy Fuels*, 2010, **25**, 456.

202.D. J. Fauth, M. L. Gray, H. W. Pennline, H. M. Krutka, S. Sjostrom and A. M. Ault, *Energy Fuels*, 2012, **26**, 2483.

203.W. Ke, S. Hongyan, L. Lin, Y. Xinlong, Y. Zifeng, L. Chenguang and Z. Qingfang, *J. Nat. Gas Chem.*, 2012, **21**, 319.

204.O. Leal, C. Bolivar, C. Ovalles, J. J. Garcia and Y. Espidel, *Inorg. Chim. Acta*, 1995, **240**, 183.

205.J. Yu, Y. Le and B. Cheng, *RSC Adv.*, 2012, **2**, 6784.

206.Y. Du, Z. Du, W. Zou, H. Li, J. Mi and C. Zhang, *J. Colloid Interface Sci.*, 2013, **409**, 132.

207.A. Goeppert, H. Zhang, M. Czaun, R. B. May, G. K. S. Prakash, G. A. Olah and S. R. Narayanan, *ChemSusChem*, 2014, **7**, 1386.

208.S. Bai, J. Liu, J. Gao, Q. Yang and C. Li, *Microporous Mesoporous Mater.*, 2012, **151**, 474.

209.Y. G. Ko, H. J. Lee, H. C. Oh and U. S. Choi, *J. Hazard Mater.*, 2013, **250-251**, 53.

210.J.-L. Liu and R.-B. Lin, *Powder Technol.*, 2013, **241**, 188.

211.H. Zhang, A. Goeppert, M. Czaun, G. K. S. Prakash and G. A. Olah, *RSC Adv.*, 2014, **4**, 19403.

212.M. Yao, Y. Dong, X. Feng, X. Hu, A. Jia, G. Xie, G. Hu, J. Lu, M. Luo and M. Fan, *Fuel*, 2014, **123**, 66.

213.F.-Q. Liu, L. Wang, Z.-G. Huang, C.-Q. Li, W. Li, R.-X. Li and W.-H. Li, *ACS Appl. Mater. Interf.*, 2014, **6**, 4371.

214.M. R. Liebl and J. Senker, *Chem. Mater.*, 2013, **25**, 970.

215.A. Wilke and J. Weber, *J. Mater. Chem.*, 2011, **21**, 5226.

216.C. F. Martín, E. Stöckel, R. Clowes, D. J. Adams, A. I. Cooper, J. J. Pis, F. Rubiera and C. Pevida, *J. Mater. Chem.*, 2011, **21**, 5475.

217.M. Kaliva, G. S. Armatas and M. Vamvakaki, *Langmuir*, 2012, **28**, 2690.

218.Y. Luo, B. Li, W. Wang, K. Wu and B. Tan, *Adv. Mater.*, 2012, **24**, 5703.

219.M. G. Rabbani and H. M. El-Kaderi, *Chem. Mater.*, 2011, **23**, 1650.

220.X. Chen, S. Qiao, Z. Du, Y. Zhou and R. Yang, *Macromol. Rapid. Commun.*, 2013, **34**, 1181.

221.L. H. Xie and M. P. Suh, *Chemistry*, 2013, **19**, 11590.

222.K. V. Rao, S. Mohapatra, C. Kulkarni, T. K. Maji and S. J. George, *J. Mater. Chem.*, 2011, **21**, 12958.

223.R. Dawson, D. J. Adams and A. I. Cooper, *Chem. Sci.*, 2011, **2**, 1173.

224.N. Ritter, I. Senkovska, S. Kaskel and J. Weber, *Macromolecules*, 2011, **44**, 2025.

225.N. Du, H. B. Park, G. P. Robertson, M. M. Dal-Cin, T. Visser, L. Scoles and M. D. Guiver, *Nat. Mater.*, 2011, **10**, 372.

226.Y. Luo, B. Li, L. Liang and B. Tan, *Chem. Commun.*, 2011, **47**, 7704.

227.W. Lu, J. P. Sculley, D. Yuan, R. Krishna and H.-C. Zhou, *J. Phys. Chem. C*, 2013, **117**, 4057.

228.T. Ben, C. Pei, D. Zhang, J. Xu, F. Deng, X. Jing and S. Qiu, *Energy Environ. Sci.*, 2011, **4**, 3991.

229. X. Zhu, S. M. Mahurin, S.-H. An, C.-L. Do-Thanh, C. Tian, Y. Li, L. W. Gill, E. W. Hagaman, Z. Bian, J.-H. Zhou, J. Hu, H. Liu and S. Dai, *Chem. Commun.*, 2014, **50**, 7933.

230. T. Ben, Y. Li, L. Zhu, D. Zhang, D. Cao, Z. Xiang, X. Yao and S. Qiu, *Energy Environ. Sci.*, 2012, **5**, 8370.

231. Z. Xiang, X. Zhou, C. Zhou, S. Zhong, X. He, C. Qin and D. Cao, *J. Mater. Chem.*, 2012, **22**, 22663.

232. H. J. Jeon, J. H. Choi, Y. Lee, K. M. Choi, J. H. Park and J. K. Kang, *Adv. Energy Mater.*, 2012, **2**, 225.

233. H. Lim, M. C. Cha and J. Y. Chang, *Macromol. Chem. Phys.*, 2012, **213**, 1385.

234. Y. Zhao, Y. Shen, L. Bai, R. Hao and L. Dong, *Environ. Sci. Technol.*, 2012, **46**, 1789.

235. J. H. Ahn, J. E. Jang, C. G. Oh, S. K. Ihm, J. Cortez and D. C. Sherrington, *Macromolecules*, 2006, **39**, 627.

236. J. Germain, F. Svec and J. M. Fré chet, *J. Chem. Mater.*, 2008, **20**, 7069.

237. P. M. Budd, N. B. McKeown and D. Fritsch, *Macromol. Sym.*, 2006, **245**, 403.

238. M. G. Schwab, B. Fassbender, H. W. Spiess, A. Thomas, X. Feng and K. Mullen, *J. Am. Chem. Soc.*, 2009, **131**, 7216.

239. W. Li, H. Shi and J. Zhang, *ChemPhysChem*, 2014, **15**, 1772.

240. Z. Xiang, D. Cao, W. Wang, W. Yang, B. Han and J. Lu, *J. Mater. Chem. C*, 2012, **116**, 5974.

241. Y. Xie, T. T. Wang, X. H. Liu, K. Zou and W. Q. Deng, *Nat. Commun.*, 2013, **4**, 1960.

242. T. Ben, H. Ren, S. Ma, D. Cao, J. Lan, X. Jing, W. Wang, J. Xu, F. Deng, J. M. Simmons, S. Qiu and G. Zhu, *Angew. Chem. Int. Ed.*, 2009, **48**, 9457.

243. W. Lu, D. Yuan, J. Sculley, D. Zhao, R. Krishna and H. C. Zhou, *J. Am. Chem. Soc.*, 2011, **133**, 18126.

244. S. Guggenheim and R. T. Martin, *Clays Clay Miner.*, 1995, **43**, 255.

245. F. Bergaya, B. K. G. Theng and G. Lagaly, *Handbook of clay science, in: Developments in Clay Science*, Elseiver, Oxford, 2006.

246. J. C. Hicks, J. H. Drese, D. J. Fauth, M. L. Gray, G. Qi and C. W. Jones, *J. Am. Chem. Soc.*, 2008, **130**, 2902.

247. L. Stevens, K. Williams, W. Y. Han, T. Drage, C. Snape, J. Wood and J. Wang, *Chem. Eng. J.*, 2013, **215**, 699.

248. E. A. Roth, S. Agarwal and R. K. Gupta, *Energy Fuels*, 2013, **27**, 4129.

249. A. Azzouz, S. Nousir, N. Platon, K. Ghomari, T. C. Shiao, G. Hersant, J.-Y. Bergeron and R. Roy, *Int. J. Greenhouse Gas Control*, 2013, **17**, 140.

250. A. Gil, M. A. Vicente and S. A. Korili, *J. Catal.*, 2005, **229**, 119.

251. R. G. Leliveld, T. G. Ros, A. J. van Dillen, J. W. Geus and D. C. Koningsberger, *J. Catal.*, 1999, **185**, 513.

252. C. Chen, D.-W. Park and W.-S. Ahn, *Appl. Surf. Sci.*, 2013, **283**, 699.

253. W. Wang, X. Wang, C. Song, X. Wei, J. Ding and J. Xiao, *Energy Fuels*, 2013, **27**, 1538.

254. C. Zhao, X. Chen and C. Zhao, *Energy Fuels*, 2010, **24**, 1009.

255. Y. Seo, S. H. Jo, C. K. Ryu and C. K. Yi, *Chemosphere*, 2007, **69**, 712.

256. S. C. Lee, B. Y. Choi, C. K. Ryu, Y. S. Ahn, T. J. Lee and J. C. Kim, *Korean J. Chem. Eng.*, 2006, **23**, 374.

257. Y. Liang, D. P. Harrison, R. P. Gupta, D. A. Green and W. A. McMichael, *Energy Fuels*, 2004, **18**, 569.

258. J. B. Lee, C. K. Ryu, J. I. Baek, J. H. Lee, T. H. Eom and S. H. Kim, *Ind. Eng. Chem. Res.*, 2008, **47**, 4465.

259. C. K. Yi, S. H. Jo, Y. Seo, S. D. Park, K. H. Moon, J. S. Yoo, J. B. Lee and C. K. Ryu, *Stud. Surf. Sci. Catal.*, 2006, **159**, 501.

260. D. P. Harrison, *Greenhouse Gas Control Technol.*, 2005, **2**, 1101.

261. Y. Liang, D. P. Harrison, R. P. Gupta, D. A. Green and W. J. McMichael, *Energy Fuels*, 2004, **18**, 569.

262. V. E. Sharonov, A. G. Okunev and Y. I. Aristov, *React. Kinet. Catal. Lett.*, 2004, **82**, 363.

263. C. Zhao, X. Chen and C. Zhao, *Chemosphere*, 2009, **75**, 1401.

264. C. K. Yi, S. H. Jo, Y. Seo, J. B. Lee and C. K. Ryu, *Int. J. Greenhouse Gas Control*, 2007, **1**, 31.

265. S. C. Lee, H. J. Chae, S. J. Lee, Y. H. Park, C. K. Ryu, C. K. Yi and J. C. Kim, *J. Mol. Catal. B: Enzym.*, 2009, **56**, 179.

266. C. K. Yi, S. H. Jo, H. J. Ryu, Y. W. Yoo, J. B. Lee and C. K. Ryu, *Greenhouse Gas Control Technol.*, 2005, **2**, 1765.

267. Y. Wu, X. Chen, W. Dong, C. Zhao, Z. Zhang, D. Liu and C. Liang, *Energy Fuels*, 2013, **27**, 4804.

268. W. Dong, X. Chen and Y. Wu, *Energy Fuels*, 2014, **28**, 3310.

269. V. S. Derevschikov, J. V. Veselovskaya, T. Y. Kardash, D. A. Trubitsyn and A. G. Okunev, *Fuel*, 2014, **127**, 212.

270. R. R. Kondakindi, G. McCumber, S. Aleksic, W. Whittenberger and M. A. Abraham, *Int. J. Greenhouse Gas Control*, 2013, **15**, 65.

271.D. K. Lee, D. Y. Min, H. Seo, N. Y. Kang, W. C. Choi and Y. K. Park, *Ind. Eng. Chem. Res.*, 2013, **52**, 9323.

272.L. w. Wang, Y. f. Diao, L. l. Wang, X. f. Shi and X. y. Tai, *Korean J. Chem. Eng.*, 2013, **30**, 1631.

273.M. Kianpour, M. A. Sobati and S. Shahhosseini, *Chem. Eng. Res. Des.*, 2012, **90**, 2041.

274.M. Freemantle, *An Introduction to Ionic Liquids*, RSC Publishing, London, 2010.

275.J. Ren, L. B. Wu and B. G. Li, *Ind. Eng. Chem. Res.*, 2012, **51**, 7901.

276.B. E. Gurkan, J. C. de la Fuente, E. M. Mindrup, L. E. Ficke, B. F. Goodrich, E. A. Price, W. F. Schneider and J. F. Brennecke, *J. Am. Chem. Soc.*, 2010, **132**, 2116.

277.Y. Y. Jiang, G. N. Wang, Z. Zhou, Y. T. Wu, J. Geng and Z. B. Zhang, *Chem. Commun.*, 2008, **4**, 505.

278.L. A. Blanchard, D. Hancu, E. J. Beckman and J. F. Brennecke, *Nature*, 1999, **399**, 28.

279.K. R. Seddon, *Nature*, 2003, **2**, 363.

280.B. F. Goodrich, J. C. de la Fuente, B. E. Gurkan, Z. K. Lopez, E. A. Price, Y. Huang and J. F. Brennecke, *J. Phys. Chem. B*, 2011, **115**, 9140.

281.H. Yu, Y. T. Wu, Y. Y. Jiang, Z. Zhou and Z. B. Zhang, *New J. Chem.*, 2009, **33**, 2385.

282.N. M. Kocherginsky, Q. Yang and L. Seelam, *Sep. Purif. Technol.*, 2007, **53**, 171.

283.P. Scovazzo, J. Kieft, D. A. Finan, C. Koval, D. DuBois and R. D. Noble, *J. Membr. Sci.*, 2004, **238**, 57.

284.L. J. Lozano, C. Godínez, A. P. d. l. Ríos, F. J. Hernández-Fernández, S. Sánchez-Segado and F. J. Alguacil, *J. Membr. Sci.*, 2011, **376**, 1.

285.R. D. Noble and D. L. Gin, *J. Membr. Sci.*, 2011, **369**, 1.

286.K. M. Gupta, Y. Chen and J. Jiang, *J. Phys. Chem. C*, 2013, **117**, 5792.

287.D. D. Iarikov, P. Hacarlioglu and S. T. Oyama, *Chem. Eng. J.*, 2011, **166**, 401.

288.S. Hanioka, T. Maruyama, T. Sotani, M. Teramoto, H. Matsuyama, K. Nakashima, M. Hanaki, F. Kubota and M. Goto, *J. Membr. Sci.*, 2008, **314**, 1.

289.J. E. Bara, E. S. Hatakeyama, C. J. Gabriel, S. Lessmann, D. L. Gin and R. D. Noble, *J. Membr. Sci.*, 2008, **316**, 186.

290.M. Eddaoudi, J. Kim, N. Rosi, D. Vodak, J. Wachter, M. O'Keefe and O. M. Yaghi, *Science*, 2002, **295**, 469.

291.Y. Chen, Z. Hu, K. M. Gupta and J. Jiang, *J. Phys. Chem.*, 2011, **115**, 21736.

292.E. I. Privalova, P. MaÈki-Arvela, D. Yu Murzin and J. P. Mikkola, *Russ. Chem. Rev.*, 2012, **81**, 435.

293.K. M. Gupta, Y. Chen, Z. Hu and J. Jiang, *Phys. Chem. Chem. Phys.*, 2012, **14**, 5758.

294.X. Wang, N. G. Akhmedov, Y. Duan, D. Luebke and B. Li, *J. Mater. Chem. A*, 2013, **1**, 2978.

295.X. Luo, Y. Guo, F. Ding, H. Zhao, G. Cui, H. Li and C. Wang, *Angew. Chem. Int. Ed.*, 2014, **53**, 7053.

296.E. I. Privalova, E. Karjalainen, M. Nurmi, P. i. M. ki-Arvela, K. E. nen, H. Tenhu, D. Y. Murzin and J.-P. Mikkola, *ChemSusChem*, 2013, **6**, 1500.

297.M. Hasib-ur-Rahman, M. Siaj and F. Larachi, *Chem. Eng. Process.*, 2010, **49**, 313.

298.J. Tang, W. Sun, H. Tang, M. Radosz and Y. Shen, *Macromolecules*, 2005, **38**, 2037.

299.S. Supasitmongkol and P. Styring, *Energy Environ. Sci.*, 2010, **3**, 1961.

300.J. Tang, H. Tang, W. Sun, M. Radosz and Y. Shen, *J. Polym. Sci. Part A*, 2005, **43**, 5477.

301.J. E. Bara, C. J. Gabriel, E. S. Hatakeyama, T. K. Carlisle, S. Lessmann, R. D. Noble and D. L. Gin, *J. Membr. Sci.*, 2008, **3**, 321.

302.S. Kato, Y. Tsujita, H. Yoshimizu, T. Kinoshita and J. S. Higgins, *Polymer*, 1997, **38**, 2807.

303.Z. Mogri and D. R. Paul, *Polymer*, 2001, **42**, 7781.

304.J. L. Budzien, J. D. McCoy, D. H. Weinkauf, R. A. LaViolette and E. S. Peterson, *Macromolecules*, 1998, **3368**, 31.

305.Y. Jiao, A. Dua, Z. Zhu, V. Rudolphb, G. Q. M. Lu and S. C. Smitha, *Catal. Today*, 2010.

306.Q. Sun, Z. Li, D. J. Searles, Y. Chen, G. M. Lu and A. Du, *J. Am. Chem. Soc.*, 2013, **135**, 8246.

307.P. Shao, X.-Y. Kuang, L.-P. Ding, J. Yang and M.-M. Zhong, *Appl. Surf. Sci.*, 2013, **285**, 350.

308.Z. Mahdavifar and N. Abbasi, *Physica. E*, 2014, **56**, 268.

309.H. Choi, Y. C. Park, Y.-H. Kim and Y. S. Lee, *J. Am. Chem. Soc.*, 2011, **133**, 2084.

310.A. Kalinkin, E. Kalinkina, O. Zalkind and T. Makarova, *Colloid J.*, 2008, **70**, 33.

311.M. T. Rodríguez and H. Pfeiffer, *Thermochim. Acta*, 2008, **473**, 92.

312.J. Ortiz-Landeros, C. Gómez-Yáñez and H. Pfeiffer, *J. Solid State Chem.*, 2011, **184**, 2257.

313.R. B. Vieira and H. O. Pastore, *Environ. Sci. Technol.*, 2014, **48**, 2472.

314.Y. Wu, X. Chen, M. Radosz, M. Fan, W. Dong, Z. Zhang and Z. Yang, *Fuel*, 2014, **125**, 50.

315.R. V. Siriwardane, C. Robinson, M. Shen and T. Simonyi, *Energy Fuels* 2007, **21**, 2088.

316.X. Wang, N. G. Akhmedov, Y. Duan, D. Luebke, D. Hopkinson and B. Li, *ACS Appl. Mater. Interf.*, 2013, **5**, 8670.

317.G. R. Williams and D. O'Hare, *J. Mater. Chem.*, 2006, **16**, 3065.

318.V. Rives and S. Kannan, *J. Mater. Chem.*, 2000, **10**, 489.

319.Y. Ding and E. Alpay, *Trans. IChemE*, 2001, **79**, 45.

320.Z. Yong and A. E. Rodrigues, *Energy Convers. Manage.*, 2002, **43**, 1865.

321.H. T. J. Reijers, S. E. A. Valster-Schiermeier, P. D. Cobden and R. W. v. d. Brink, *Ind. Eng. Chem. Res.*, 2006, **45**, 2522.

322.M. S. San Román, M. J. Holgado, C. Jaubertie and V. Rives, *Solid State Sci.*, 2008, **10**, 1333.

323.U. Sharma, B. Tyagi and R. V. Jasra, *Ind. Eng. Chem. Res.*, 2008, **47**, 9588.

324.M. K. Ram Reddy, Z. P. Xu, G. Q. (Max) Lu and J. C. Diniz da Costa, *Ind. Eng. Chem. Res.*, 2008, **47**, 2630.

325.S. P. Reynolds, A. D. Ebner and J. A. Ritter, *Ind. Eng. Chem. Res.*, 2006, **45**, 4278.

326.Y. Ding and E. Alpay, *Chem. Eng. Sci.*, 2000, **55**, 3461.

327.E. L. G. Oliveira, C. A. Grande and A. E. Rodrigues, *Sep. Purif. Technol.*, 2008, **62**, 137.

328.A. D. Ebner, S. P. Reynolds and J. A. Ritter, *Ind. Eng. Chem. Res.*, 2006, **45**, 6387.

329.K. B. Lee, A. Verdooren, H. S. Caram and S. Sircar, *J. Colloid Interface Sci.*, 2007, **308**, 30.

330.S. Walspurger, L. Boels, P. D. Cobden, G. D. Elzinga, W. G. Haije and R. W. van den Brink, *ChemSusChem*, 2008, **1**, 643.

331.M. Dadwhal, T. Kim, M. Sahimi and T. T. Tsotsis, *Ind. Eng. Chem. Res.*, 2008, **47**, 6150.

332.M. R. Othman, N. M. Rasid and W. J. N. Fernando, *Chem. Eng. Sci.*, 2006, **61**, 1555.

333.N. N. A. H. Meis, J. H. Bitter and K. P. d. Jong, *Ind. Eng. Chem. Res.*, 2010, **49**, 1229.

334.Q. Wang, Z. Wu, H. H. Tay, L. Chen, Y. Liu, J. Chang, Z. Zhong, J. Luo and A. Borgna, *Catal. Today*, 2011, **164**, 198.

335.Q. Wang, H. H. Tay, Z. Zhong, J. Luo and A. Borgna, *Energy Environ. Sci.*, 2012, **5**, 7526.

336.A. Garcia-Gallastegui, D. Iruretagoyena, V. Gouvea, M. Mokhtar, A. M. Asiri, S. N. Basahel, S. A. Al-Thabaiti, A. O. Alyoubi, D. Chadwick and M. S. P. Shaffer, *Chem. Mater.*, 2012, **24**, 4531.

337.K. Ariga, J. P. Hill, M. V. Lee, A. Vinu, R. Charvet and S. Acharya, *Sci. Technol. Adv. Mater.*, 2008, **9**, 1.

338.L. H. Zhang, F. Li, D. G. Evans, X. Duan and J. M. Sci., *J. Mater. Sci.*, 2010, **45**, 3741.

339.A. Inayat, M. Klumpp and W. Schwieger, *Appl. Clay Sci.*, 2011, **51**, 452.

340.P. Benito, I. Guinea, F. M. Labajos and V. Rives, *J. Solid State Chem.*, 2008, **181**, 987.

341.S. P. Paredes, G. Fetter, P. Bosch and S. Bulbulian, *J. Mater. Sci.*, 2006, **41**, 3377.

342.A. Tsujimura, M. Uchida and A. Okuwaki, *J. Hazard Mater.*, 2007, **143**, 582.

343.G. Hu, N. Wang, D. O'Hare and J. Davis, *Chem. Commun.*, 2006, 287.

344.S. Li, J. Lu, M. Wei, D. G. Evans and X. Duan, *Adv. Funct. Mater.*, 2010, **20**, 2848.

345.M. J. Climent, A. Corma, S. Iborra, K. Epping and A. Velty, *J. Catal.*, 2004, **225**, 316.

346.P. Benito, M. Herrero, F. M. Labajos and V. Rives, *Appl. Clay Sci.*, 2010, **48**, 218.

347.T. Xiao, Y. Tang, Z. Jia, D. Li, X. Hu, B. Li and L. Luo, *Nanotechnology*, 2009, **20**, 475603.

348.R. Ma, K. Takada, K. Fukuda, N. Iyi, Y. Bando and T. Sasaki, *Angew Chem. Int. Ed.*, 2008, **47**, 86.

349.Q. Wang, Y. Gao, J. Luo, Z. Zhong, A. Borgna, Z. Guo and D. O'Hare, *RSC Adv.*, 2013, **3**, 3414.

350.Q. Wang, H. H. Tay, L. Chen, Y. Liu, J. Chang, Z. Zhong, J. Luo and A. Borgna, *J. Nanoeng. Nanomanuf.*, 2011, **1**, 298.

351.Y. Gao, Z. Zhang, J. Wu, X. Yi, A. Zheng, A. Umar, D. O'Hare and Q. Wang, *J. Mate. Chem. A*, 2013, **1**, 12782.

352.J. C. G. Carroll, J. Corish, B. Henderson and W. C. Mackrodt, *J. Mater. Sci.*, 1988, **23**, 2824.

353.B. Feng, H. An and E. Tan, *Energy Fuels*, 2007, **21**, 426.

354.S. Choi, J. H. Drese and C. W. Jones, *ChemSusChem*, 2009, **2**, 796.

355.R. Philipp and K. Fujimoto, *J. Phys. Chem.*, 1992, **96**, 9035.

356.C. D. Daub, G. N. Patey, D. B. Jack and A. K. Sallabi, *J. Chem. Phys.*, 2006, **124**, 114706.

357.D. L. Meixner, D. A. Arthur and S. M. George, *Surf. Sci.*, 1992, **261**, 141.

358.G. Pacchioni, *Surf. Sci.*, 1993, **281**, 207.

359.M. B. Jensen, L. G. M. Pettersson, O. Swang and U. Olsbye, *J. Phys. Chem. B*, 2005, **109**, 16774.

360.M. Bhagiyalakshmi, J. Y. Lee and H. T. Jang, *Int. J. Greenhouse Gas Control*, 2010, **4**, 51.

361.S.-W. Bian, J. Baltrusaities, P. Galhotra and V. H. Grassian, *J. Mate. Chem.*, 2010, **20**, 8705.

362.A. M. Ruminski, K.-J. Jeon and J. J. Urban, *J. Mater. Chem.*, 2011, **21**, 11486.

363.M. B. Yue, Y. Chun, Y. Cao, X. Dong and J. H. Zhu, *Adv. Funct. Mater.*, 2006, **16**, 1717.

364.F. N. Gu, F. Wei, J. Y. Yang, Y. Wang and J. H. Zhu, *J. Phys. Chem. C*, 2010, **114**, 8431.

365.L. Li, X. Wen, X. Fu, F. Wang, N. Zhao, F. Xiao, W. Wei and Y. Sun, *Energy Fuels*, 2010, **24**, 5773.

366.K. K. Han, Y. Zhou, W. G. Lin and J. H. Zhu, *Microporous Mesoporous Mater.*, 2013, **169**, 112.

367.M. Bhagiyalakshmi, P. Hemalatha, M. Ganesh, P. M. Mei and H. T. Jang, *Fuel*, 2011, **90**, 1662.

368.H. Jeon, Y. J. Min, S. H. Ahn, S.-M. Hong, J.-S. Shin and J. H. Kim, *Colloids Surf. A*, 2012, **414**, 75.

369.S.-W. Bian, J. Baltrusaitis, P. Galhotra and V. H. Grassian, *J. Mater. Chem.*, 2010, **20**, 8705.

370.L. She, J. Li, Y. Wan, X. Yao, B. Tu and D. Zhao, *J. Mater. Chem*, 2011, **21**, 795.

371.Y. Y. Li, K. K. Han, W. G. Lin, M. M. Wan, Y. Wang and J. H. Zhu, *J. Mater. Chem. A*, 2013, **1**, 12919.

372.W. J. Liu, H. Jiang, K. Tian, Y. W. Ding and H. Q. Yu, *Environ. Sci. Technol.*, 2013, **47**, 9397.

373.G. W. Huber, S. Iborra and A. Corma, *Chem. Rev.*, 2006, **106**, 4044.

374.T. K. Kim, K. J. Lee, J. Yuh, S. K. Kwak and H. R. Moon, *New J. Chem.*, 2014, **38**, 1606.

375.K. B. Lee, M. G. Beaver, H. S. Caram and S. Sircar, *Ind. Eng. Chem. Res.*, 2008, **47**, 8048.

376.G. Xiao, R. Singh, A. Chaffee and P. Webley, *Int. J. Greenhouse Gas Control*, 2011, **5**, 634.

377.M. Liu, C. Vogt, A. L. Chaffee and S. L. Y. Chang, *J. Phys. Chem. C*, 2013, **117**, 17514.

378.M.A. Aramendia, V. Borau, C. Jimenez, A. Marinas, J.M. Marinas, J.R. Ruiz and F.J. Urbano, *J. Mol. Catal. A: Chem.*, 2004, **218**, 81.

379.H. Jeon, Y. J. Min, S. H. Ahn, S.-M. Hong, J.-S. Shin, J. H. Kim and K. B. Lee, *Colloids Surf. A*, 2012, **414**, 75.

380.S. J. Han, Y. Bang, H. J. Kwon, H. C. Lee, V. Hiremath, I. K. Song and J. G. Seo, *Chem. Eng. J.*, 2014, **242**, 357.

381.S. Wang, S. Yan, X. Ma and J. Gong, *Energy Environ. Sci.*, 2011, **4**, 3805.

382.S. Li, Y. Shi, Y. Yang, Y. Zheng and N. Cai, *Energy Fuels*, 2013, **27**, 5352.

383.M. Alonso, Y. A. Criado, J. C. Abanades and G. Grasa, *Fuel*, 2014, **127**, 52.

384.J. Blamey, E. J. Anthony, J. Wang and P. S. Fennell, *Prog. Energ. Combust. Sci.*, 2010, **36**, 260.

385.M. E. Boot-Handford, J. C. Abanades, E. J. Anthony, M. J. Blunt, S. Brandani, N. Mac Dowell, J. R. Fernandez, M.-C. Ferrari, R. Gross, J. P. Hallett, R. S. Haszeldine, P. Heptonstall, A. Lyngfelt, Z. Makuch, E. Mangano, R. T. J. Porter, M. Pourkashanian, G. T. Rochelle, N. Shah, J. G. Yao and P. S. Fennell, *Energy Environ. Sci.*, 2014, **7**, 130.

386.M. Alonso, N. Rodríguez, B. Gonzalez, B. Arias and J. C. Abanades, *Ind. Eng. Chem. Res.*, 2011, **50**, 6982.

387.J. R. Fernández, J. C. Abanades, R. Murillo and G. Grasa, *Int. J. Greenhouse Gas Control*, 2012, **6**, 126.

388.I. Martínez, G. Grasa, R. Murillo, B. Arias and J. C. Abanades, *Energy Fuels*, 2012, **26**, 1432.

389.K. Sasaki, K. Wakuta, N. Tokuda, R. V. Belosludov, S. Ueda, R. Inoue, Y. Kawazoe and T. Ariyama, *ISIJ International*, 2012, **52**, 1233.

390.M. Olivares-Marín, E. M. Cuerda-Correa, A. Nieto-Sánchez, S. García, C. Pevida and S. Román, *Chem. Eng. J.*, 2013, **217**, 71.

391.D. Karami and N. Mahinpey, *Ind. Eng. Chem. Res.*, 2012, **51**, 4567.

392.E. T. Santos, C. Alfonsín, A. J. S. Chambel, A. Fernandes, A. P. S. Dias, C. I. C. Pinheiro and M. F. Ribeiro, *Fuel*, 2012, **94**, 624.

393.P. Xu, M. Xie, Z. Cheng and Z. Zhou, *Ind. Eng. Chem. Res.*, 2013, **52**, 12161.

394.C. Luo, Y. Zheng, C. Zheng, J. Yin, C. Qin and B. Feng, *Int. J. Greenhouse Gas Control*, 2013, **12**, 193.

395.A. M. López-Periago, J. Fraile, P. López-Aranguren, L. F. Vega and C. Domingo, *Chem. Eng. J.*, 2013, **226**, 357.

396.F.-Q. Liu, W.-H. Li, B.-C. Liu and R.-X. Li, *J. Mate. Chem. A*, 2013, **1**, 8037.

397.F. N. Ridha, V. Manovic, A. Macchi, M. A. Anthony and E. J. Anthony, *Fuel Process. Technol.*, 2013, **116**, 284.

398.M. J. Al-Jeboori, M. Nguyen, C. Dean and P. S. Fennell, *Ind. Eng. Chem. Res.*, 2013, **52**, 1426.

399.Y. Li, C. Zhao, H. Chen, C. Liang, L. Duan and W. Zhou, *Fuel*, 2009, **88**, 697.

400.F. N. Ridha, V. Manovic, Y. Wu, A. Macchi and E. J. Anthony, *Int. J. Greenhouse Gas Control*, 2013, **16**, 21.

401.Z. S. Li, N. S. Cai, Y. Y. Huang and H. J. Han, *Energy Fuels*, 2005, **19**, 1447.

402.B. Feng, W. Q. Liu, X. Li and H. An, *Energy Fuels*, 2006, **20**, 2417.

403.V. Manovic and E. J. Anthony, *Ind. Eng. Chem. Res.*, 2010, **49**, 6916.

404.A. M. Kierzkowska, L. V. Poulikakos, M. Broda and C. R. Müller, *Int. J. Greenhouse Gas Control*, 2013, **15**, 48.

405.C.-T. Yu and W.-C. Chen, *Fuel*, 2014, **122**, 179.

406.Wenqiang Liu, Bo Feng, Yueqin Wu, Guoxiong Wang, John Barry and J. C. D. d. Costa, *Environ. Sci. Technol.*, 2010, **44**, 3093.

407.L. Li, D. L. King, Z. Nie and C. Howard, *Ind. Eng. Chem. Res.*, 2009, **48**, 10604.

408.S. F. Wu and Y. Q. Zhu, *Ind. Eng. Chem. Res.*, 2010, **49**, 2701.

409.Y. J. Li, C. S. Zhao, H. C. Chen, L. B. Duan and X. P. Chen, *Fuel*, 2010, **89**, 642.

410.C. H. Huang, K. P. Chang, C. T. Yu, P. C. Chiang and C. F. Wang, *Chem. Eng. J.*, 2010, **161**, 129.

411.K. B. Yi, C. H. Ko, J.-H. Park and J.-N. Kim, *Catal. Today*, 2009, **146**, 241.

412.C. Luo, Y. Zheng, N. Ding, Q. Wu, G. Bian and C. Zheng, *Ind. Eng. Chem. Res.*, 2010, **49**, 11778.

413.M. Zhao, M. Bilton, A. P. Brown, A. M. Cunliffe, E. Dvininov, V. Dupont, T. P. Comyn and S. J. Milne, *Energy Fuels*, 2014, **28**, 1275.

414.P. Gruene, A. G. Belova, T. M. Yegulalp, R. J. Farrauto and M. J. Castaldi, *Ind. Eng. Chem. Res.*, 2011, **50**, 4042.

415.C. S. Martavaltzi and A. A. Lemonidou, *Microporous Mesoporous Mater.*, 2008, **110**, 119.

416.Z. Zhou, Y. Qi, M. Xie, Z. Cheng and W. Yuan, *Chem. Eng. Sci.*, 2012, **74**, 172.

417.N. J. Amos, M. Widyawati, S. Kureti, D. Trimis, A. I. Minett, A. T. Harris and T. L. Church, *J. Mater. Chem. A*, 2014, **2**, 4332.

418.P. Lan and S. Wu, *Chem. Eng. Technol.*, 2014, **37**, 580.

419.J. C. Mabry and K. Mondal, *Environ. Technol.*, 2011, **32**, 55.

420.P. E. Sanchez-Jimenez, L. A. Perez-Maqueda and J. M. Valverde, *Appl. Energy*, 2014, **118**, 92.

421.C.-C. Li, U.-T. Wu and H.-P. Lin, *J. Mater. Chem. A*, 2014, **2**, 8252.

422.B. González, M. Alonso and J. C. Abanades, *Fuel*, 2010, **89**, 2918.

423.H. Chen, C. Zhao, Y. Yang and P. Zhang, *Appl. Energy*, 2012, **91**, 334.

424.H. Chen, C. Zhao and Y. Yang, *Fuel Process. Technol.*, 2013, **116**, 116.

425.N. Phalak, N. Deshpande and L. S. Fan, *Energy Fuels*, 2012, **26**, 3903.

426.J. M. Valverde, P. E. Sanchez-Jimenez and L. A. Perez-Maqueda, *Fuel*, 2014, **123**, 79.

427.K. Kuramoto, S. Fujimoto, A. Morita, S. Shibano, Y. Suzuki, H. Hatano, S. Shi-Ying, M. Harada and T. Takarada, *Ind. Eng. Chem. Res.*, 2003, **42**, 975.

428.A. Coppola, P. Salatino, F. Montagnaro and F. Scala, *Fuel*, 2014, **127**, 109.

429.Y. Wu, J. Blamey, E. J. Anthony and P. S. Fennell, *Energy Fuels*, 2010, **24**, 2768.

430.F. Yu, N. Phalak, Z. Sun and L.-S. Fan, *Ind. Eng. Chem. Res.*, 2012, **51**, 2133.

431.J. Yin, C. Zhang, C. Qin, W. Liu, H. An, G. Chen and B. Feng, *Chem. Eng. J.*, 2012, **198-199**, 38.

432.Y. J. Li, C. S. Zhao, C. R. Qu, L. B. Duan, Q. Z. Li and C. Liang, *Chem. Eng. Technol.*, 2008, **31**, 237.

433.H. Chen, C. Zhao, M. Chen, Y. Li and X. Chen, *Fuel. Process. Technol.*, 2011, **92**, 1144.

434.I. Martínez, G. Grasa, R. Murillo, B. Arias and J. C. Abanades, *Energy Fuels*, 2011, **25**, 1294.

435.J. M. Cordero, M. Alonso, B. Arias and J. C. Abanades, *Energy Fuels*, 2014, **28**, 1325.

436.C. Luo, Y. Zheng, J. Guo and B. Feng, *Fuel*, 2014, **127**, 124.

437.R. H. Borgwardt, *Environ. Sci. Technol.*, 1970, **4**, 59.

438.C. Tullin and E. Ljungstrom, *Energy Fuels*, 1989, **3**, 284.

439.P. Sun, J. R. Grace, C. J. Lim and E. J. Anthony, *Energy Fuels*, 2006, **21**, 163.

440.B. Arias, J. M. Cordero, M. Alonso and J. C. Abanades, *AIChE J.*, 2011, **58**, 2262.

441.P. Sun, J. R. Grace, C. J. Lim and E. J. Anthony, *Energy Fuels*, 2007, **21**, 163.

442.H. Ryu, J. Grace and C. Lim, *Energy Fuels*, 2006, **20**, 1621.

443.H. Lu and P. Smirniotis, *Ind. Eng. Chem. Res.*, 2009, **48**, 545.

444.R. T. Symonds, D. Y. Lu, V. Manovic and E. J. Anthony, *Ind. Eng. Chem. Res.*, 2012, **51**, 7177.

445.R. Hughes, D. Lu, E. J. Anthony and A. Macchi, *Fuel Process. Technol.*, 2005, **86**, 1523.

446.F. N. Ridha, V. Manovic, Y. Wu, A. Macchi and E. J. Anthony, *Int. J. Greenhouse Gas Control*, 2013, **17**, 357.

447.F.-Q. Liu, W.-H. Li, B.-C. Liu and R.-X. Li, *J. Mater. Chem. A*, 2013, **1**, 8037.

448.K. B. Yi and D. O. Eriksen, *Sep. Sci. Technol.*, 2006, **41**, 283.

449.E. Ochoa-Fernandez, M. Ronning, T. Grande and D. Chen, *Chem. Mater.*, 2006, **18** 1383.

450.Q. Xiao, Y. F. Liu, Y. J. Zhong and W. D. Zhu, *J. Mater. Chem.*, 2011, **21**, 3838.

451.D. Barraza Jiménez, M. A. Escobedo Bretado, D. Lardizábal Gutiérrez, J. M. Salinas Gutiérrez, A. López Ortiz and V. Collins-Martínez, *Int. J. Hydrogen Energy*, 2013, **38**, 2557.

452.Y. Duan, *Phys. Chem. Chem. Phys.*, 2013, **15**, 9752.

453.M. Y. Veliz-Enriquez, G. Gonzalez and H. Pfeiffer, *J. Solid State Chem.*, 2007, **180**, 2485.

454.V. L. Mejı´a-Trejo, E. Fregoso-Israel and H. Pfeiffer, *Chem. Mater.*, 2008, **20**, 7171.

455.F. Durán-Muñoz, I. C. Romero-Ibarra and H. Pfeiffer, *J. Mater. Chem. A*, 2013, **1**, 3919.

456.Y. Duan, H. Pfeiffer, B. Li, I. C. Romero-Ibarra, D. C. Sorescu, D. R. Luebke and J. W. Halley, *Phys. Chem. Chem. Phys.*, 2013, **15**, 13538.

457.M. Wang and C.-G. Lee, *Energy Convers. Manage.*, 2009, **50**, 636.

458.C. Zanzottera, M. Armandi, S. Esposito, E. Garrone and B. Bonelli, *J. Phys. Chem. C*, 2012, **116**, 38.

459.K. M. and N. K., *J. Ceram. Soc. Jpn.*, 2001, **109**, 911.

460.K. M., Y. S. and N. K., *J. Mater. Sci. Lett.*, 2002, **21**, 485.

461.K. Essaki, K. Nakagawa, M. Kato and H. Uemoto, *J. Chem. Eng. Jpn.*, 2004, **37**, 772.

462.M. Seggiani, M. Puccini and S. Vitolo, *Int. J. Greenhouse Gas Control*, 2013, **17**, 25.

463.M. Kato, K. Nakagawa, K. Essaki, Y. Maezawa, S. Takeda, R. Kogo and Y. Hagiwara, *Int. J. Appl. Ceram. Technol.*, 2005, **2**, 467.

464.M. Kato, S. Yoshikawa and K. Nakagawa, *J. Mater. Sci. Lett.*, 2002, **21**, 485.

465.K. Essaki and M.Kato, *J. Mater. Sci.*, 2005.

466.E. Ochoa-Fernández, T. Zhao, M. Rønning and D. Chen, *J. Environ. Eng.*, 2009, **135**, 397.

467.R. Pacciani, J. Torres, P. Solsona, C. Coe, R. Quinn, J. Hufton, T. Golden and L. F. Vega, *Environ. Sci. Technol.*, 2011, **45**, 7083.

468.I. C. Romero-Ibarra, J. Ortiz-Landeros and H. Pfeiffer, *Thermochim. Acta*, 2013, **567**, 118.

469.M. Seggiani, M. Puccini and S. Vitolo, *Int. J. Greenhouse Gas Control*, 2011, **5**, 741.

470.R. Xiong, J. Ida and Y. S. Lin, *Chem. Eng. Sci.*, 2003, **58**, 4377.

471.J. F. Stebbins, Z. Xu and D. Vollath, *Solid State Ionics*, 1995, **78**, L1.

472.K. Jackowska and A. R. West, *J. Mater. Sci.*, 1983, **18**, 2380.

473.C. Gauer and W. Heschel, *J. Mater. Sci.*, 2006, **41**, 2405.

474.J. Ortiz-Landeros, C. Gomez-Yanez, L. M. Palacios-Romero, E. Lima and H. Pfeiffer, *J. Phys. Chem. A*, 2012, **116**, 3163.

475.H. Pfeiffer, E. Lima and P. Bosch, *Chem. Mater.*, 2006, **18**, 2642.

476.H. Pfeiffer, C. Vazquez, V. H. Lara and P. Bosch, *Chem. Mater.*, 2007, **19**, 922.

477.M. Y. Veliz-Enriquez, G. Gonzalez and H. J. Pfeiffer, *Solid State Chem.*, 2007, **180**, 2485.

478.J. I. Ida, R. Xiong and Y. S. Lin, *Sep. Purif. Technol.*, 2004, **36**, 41.

479.R. Quinn, R. J. Kitzhoffer, J. R. Hufton and T. C. Golden, *Ind. Eng. Chem. Res.*, 2012, **51**, 9320.

480.S. Shan, Q. Jia, L. Jiang, Q. Li, Y. Wang and J. Peng, *Ceram. Int.*, 2013, **39**, 5437.

481.M. Olivares-Marín and M. M. Maroto-Valer, *Greenhouse Gases Sci. Technol.*, 2012, **2**, 20.

482. UNEP, presented in part at the Compendium of Technologies Osaka/Shiga, Japan, 2009.

483. M. G. Plaza, S. García, F. Rubiera, J. J. Pis and C. Pevida, *Sep. Purif. Technol.*, 2011, **80**, 96.

484. A. S. González, M. G. Plaza, F. Rubiera and C. Pevida, *Chem. Eng. J.*, 2013, **230**, 456.

485. A. S. Ello, L. K. C. de Souza, A. Trokourey and M. Jaroniec, *Microporous Mesoporous Mater.*, 2013, **180**, 280.

486. D. P. Vargas, L. Giraldo and J. C. Moreno-Pirajan, *Int. J. Mol. Sci.*, 2012, **13**, 8388.

487. G. Dobele, T. Dizhbite, M. V. Gil, A. Volperts and T. A. Centeno, *Biomass Bioenergy*, 2012, **46**, 145.

488. J. Song, W. Shen, J. Wang and W. Fan, *Carbon*, 2014, **69**, 255.

489. M. G. Plaza, A. S. González, C. Pevida, J. J. Pis and F. Rubiera, *Appl. Energy*, 2012, **99**, 272.

490. A. Boonpoke, S. Chiarakorn, N. Laosiripojana, S. Towprayoon and A. Chidthaisong, *Korean J. Chem. Eng.*, 2011, **29**, 89.

491. R. Wang, P. Wang, X. Yan, J. Lang, C. Peng and Q. Xue, *ACS Appl. Mater. Interf.*, 2012, **4**, 5800.

492. Z. Zhang, K. Wang, J. D. Atkinson, X. Yan, X. Li, M. J. Rood and Z. Yan, *J. Hazard. Mater.*, 2012, **229**, 183.

493. M. G. Plaza, C. Pevida, B. Arias, J. Fermoso, M. D. Casal, C. F. Martín, F. Rubiera and J. J. Pis, *Fuel*, 2009, **88**, 2442.

494. M. G. Plaza, C. Pevida, C. F. Martín, J. Fermoso, J. J. Pis and F. Rubiera, *Sep. Purif. Technol.*, 2010, **71**, 102.

495. M. A. Silva, S. A. Nebra, M. J. Machado Silva and C. G. Sanchez, *Biomass Bioenergy*, 1998, **14**, 457.

496. A. Wahby, J. M. Ramos-Fernandez, M. Martinez-Escandell, A. Sepulveda-Escribano, J. Silvestre-Albero and F. Rodriguez-Reinoso, *ChemSusChem*, 2010, **3**, 974.

497. M. E. Casco, M. Martinez-Escandell, J. Silvestre-Albero and F. Rodriguez-Reinoso, *Carbon*, 2014, **67**, 230.

498. S.-Y. Lee, H.-M. Yoo, S. W. Park, S. H. Park, Y. S. Oh, K. Y. Rhee and S.-J. Park, *J. Solid State Chem.*, 2014, **215**, 201.

499. L.-Y. Lin and H. Bai, *Microporous Mesoporous Mater.*, 2013, **170**, 266.

500. M. Ives, R. C. Mundy, P. S. Fennell, J. F. Davidson, J. S. Dennis and A. N. Hayhurst, *Energy Fuels*, 2008, **22**, 3852.

501. E. R. Sacia, S. Ramkumar, N. Phalak and L.-S. Fan, *ACS Sustainable. Chem. Eng.*, 2013, **1**, 903.

502. S. Castilho, A. Kiennemann, M. F. Costa Pereira and A. P. Soares Dias, *Chem. Eng. J.*, 2013, **226**, 146.

503. M. Mohammadi, P. Lahijani and A. R. Mohamed, *Chem. Eng. J.*, 2014, **243**, 455.

504. Y. Li, C. Liu, R. Sun, H. Liu, S. Wu and C. Lu, *Ind. Eng. Chem. Res*, 2012, **51**, 16042.

505. S. Yoo, J. S. Hsieh, P. Zou and J. Kokoszka, *Bioresource Technol.*, 2009, **100**, 6416.

506. H. V. Walton, O. J. Cotterill and J. M. Vandepopuliere, *Poultry Sci.*, 1973, **52**, 1192.

507. M. Olivares-Marin, T. C. Drage and M. Mercedes Maroto-Valer, *Int. J. Greenhouse Gas Control*, 2010, **4**, 623.

508. K. Wang, X. Guo, P. Zhao, F. Wang and C. Zheng, *J. Hazard Mater.*, 2011, **189**, 301.

509. S. Shan, Q. Jia, L. Jiang, Q. Li, Y. Wang and J. Peng, *Chin. Sci. Bull.*, 2012, **57**, 2475.

510. K. Wang, X. Guo∗, P. Zhao, F. Wang and C. Zheng, *J. Hazard. Mater.*, 2011, **189**, 306.

511. M. Zhao, A. I. Minett and A. T. Harris, *Energy Environ. Sci.*, 2013, **6**, 25.

512. T. F. Hurst, T. T. Cockerill and N. H. Florin, *Energy Environ. Sci.*, 2012, **5**, 7132.

513. C. C. Dean, D. Dugwell and P. S. Fennell, *Energy Environ. Sci.*, 2011, **4**, 2050.

514. N. Berghout, M. van den Broek and A. Faaij, *Int. J. Greenhouse Gas Control*, 2013, **17**, 259.

515. K. Vatopoulos and E. Tzimas, *J. Cleaner Production*, 2012, **32**, 251.

516. M. Gazzani, E. Macchi and G. Manzolini, *Int. J. Greenhouse Gas Control*, 2013, **12**, 493.

517. M. M. J. Knoope, J. C. Meerman, A. Ramírez and A. P. C. Faaij, *Int. J. Greenhouse Gas Control*, 2013, **16**, 287.

518. S. Chen, W. Xiang, D. Wang and Z. Xue, *Appl. Energy*, 2012, **95**, 285.